PHILOSOPHICAL TRANSACTIONS OF THE ROYAL SOCIETY B BIOLOGICAL SCIENCES

The Postcranial Skeletal Anatomy of the Carboniferous Tetrapod Greererpeton burkemorani Romer, 1969

S. J. Godfrey

Phil. Trans. R. Soc. Lond. B 1989 **323**, 75-133
doi: 10.1098/rstb.1989.0002

Phil. Trans. R. Soc. Lond. B **323**, 75–133 (1989) [75]
Printed in Great Britain

THE POSTCRANIAL SKELETAL ANATOMY OF THE CARBONIFEROUS TETRAPOD *GREERERPETON BURKEMORANI* ROMER, 1969

By S. J. GODFREY

Redpath Museum, McGill University, 859 Sherbrooke Street West, Montreal, Quebec, Canada H3A 2K6

(*Communicated by H. B. Whittington, F.R.S.* – *Received* 16 *July* 1987 – *Revised* 22 *April* 1988)

[Pullouts 1 and 2]

CONTENTS

Vol. 323. B 1213 11 [Published 2 February 1989

The discovery of well-preserved skeletal remains of *Greererpeton burkemorani* Romer, 1969, from the Upper Mississippian at Greer, West Virginia, has prompted a redescription of its postcranial skeletal anatomy. The vertebrae are rhachitomous, more specifically schizomerous. The presacral count is approximately 41. Neural arch elements of the atlas–axis complex consist of paired pro- and atlas arches and a relatively massive axis arch. All presacral vertebrae appear to have borne short, gently curved ribs, most of which developed a flange or stiletto-like uncinate process. The sacral rib is long. In adults, the scapulocoracoid and the dermal pectoral girdle are large and well ossified. The ascending iliac blade is undivided and the pubis is poorly ossified.

A cladistic analysis indicates that *Greererpeton burkemorani* shares a more recent common ancestor with the anthracosaur *Proterogyrinus scheelei* than it does with either *Crassigyrinus scoticus* or *Ichthyostega* sp.

Introduction

Although our knowledge of the cranial morphology of Carboniferous tetrapods has improved significantly over the past 20 years, much less is known of the postcranial skeletal anatomy of many forms, owing primarily to the paucity of articulated specimens.

Between 1969 and 1973, field parties from the Cleveland Museum of Natural History recovered a large number of vertebrate skeletons from a commercial quarry operated by the Greer Limestone Company in the valley of Deckers Creek, Monongalia County, West Virginia. Detailed descriptions of the site are provided by Hotton (1970) and Romer (1969, 1970). By far the largest number of vertebrate remains recovered from this Upper Mississippian locality belong to *Greererpeton burkemorani* (Romer 1969) (figure 1).

Although not closely related to them, *G. burkemorani* resembled the giant Asian salamanders of the genus *Andrias* in its general skeletal proportions. As an adult, *G. burkemorani* attained an overall length of 1.0–1.4 m. It possessed diminutive limbs and an elongate vertebral column. From the snout to the pelvic girdle, *G. burkemorani* was dorsoventrally compressed. The skull was flattened and the ribs were short, slightly curved, and directed primarily laterally. The laterally compressed tail appears to have accounted for approximately one third of the total body length. Unlike most modern frogs and salamanders, which lack dermal ossifications, *G. burkemorani* was clad in a virtually complete covering of dermal scales.

Synopsis of previous work on *Greererpeton*

The original description of *G. burkemorani* (Romer 1969) was based on a single incomplete specimen (figure 2). Although the holotype includes much of the anterior portion of the skeleton, it was not fully prepared before publication; consequently the original description was incomplete and in some cases inaccurate. Since then, several virtually complete individuals have been collected and prepared by the Cleveland Museum. These exquisite specimens formed the basis of subsequent publications. In 1972, Romer published a brief description of the dermal armour investing *G. burkemorani*. From this study he concluded that primitive amphibians clad with a dense dermal armour of the type found in *G. burkemorani* would not have been able to engage in cutaneous respiration as practised by modern amphibians.

More recently Carroll (1980), in a study of the stapes of *G. burkemorani*, demonstrated that this element was essential for bracing and stabilizing the braincase beneath the dermal skull

PHILOSOPHICAL TRANSACTIONS OF THE ROYAL SOCIETY B BIOLOGICAL SCIENCES

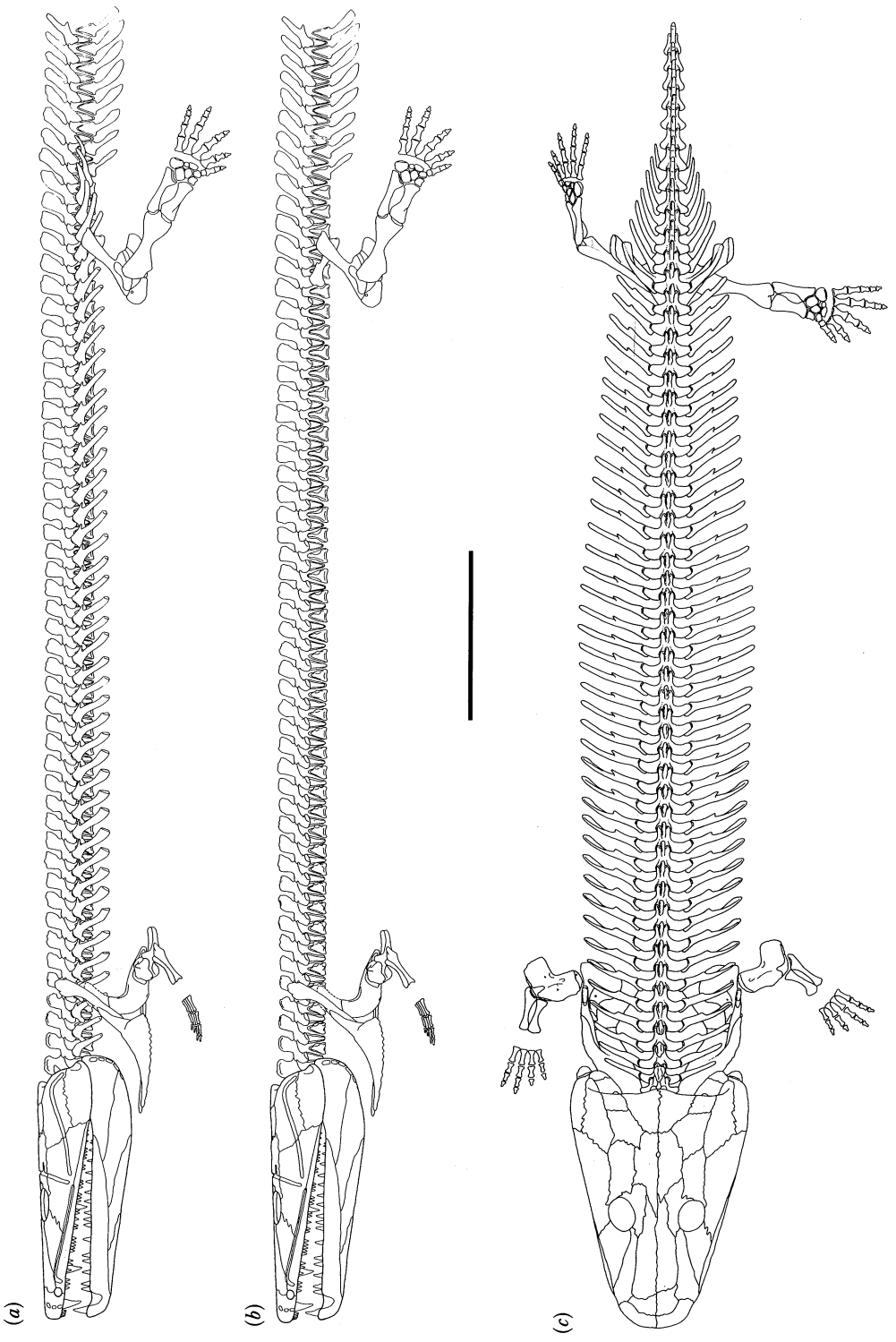

FIGURE 1. *Greererpeton burkemorani* Romer, skeletal restoration. (*a*) Left lateral view; (*b*) left lateral view with the ribs omitted to reveal details of vertebral structure; (*c*) dorsal view. Scale bar 10 cm.

PHILOSOPHICAL TRANSACTIONS OF THE ROYAL SOCIETY B BIOLOGICAL SCIENCES

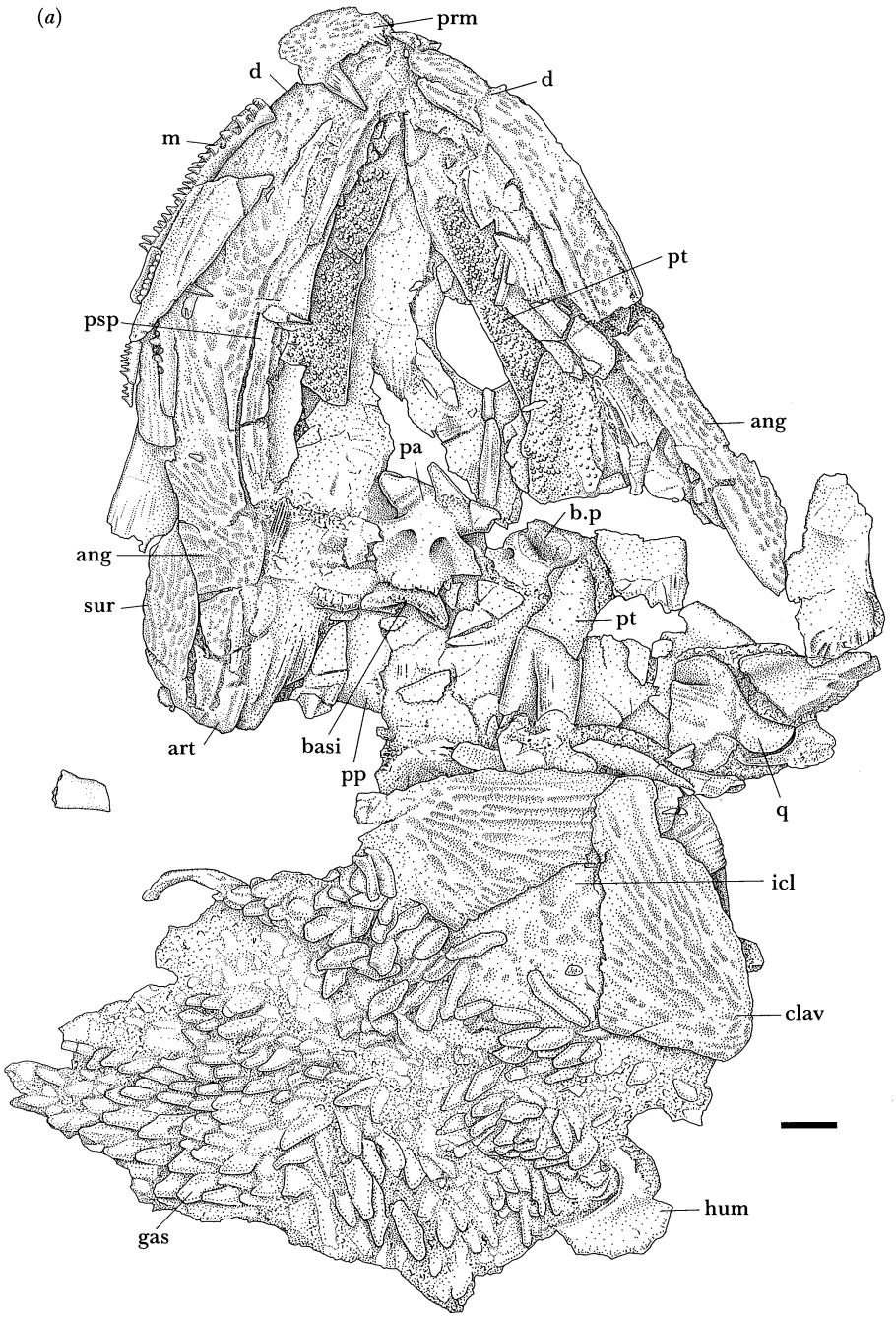

FIGURE 2*a*. For description see opposite.

roof. As such, it did not function as a transmitter of airborne vibrations from a membranous typanum to the inner ear. This study renewed interest in the (in)ability of early tetrapods to receive airborne sounds through an aerial impedance matching ear. In a redescription of the hyomandibular of *Eusthenopteron foordi* Whiteaves, Smithson & Thomson (1982) also provided a brief account of the stapes and otic region of *G. burkemorani* and its bearing upon the early evolution of the tetrapod stapes.

PHILOSOPHICAL TRANSACTIONS OF THE ROYAL SOCIETY B BIOLOGICAL SCIENCES

FIGURE 2. *Greererpeton burkemorani* Romer, CMNH 10931. (*a*) Anterior portion of the Holotype in ventral view; (*b*) abdominal section of the Holotype in dorsal view. Scale bar 1 cm.

PHILOSOPHICAL TRANSACTIONS OF THE ROYAL SOCIETY B BIOLOGICAL SCIENCES

The right humerus of *G. burkemorani* (CMNH 11090) was illustrated by Holmes (1980) to show its remarkable similarity to that of the contemporary Greer embolomere, *Proterogyrinus scheelei* Romer.

Smithson (1982) provided a detailed description of the cranial morphology of *G. burkemorani* with particular emphasis placed upon the structure of the palatoquadrate, braincase and stapes. Finally, Godfrey (1989) described ontogenetic changes in a growth series of *G. burkemorani*. Conspicuous changes were noted in the relative size of some circumorbital bones, the braincase and stapes.

It is evident that most publications have concentrated primarily on various aspects of the cranial anatomy of *G. burkemorani*. With several virtually complete individuals at hand, such as CMNH 11090 and CMNH 11068 (figure 3, pullouts 1 and 2, and figure 4), a thorough redescription of the postcranial skeleton is warranted.

The advent of phylogenetic systematics, or cladism, has revolutionized systematic procedures and prompted a re-evaluation of the 'diagnostic features' employed to delineate taxonomic assemblages. Not unlike traditional systematic procedures, cladistic methodology places a premium on detailed and accurate descriptions because the conclusions of a cladistic analysis are only as good as the anatomical information on which they are based. Although *G. burkemorani* is not on the main evolutionary line leading to extant amphibians or amniotes, an analysis of its skeletal anatomy will help to clarify aspects of the early evolution of tetrapods, and the sequence in which characters diagnostic of smaller taxonomic groups arose. The results of this study are incorporated into a cladogram in an attempt to determine the interrelations of some of the earliest tetrapods.

Materials and methods

The specimens of *G. burkemorani* that formed the basis of this study were loaned to the Redpath Museum by the Cleveland Museum of Natural History (CMNH) and the Museum of Comparative Zoology, Harvard University (MCZ) (a brief description of each specimen studied is provided in Appendix 1). Almost all the material had been prepared by the staff of the Cleveland Museum with an S. S. White Industrial Airbrasive machine. Although most specimens were well prepared, bone surfaces show varying degrees of dolomite powder abrasion that has reduced or obliterated some fine surface detail, such as muscle scars. Additional preparation of some specimens was undertaken by T. R. Smithson and the author, with an Airbrasive unit, a Chicago Pneumatic Scribe (air-driven reciprocal chisel), dental drills and mounted needles, all under a binocular dissecting microscope.

The grey-green medium-grained micaceous sandstone in which the fossils are preserved softens when left standing in water for approximately 15 minutes. This discovery greatly facilitated the removal of the matrix from around the bone by using mounted needles. Fractured or broken material was consolidated with dilute Glyptal Cement (Canadian General Electric, G-1276). Glyptal was also applied liberally to exposed bone before airbrasive preparation to prevent the loss of surface detail. Because most bones suffered little or no *post mortem* crushing, it was possible to prepare many elements for three-dimensional study by embedding exposed surfaces in Carbowax (polyethylene glycol) before removing the remaining matrix.

Because *G. burkemorani* is represented by numerous specimens, tabulations of some postcranial dimensions are included in Appendix 2. The measurements were made with dial calipers and are accurate to the nearest millimetre, unless otherwise specified.

PHILOSOPHICAL TRANSACTIONS OF THE ROYAL SOCIETY B BIOLOGICAL SCIENCES

PHILOSOPHICAL TRANSACTIONS OF THE ROYAL SOCIETY B BIOLOGICAL SCIENCES

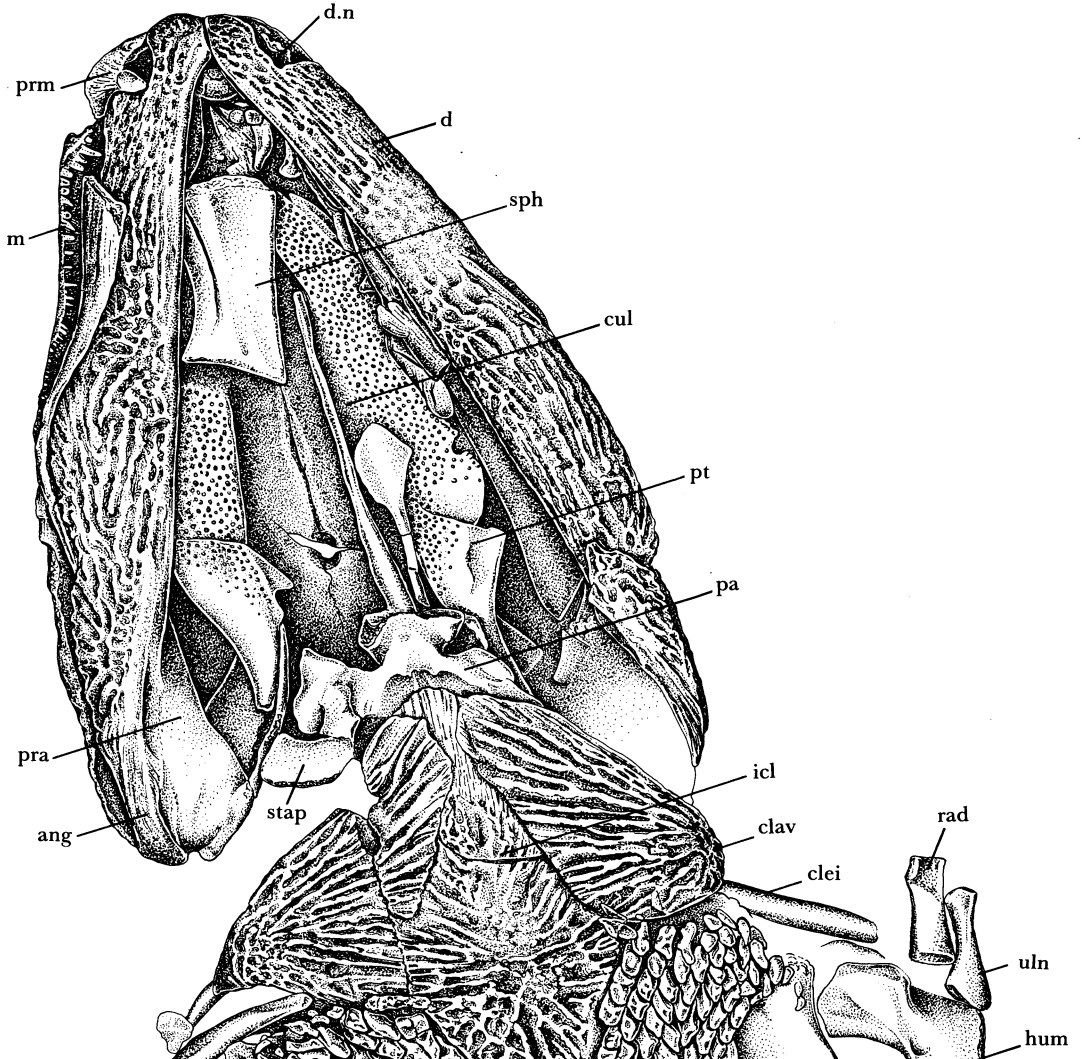

PHILOSOPHICAL TRANSACTIONS OF THE ROYAL SOCIETY B BIOLOGICAL SCIENCES

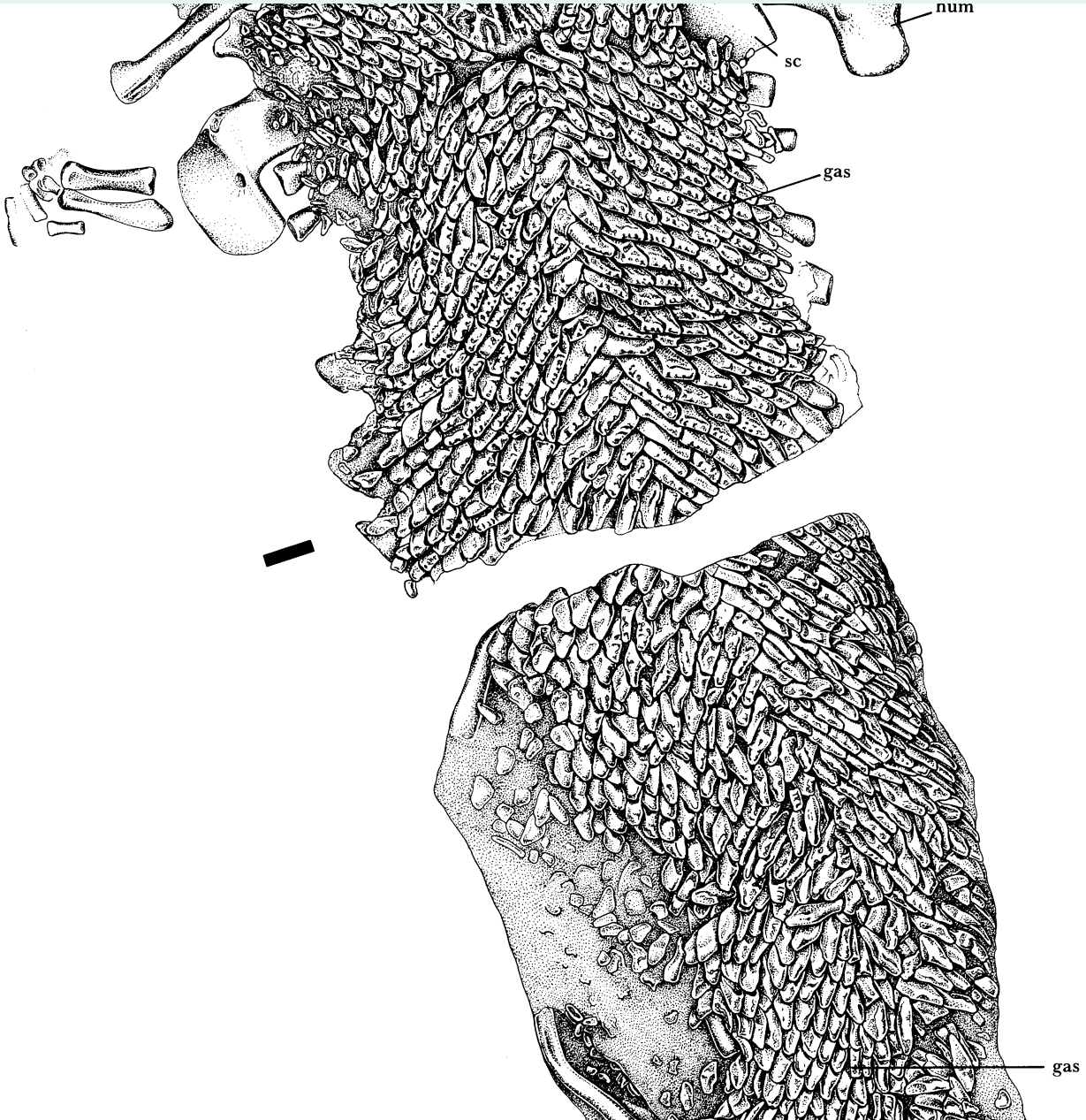

FIGURE 3*a*. *Greererpeton burkemorani* Romer, C

PHILOSOPHICAL TRANSACTIONS OF THE ROYAL SOCIETY B BIOLOGICAL SCIENCES

CMNH 11090. Articulated skeleton in ventral view. Scale bar 1 cm.

PHILOSOPHICAL TRANSACTIONS OF THE ROYAL SOCIETY B BIOLOGICAL SCIENCES

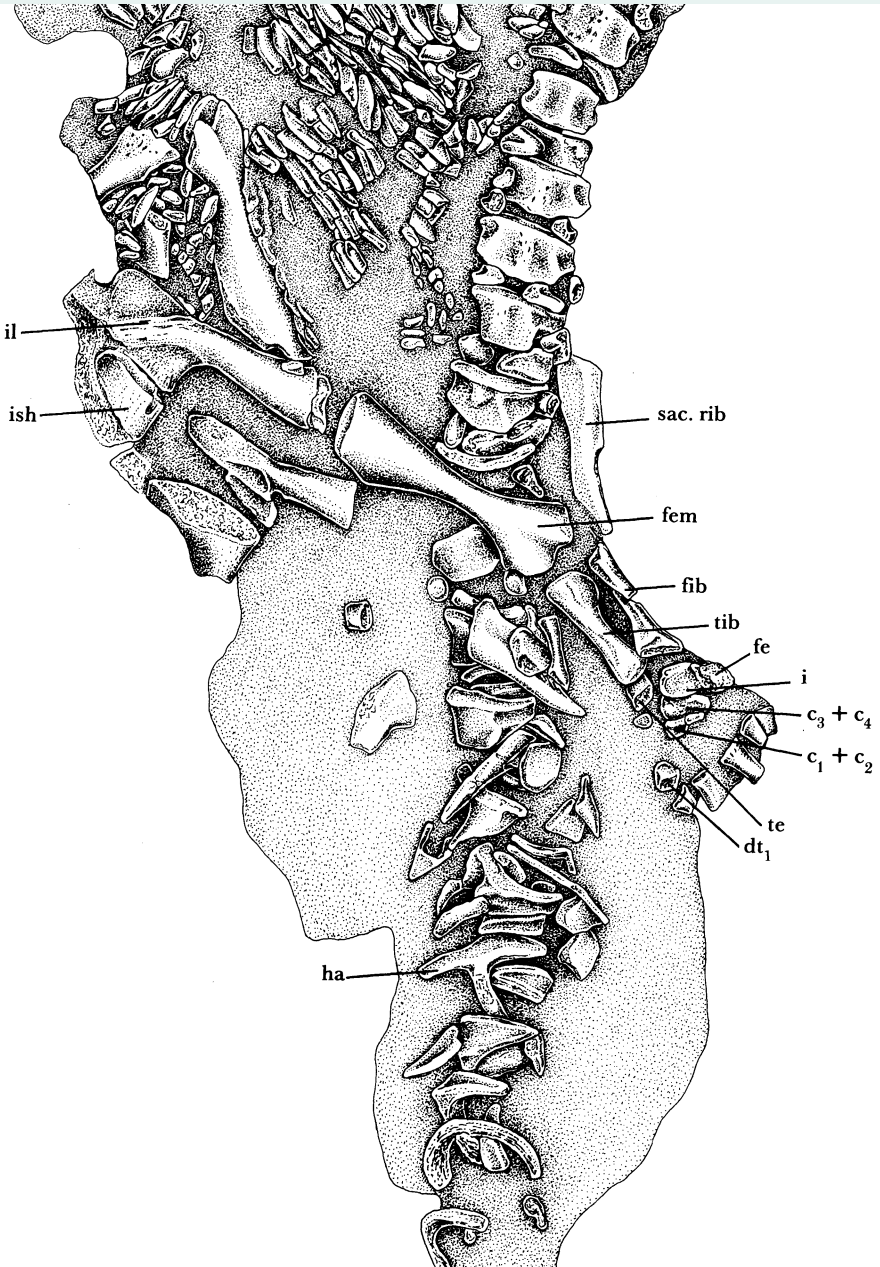

Godf

PHILOSOPHICAL TRANSACTIONS OF THE ROYAL SOCIETY B BIOLOGICAL SCIENCES

PHILOSOPHICAL TRANSACTIONS OF THE ROYAL SOCIETY B BIOLOGICAL SCIENCES

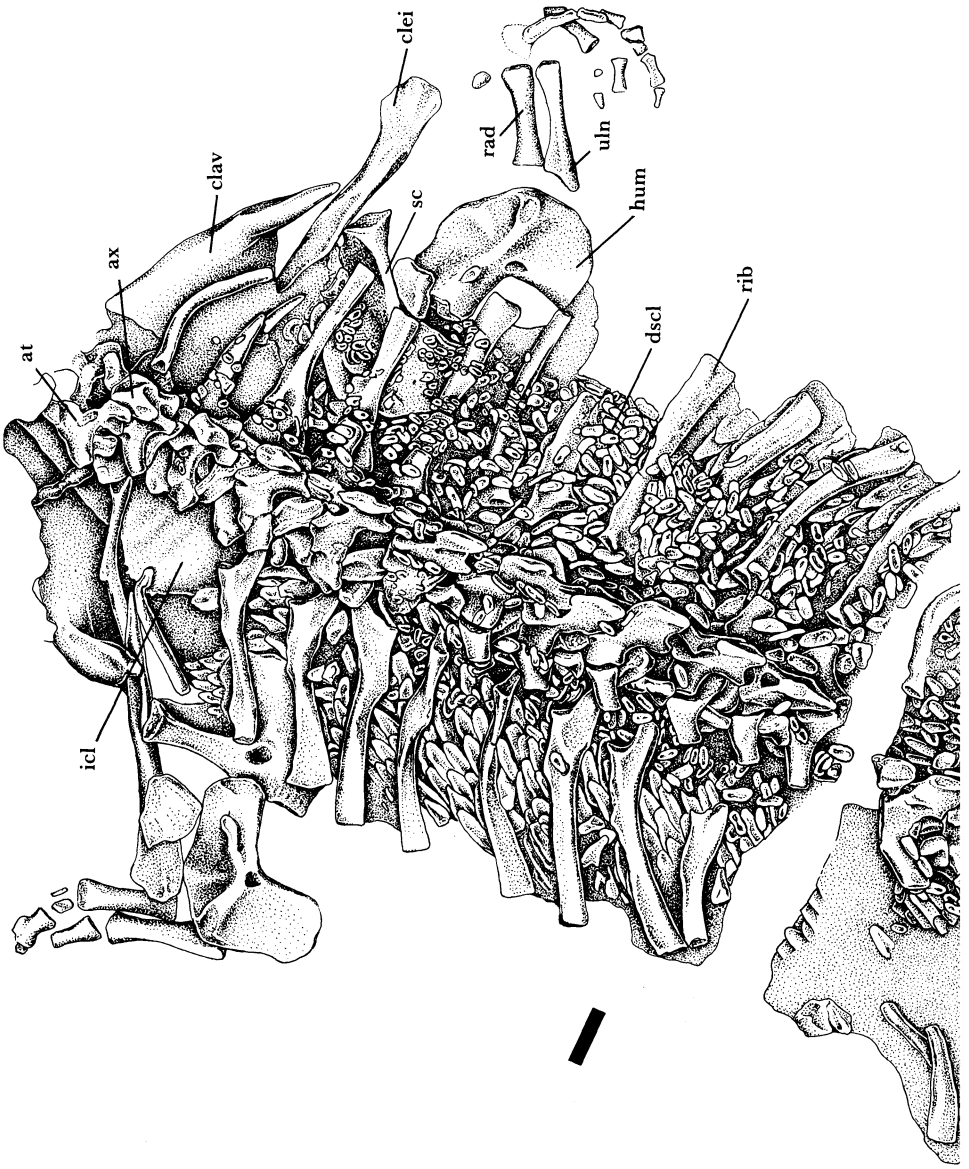

PHILOSOPHICAL TRANSACTIONS OF THE ROYAL SOCIETY B BIOLOGICAL SCIENCES

PHILOSOPHICAL TRANSACTIONS OF THE ROYAL SOCIETY B BIOLOGICAL SCIENCES

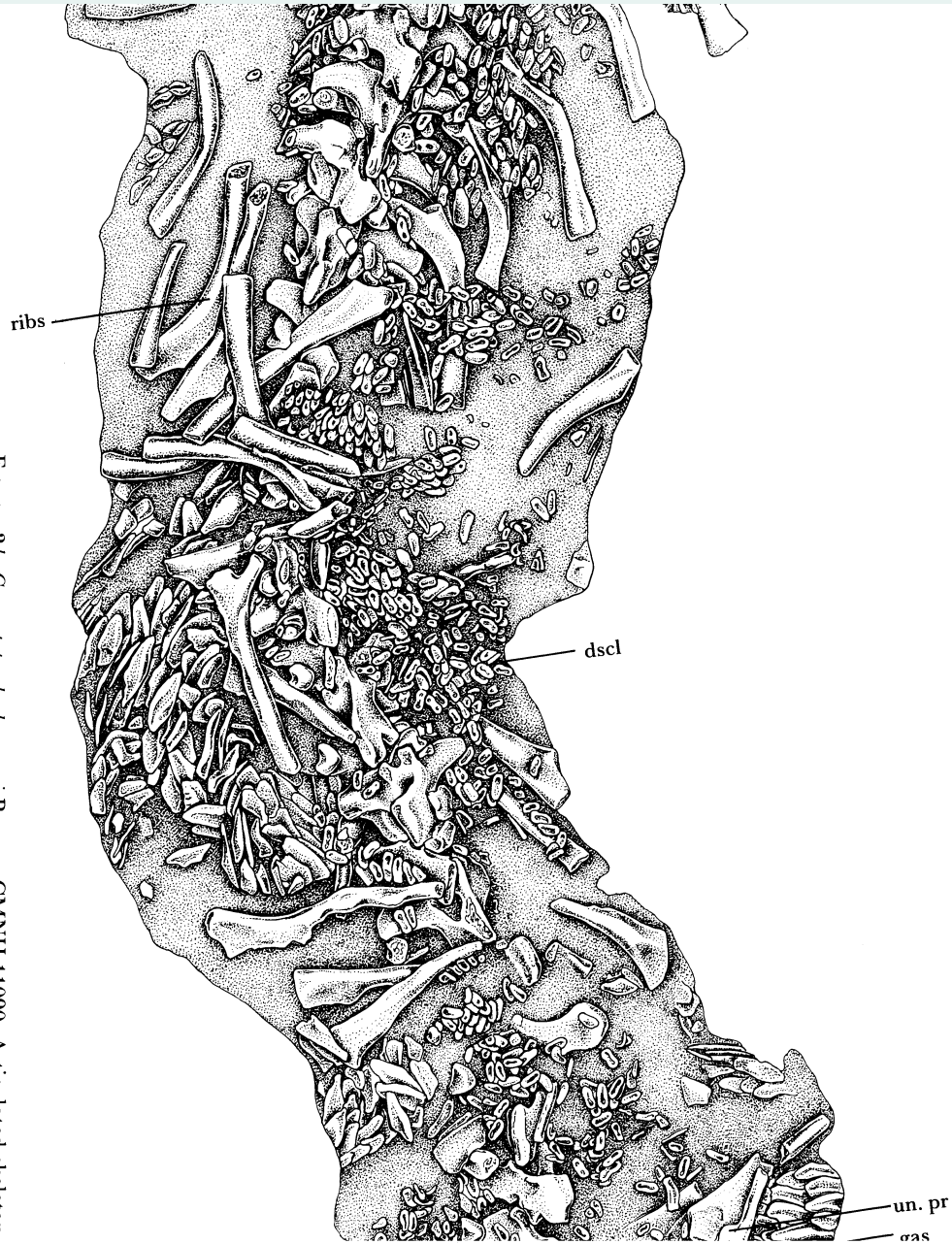

FIGURE 3*b*. *Greererpeton burkemorani* Romer, CMNH 11090. Articulated skeleton

PHILOSOPHICAL TRANSACTIONS OF THE ROYAL SOCIETY B BIOLOGICAL SCIENCES

on in dorsal view. Scale bar 1 cm.

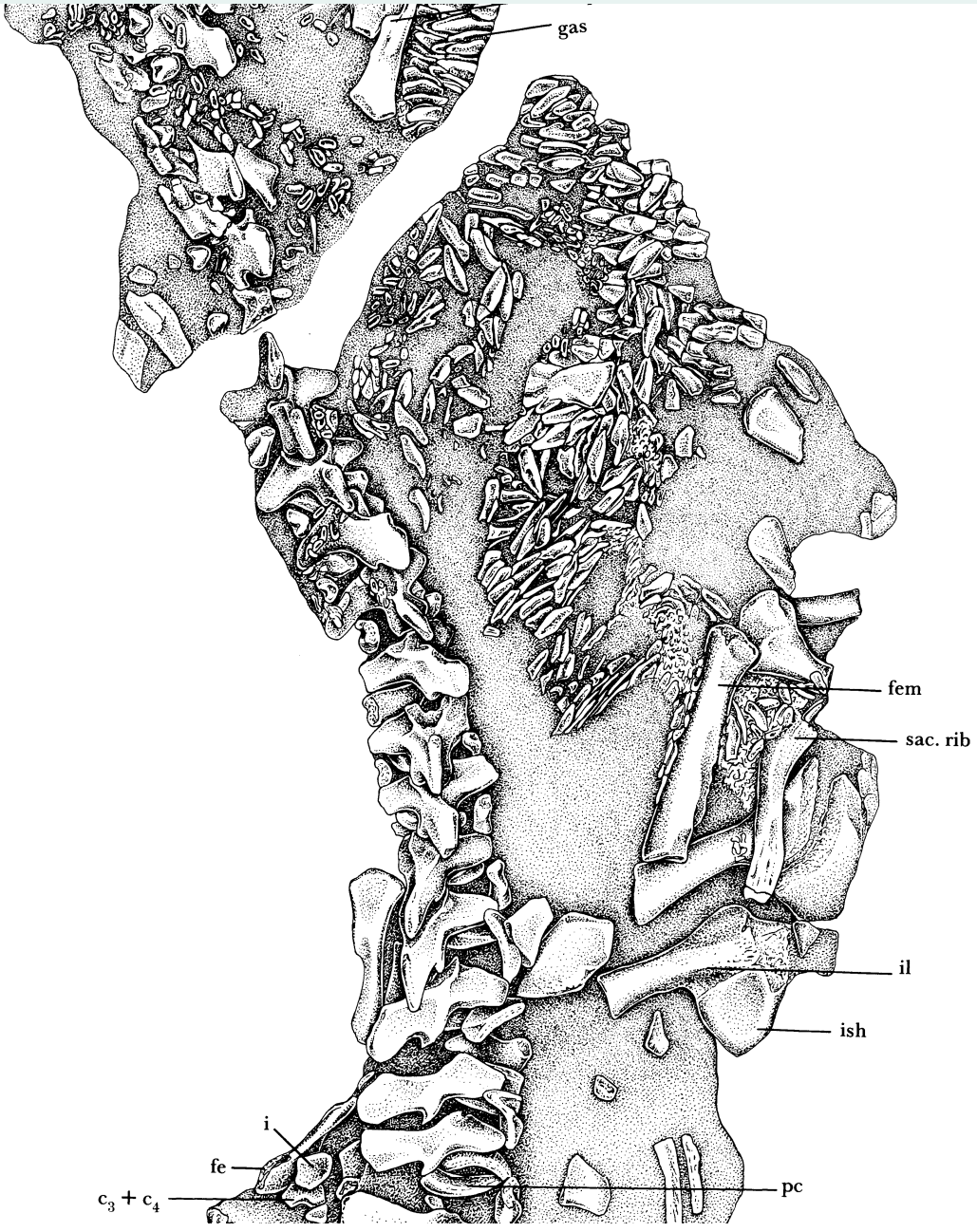

PHILOSOPHICAL TRANSACTIONS OF THE ROYAL SOCIETY B BIOLOGICAL SCIENCES

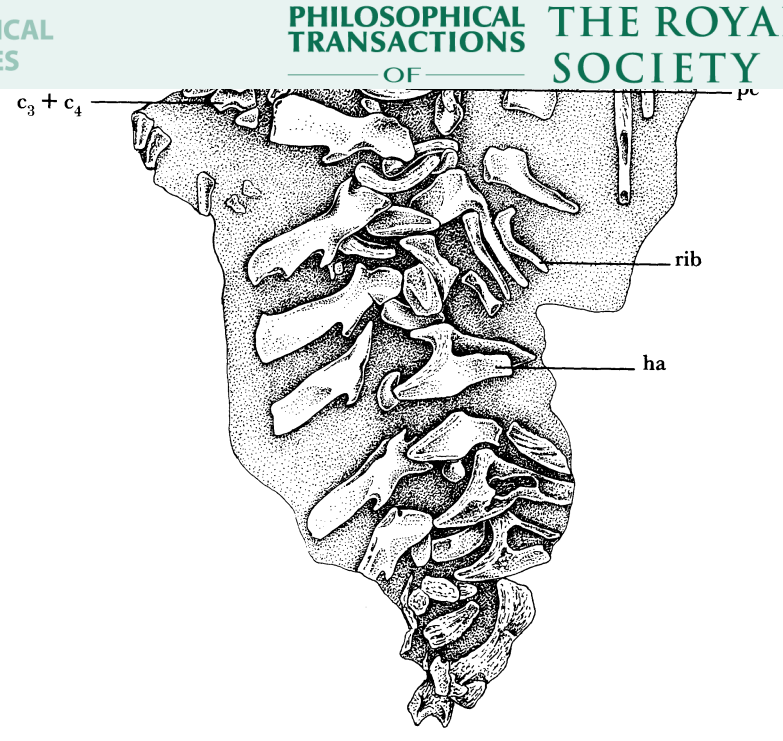

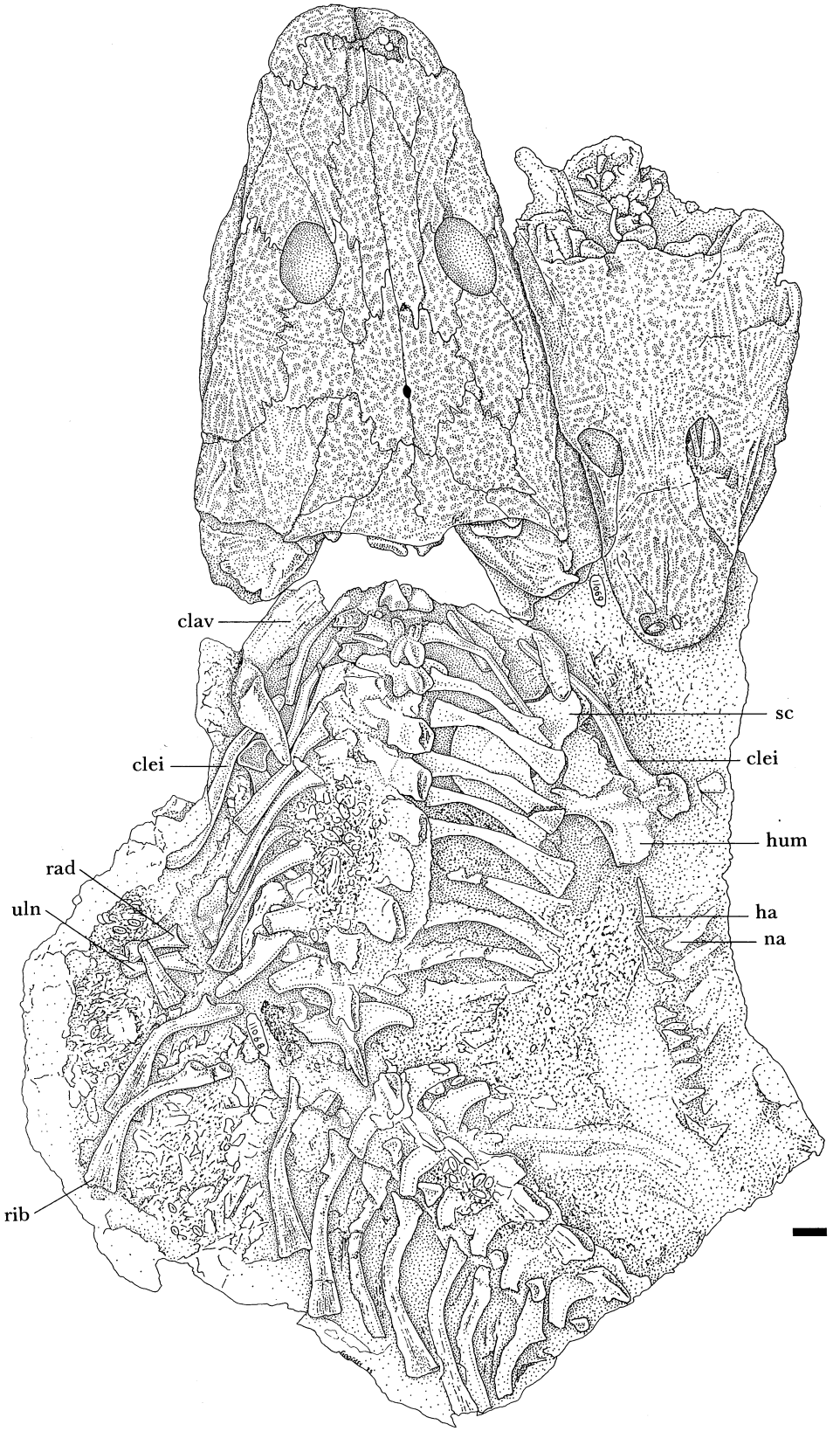

FIGURE 4. *Greererpeton burkemorani* Romer. Includes the articulated remains of three individuals: CMNH 11068, skull and articulated anterior vertebrae; CMNH 11069, smaller skull with a few cervical vertebrae; and CMNH 11070, distal caudal vertebrae. Scale bar 1 cm.

PHILOSOPHICAL TRANSACTIONS OF THE ROYAL SOCIETY B BIOLOGICAL SCIENCES

Systematics

Class **AMPHIBIA**

Order TEMNOSPONDYLI

Superfamily Colosteoidea Tatarinov 1964

sensu novo (Hook 1983)

Diagnosis. (Revised from Smithson (1982) and Hook (1983).) Tetrapods characterized by a massive stapes; an extensive tabular–squamosal contact and no squamosal embayment ('otic notch'); an elongate prefrontal extending to the external naris contacting the premaxilla and maxilla and excluding the lacrimal and nasal from the narial opening; the intertemporal is minute or absent; a broad postorbital–parietal contact; a single pair of premaxillary tusks on a posterolateral palatal flange; large premaxillary tusk and an accommodating dentary notch; parasymphysial tusk not bounded laterally by marginal teeth; dentary teeth larger than maxillary teeth; a single, elongate Meckelian fenestra; approximately 40 presacral vertebrae; loss of the supraglenoid foramen on the scapulocoracoid; extensive dorsal and ventral scalation; ventral scales rhomboidal with crenulated posterior margin.

Family Colosteidae Cope 1875

Diagnosis. As for the superfamily.

Genus *Greererpeton* Romer, 1969

Diagnosis. Four teeth on coronoid 1; dorsal squamation consisting of a mosaic of small subcircular scales.

Greererpeton burkemorani Romer, 1969

Diagnosis. As for genus. The Westphalian D colosteid, *Colosteus scutellatus* (Newberry), differs from *G. burkemorani* in possessing the following autapomorphies: (1) the orbital margin is formed by only three bones, the jugal, lacrimal, and postfrontal; (2) the coronoids possess a single row of minute coronoid teeth (may be plesiomorphic for tetrapods, see below); and (3) dorsal scalation resembles gastralia (Hook 1983). The Viséan colosteid, *Pholidogaster pisciformis* Huxley, is only known from two poorly preserved and incomplete specimens (Panchen 1975). Attempts to ascertain whether differences between it, *G. burkemorani*, and *C. scutellatus* are real or attributable to the poor quality of the fossils, must await further discoveries of *P. pisciformis*.

The vertebral column

The vertebral column of *G. burkemorani* is preserved in several specimens which collectively range from a few elements to almost complete columns, lacking only the distal portion of the tail (figures 3, 4 and 5). Articulated presacral vertebrae of *G. burkemorani* are most often preserved with the sagittal plane through the neural spines perpendicular to the bedding plane. The very broad transverse processes and the gently curved ribs appear to have ensured this orientation. Caudal vertebrae, except for the first six, lack ribs and display short transverse processes and long haemal arches (figure 1). They are invariably preserved with their vertical axis lying parallel to the bedding plane.

PHILOSOPHICAL TRANSACTIONS OF THE ROYAL SOCIETY B BIOLOGICAL SCIENCES

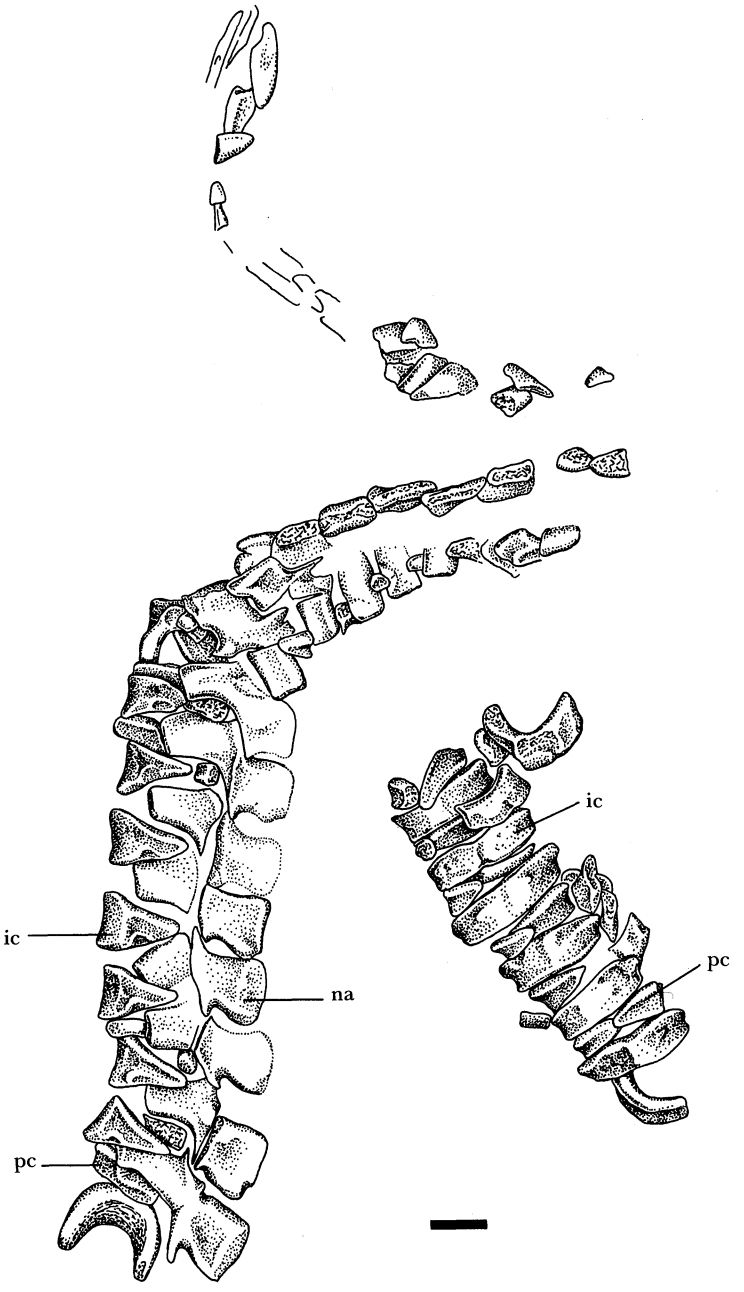

FIGURE 5. *Greererpeton burkemorani* Romer, CMNH 11092. Articulated segments of anterior (lower right) and posterior (L-shaped series, left and centre) presacral vertebrae. Scale bar 1 cm.

The similarity of the vertebrae in all *G. burkemorani* specimens makes a detailed description of each specimen unnecessary. Ontogenetic and regional variations are described where they exist. Although the most complete columns are preserved in CMNH 11090, CMNH 11068, and CMNH 11070, many other specimens were used to give a virtually complete picture of vertebral morphology.

The presacral column of *G. burkemorani* appears to be composed of 41 ± 1 vertebrae. Uncertainty arises from the fact that no column is completely articulated, and in many

specimens much of the column is obscured by a profusion of dorsal and ventral scales. Although only 12 caudal vertebrae are restored in figure 1 (which is based on CMNH 11090) at least 33 caudals are preserved in a smaller individual, CMNH 11070. Judging from their size, it is not unreasonable to suggest that there may have been as many as 40 caudal vertebrae in *G. burkemorani*, for approximately 80 vertebrae in all.

Each vertebra of *G. burkemorani* conforms to the basic rhachitomous pattern, being composed of a neural arch and a multipartite centrum. The centrum is formed by an anterior crescent-shaped intercentrum and a paired posterior pleurocentrum which bears facets to support the neural arch. The mass of bone in one intercentrum is approximately equivalent to that in the two halves of the pleurocentrum.

The basic structure of the intercentra in *G. burkemorani* (figure 6 *a–f*) is similar thoughout the presacral vertebral column, conforming to the quintessential rhacitomous pattern. Each intercentrum forms a crescentic, ventrally robust band of bone with wedge-shaped upturned

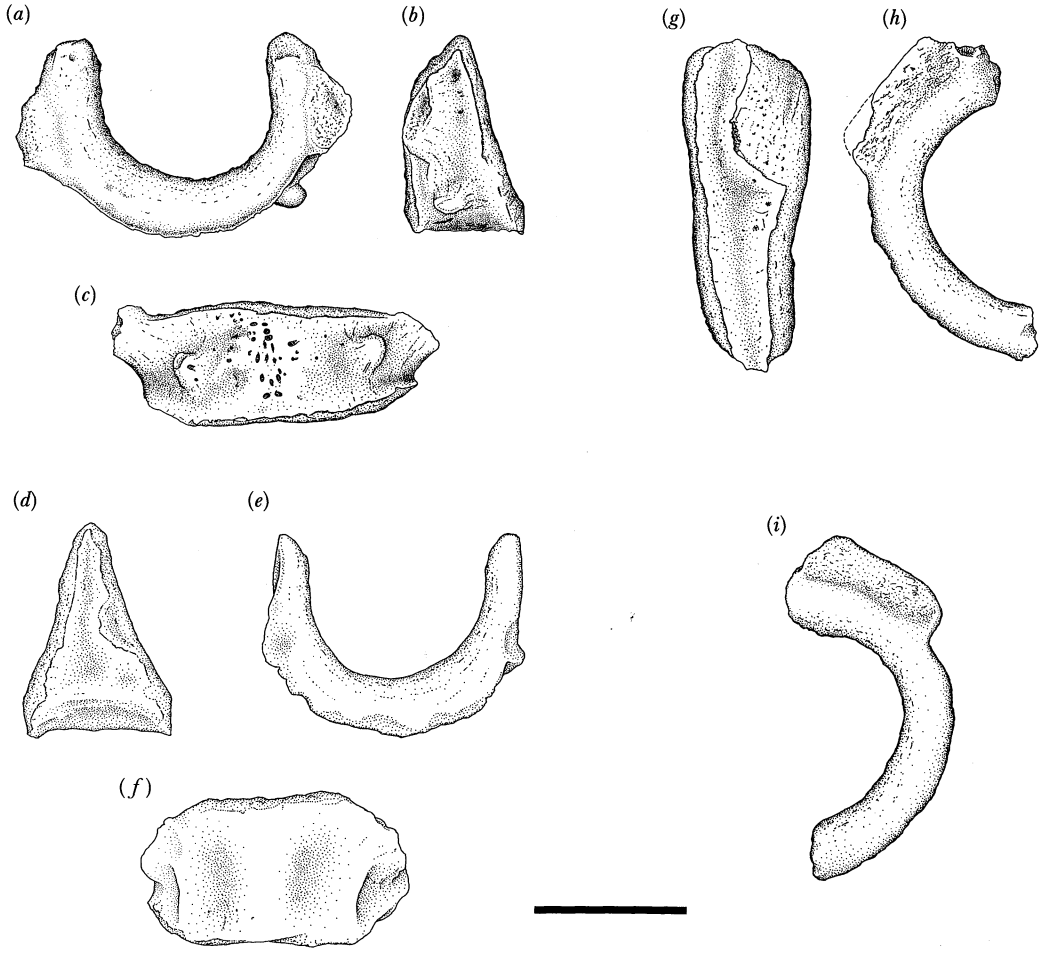

FIGURE 6. Isolated intercentra and pleurocentra of *Greererpeton burkemorani* Romer. (*a–c*) Presacral intercentrum (cervical 5 (?)) of CMNH 11319 in posterior, right lateral and ventral views respectively; (*d–f*) posterior presacral intercentrum of CMNH 11092 (exact position uncertain, behind presacral 20) in left lateral, posterior and ventral views respectively; (*g–i*) anterior presacral pleurocentra (halves) of CMNH 11240 (exact position uncertain, between vertebrae 7 and 11), (*g*, *h*) right lateral and anterior views respectively, (*i*) adjacent segment (left side) in anterior view. Scale bar 1 cm.

PHILOSOPHICAL TRANSACTIONS OF THE ROYAL SOCIETY B BIOLOGICAL SCIENCES

sides that wrap around the notochordal space. The periosteal bone is limited to its concave ventral and lateral surfaces. Internally, the notochordal surface is pitted and rugose. This texture extends onto its anterior and posterior margins. The finished external surface bears clusters of minute pits.

The ventral surface of the intercentrum is thickest along its anterior and posterior margins. A low ridge runs in the sagittal plane along the ventral surface of the element and demarcates the zone of fusion between the two halves of the intercentrum during ontogeny. In immature individuals (CMNH 11231, 11073 and 11092, for example), the intercentra were in the process of fusing at the time of death, for a line of weakness is present between adjacent halves (figure 5).

Paired intercentra are not restricted to *G. burkemorani*. Steen (1937) described paired intercentra in *Acanthostoma*, Howie (1972, figure 3) illustrated paired vertebral elements in *Rewana*, and Parrington (1948) described a series of six lydekkerinid intercentra that were split along the midline. Romer (1947, p. 65) did not believe that intercentra were paired: 'There is ... no evidence of more than two types of arcualia in a segment – anteriorly an intercentrum (never, as far as known, paired) ...'. However, it is now evident, both ontogenetically and phylogenetically (in osteolepiform fish with so-called apsidospondylous vertebrae, all vertebral elements are paired), that the intercentrum forms from two centres of ossification. This pairing is rarely observed in early tetrapods because co-ossification of the two antimeres probably occurred very early in development. Time of fusion of the intercentrum may depend upon the functional requirements of the given taxa (e.g. terrestriality) and/or their absolute adult size (Hanken 1982).

Hook (1983) has shown that the ventromedially situated ridge in *C. scutellatus* is flanked by two lesser ridges that mark the roots of the ascending processes. In *G. burkemorani*, however, these lesser ridges are not present on anterior presacral intercentra. Instead, this area is occupied by a posterolaterally directed tubercle (figure 6*a–c*). In more posterior segments, the tubercles diminish in size and are replaced by the aforementioned ridges. These tubercles may serve to differentiate between anterior and posterior presacral intercentra in colosteids. Tubercles on anterior intercentra are also present in *Trimerorhachis* (Case 1935) and *Dendrerpeton*, and they may be homologous with those seen on anterior presacral intercentra in *Proterogyrinus* (Holmes 1984) and *Archeria* (R. Holmes, personal communication). The functional significance of these tubercles is uncertain but they may have been the site of origin of hypaxial musculature.

The periosteal bone above the tubercles or lesser ridges is drawn out to form a posterolaterally directed semicircular articular face that received the capitulum of the rib. The parapophyses are well developed on anterior presacral intercentra, extending laterally up to 4 mm. The lateral exposure and overall surface area of these facets diminishes posteriorly, reflecting the concomitant decrease in the length of the transverse processes posteriorly. In *G. burkemorani*, the height of the ascending processes increases towards the sacrum.

The sacral intercentrum is not completely exposed in any specimen. Caudal intercentra in *G. burkemorani* are similar to posterior presacral intercentra (figures 1*a* and 7*c*). The first five caudal intercentra do not develop haemal arches, but do exhibit large parapophyses. Caudal intercentrum six appears to bear the last rib facet and the first haemal arch, which develops along the posterior half of the intercentrum's ventrolateral margin. The haemal arch consists of two mesiolaterally flattened shafts, which arise from expanded parasagittal bases. The shafts fuse distally for less than half their total length. The arch is inclined posteriorly at an angle of

PHILOSOPHICAL TRANSACTIONS OF THE ROYAL SOCIETY B BIOLOGICAL SCIENCES

about 50° from the horizontal. The base of the first haemal arch is only slightly longer (anteroposteriorly) than half the ventral length of the intercentrum. The anteroposterior length of the arch base increases rapidly to three quarters of the length of the intercentrum on caudal eight and nine. Thereafter, the base gradually decreases in length.

Immediately below the base of each haemal arch, the shaft is gently constricted in lateral view. Further distally, it expands before terminating in a bluntly pointed tip. Beyond caudal 15, the haemal arches are not well preserved in any specimen.

The pleurocentra of *G. burkemorani* (figure 6*g–i*) are easily distinguished from broken or crushed intercentra by a number of diagnostic features. Viewed laterally, a pleurocentrum resembles an elongate wedge: widest dorsally and tapering ventrally to a point, either blunt or acuminate. In a number of adult specimens, opposing halves of one pleurocentrum, in the anterior presacral region, appear to have abutted ventrally and perhaps dorsally as well. It is possible that pleurocentral cartilage formed a broad contact beneath the spinal cord, as proposed for *Eryops* (Moulton 1974). The anterior and posterior margins of a pleurocentrum are formed by prominent bands of pitted and rugose unfinished bone, continuous with the internal or notochordal surface. In lateral aspect, a concave strip forms a shallow trough of periosteal bone that runs from the anterodorsal corner, posterior to the articular facet for the pedicel of the neural arch, then tapers ventrally to terminate along the ventromesial margin of the element. The dorsomesial margin of the pleurocentrum displays a tiny notch or groove, finished wih periosteal bone, which runs in an anteroposterior direction (figure 6*h*). Lying ventromesial and perpendicular to the groove for the spinal nerve, this notch probably marks the lateral limit of the floor for the neural canal. In life, the floor of the neural canal must have been cartilaginous.

The conspicuous articular facet on the dorsolateral side of the pleurocentrum faces anterodorsally at an angle of about 45° from the horizontal. This broad facet receives the complementary articular surface on the pedicel of the neural arch.

The basic structure of the pleurocentrum is similar thoughout the column (figure 7). The largest pleurocentra are those in the anterior presacral region. Here contralateral halves formed large crescents, which probably abutted ventromedially. Further posteriorly, their acuminate ventral margins were probably prevented from meeting along the midline by longer intercentra. The dorsolateral margin of the articular facet that accommodates the pedicel of the neural arch on the anterior presacral pleurocentra is protuberant, whereas further posteriorly it decreases in lateral exposure. On caudal pleurocentra, this facet is significantly smaller, displaying a triangular rather than a rectangular outline in dorsolateral view. Some pleurocentra in *C. scutellatus* (Hook 1983), *Neldasaurus* (Chase 1965), and a trimerorhachoid from the Upper Pennsylvanian of Kansas (Chorn 1984), display a reflected demifacet on the anterolateral margin below the articular facet that presumably shared with the intercentrum in the support of the capitulum of the rib. Such a facet is unknown in *G. burkemorani*.

The neural arches of *G. burkemorani* are characterized by strikingly broad pedicels and transverse processes that bear broad diapophyses distally. The transverse width between diapophyses in the anterior presacral region is twice the overall arch height (figure 7*a*, *d*). Posteriorly, the widths of the processes diminish gradually to equal the height of the arch in the immediate presacral region. Behind the sacrum the spines increase in height, whereas the transverse processes are further reduced. Viewed posteriorly, the pedicels and transverse processes sweep ventrolaterally below the zygapophyses. Beyond the pedicels

PHILOSOPHICAL TRANSACTIONS OF THE ROYAL SOCIETY B BIOLOGICAL SCIENCES

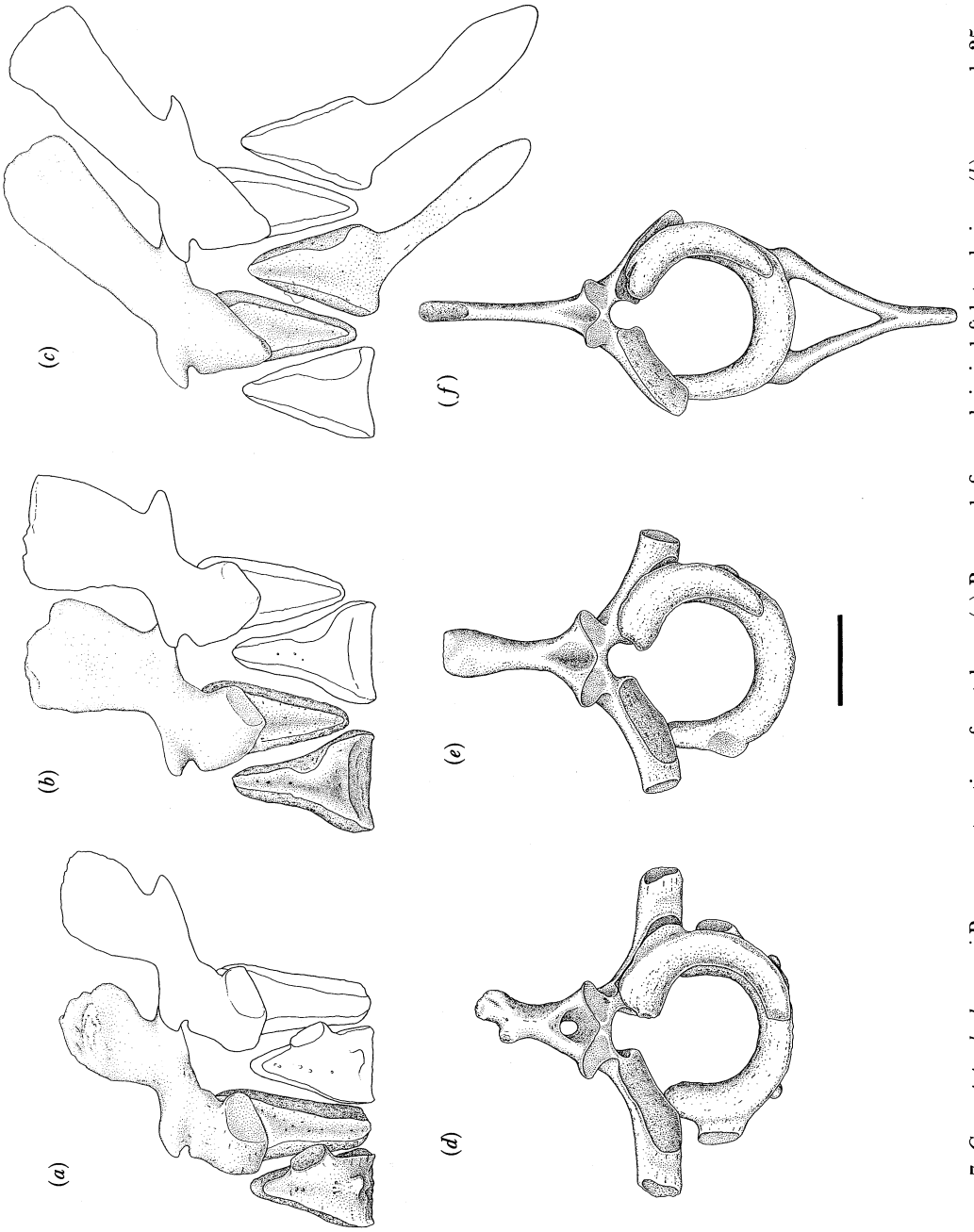

FIGURE 7. *Greererpeton burkemorani* Romer, restoration of vertebrae. (*a*) Presacrals five and six in left lateral view; (*b*) presacrals 35 and 36 in lateral view; (*c*) caudals five and six in left lateral view; (*d*) presacral five in posterior view; (*e*) presacral 35 in posterior view; (*f*) caudal six in posterior view. Scale bar 1 cm.

PHILOSOPHICAL TRANSACTIONS OF THE ROYAL SOCIETY B BIOLOGICAL SCIENCES

the transverse processes are directed laterally or slightly posterolaterally. The dorsal surface of the transverse processes are gently concave in posterior view. In dorsal aspect, the pedicels and transverse processes are curved posterolaterally. As a result of this curvature, the diapophyses face posterolaterally. Immediately below the anterior zygapophyses, on the ventral surface of the arch, are the gently concave articular facets of the pedicels. They face posteroventrally and are angled to receive the anterodorsally directed facets on the pleurocentrum. The rectangular-shaped facets cover the entire ventral surface of the pedicel and are usually slightly larger than the facets on the pleurocentrum. Below the anterior and posterior zygapophyses, and mesial to the pedicels, is the tubular groove for the spinal cord (figure 7*d–f*). This cylindrical groove is open ventrally, but was presumably completed with cartilage in life. A relatively thin, essentially vertical strip of bone, lateral to the neural canal, joins the pedicels and transverse processes to the anterior zygapophyses and dorsal segment of the neural arch. The dorsomesially facing prezygapophyses and ventrolaterally facing postzygapophyses of all presacral and most caudal arches form an angle of between 20° and 30° with the horizontal. In lateral view, each prezygapophysis is tilted to face anterodorsally, the long axis making an angle of about 20° with the horizontal plane. The posteroventrally facing postzygapophyses are inclined a similar amount. Viewed dorsally, the long axes of the diverging pre- and postzygapophyses form an angle of about 40° with the sagittal plane.

The anterior presacral neural spines in *G. burkemorani* show a supraneural space above the neural canal. A horizontal shelf of bone that runs from mid-prezygapophyses to mid-postzygapophyses extends between the two halves at the level of the zygapophyses, separating the dorsal space from the neural canal (figure 7*d*). The canal closes in the mid-thoracic region, leaving depressions, probably for the insertion of an intervertebral ligament (figure 7*e*).

The height of the neural spines increases gradually by one third from the front of the column to the back. Their maximum height is attained in the area between caudal two and seven. Although most presacral neural spines are inclined only slightly posteriorly (the anterior margin forms an angle of about 10° from the vertical), the spines of posterior presacral and caudal vertebrae become progressively more posteriorly inclined (beyond caudal four the spines form an angle of about 40° with the vertical).

The atlas–axis complex

Portions of the atlas–axis complex are preserved in several specimens, the most complete of which is CMNH 11090. The atlas–axis complex of *G. burkemorani* (figure 7) is basically similar to that of *Gephyrostegus* (Carroll 1970), *Proterogyrinus* (Holmes 1984), and *Eryops* (Moulton 1974).

Proatlantal arches are preserved in CMNH 11090 and 11079. Each proatlas is half a small neural arch with its long axis running anterolaterally and posteromesially (figure 8*b*). An anterolaterally directed tubercle bears a facet on its anterior margin which abutted against the posterodorsally directed articular surface on the exoccipital. Posterior to the proatlantal facet, the tubercle is gently constricted before giving rise to the main body of the proatlas. There is no evidence to show that the proatlantes were fused medially. They may have been held in position by cartilage, connective tissue, or muscle. Below the main body of the proatlas, a relatively large subcircular and gently concave articular facet receives the atlas prezygapophysis.

The atlas of *G. burkemorani* is composed of five elements: a paired neural arch, two pleurocentral ossifications and an intercentrum that is paired in immature individuals. In

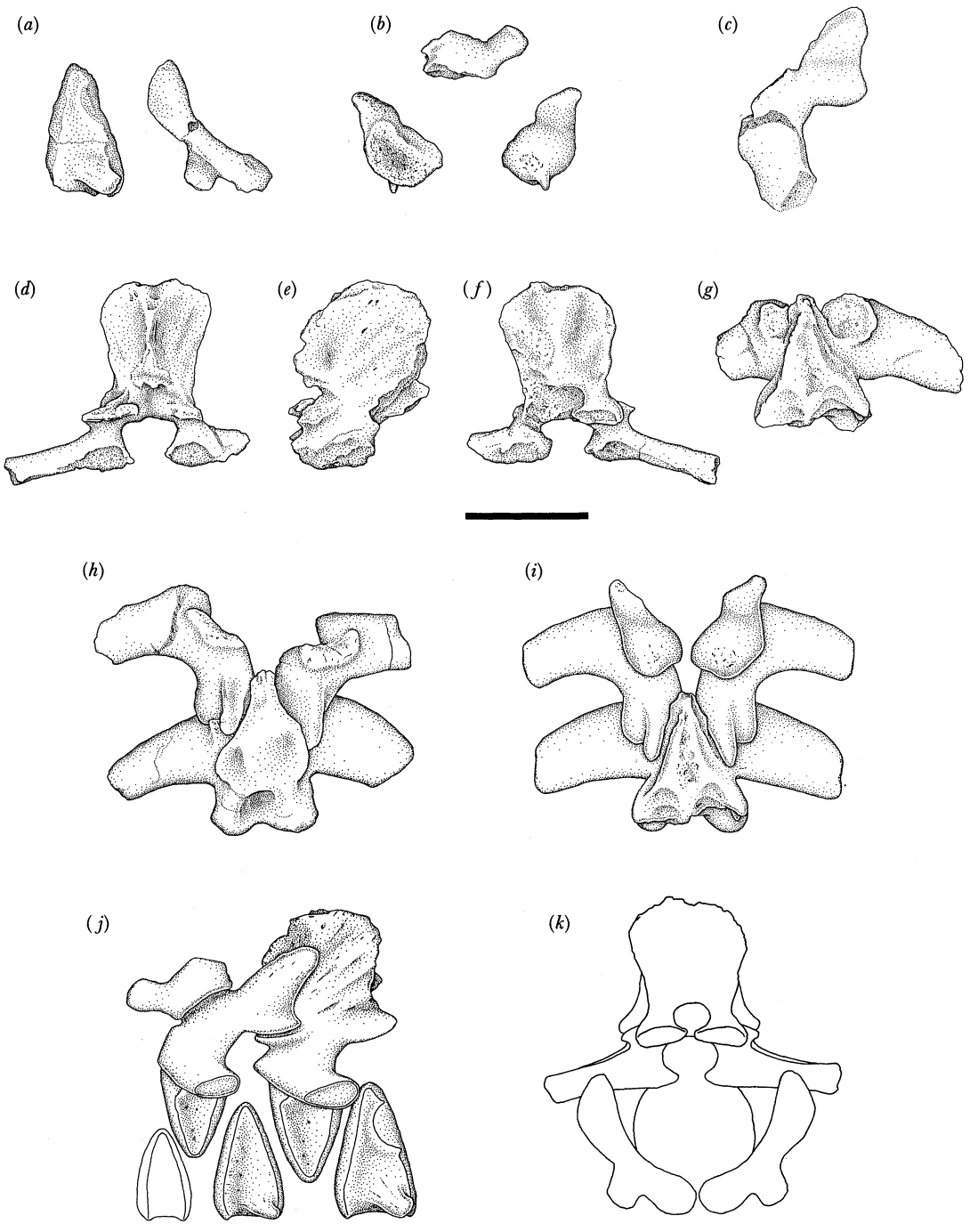

FIGURE 8. *Greererpeton burkemorani* Romer, elements of the atlas–axis complex. (*a*) The left half of the axis intercentrum of CMNH 11132 in lateral and posterior views; (*b*) the right proatlas of CMNH 11090 in lateral, ventral, and dorsal views; (*c*) the left atlas of CMNH 11090 in lateral view; (*d–g*) axis of CMNH 11132 in anterior, left lateral, posterior, and dorsal views respectively; (*h*) specimen drawing of the atlas–axis of CMNH 11090 in dorsal view; (*i–k*) restoration of the atlas–axis complex in dorsal, left lateral, and posterior views respectively. Scale bar 1 cm.

PHILOSOPHICAL TRANSACTIONS OF THE ROYAL SOCIETY B BIOLOGICAL SCIENCES

lateral view, each arch half has a small triangular neural spine. The two halves are separate in CMNH 11090, but they may have abutted medially or been held by a cartilaginous shelf immediately above the neural canal. The atlas arch is similar to thoracic arches except that the spines are always separate to accommodate the anterior margin of the axis neural spine. Viewed anteriorly, the spines are wedge-shaped, tapering dorsally. They are inclined posterodorsally at an angle of about 40° from the horizontal, and rest in shallow grooves on the expanded anterior surface of the axis spine. The relatively large crescentic, dorsally convex prezygapophyses of the atlas arch face anterodorsally to receive the concave articular facets on the proatlantes. The roughly circular postzygapophyses are directed ventrally. In dorsal view, the transverse processes curve gently posterolaterally. Although well-developed diapophyses are present, no atlantal rib has been found in any specimen.

The contralateral halves of the atlantal pleurocentrum are only about half as long as those posterior to the axis. They would not have met beneath the notochord. Although the atlantal intercentrum is incompletely known, it appears to lack parapophyses and is significantly smaller than other intercentra.

The axis arch of *G. burkemorani* is well preserved in CMNH 11079 and 11090. It is a relatively massive structure with an anteroposteriorly elongate spine and greatly thickened dorsal and posterior margins (figure 8*d–g*). The spine projects beyond the anterior margin of the prezygapophyses in a long sweeping curve between the atlantal arch halves. A 'sagittal crest' arises on the thick dorsal border of the spine and becomes more pronounced on the expanded posterior border, gradually attenuating, however, to a small ridge posteroventrally. On either side of the ridge are two deep trough-like depressions, with one usually more pronounced than the other. These grooves are bordered laterally by large ridges, which form the dorsolateral and posterolateral margins of the axis spine. The lateral ridges attenuate just above the dorsal surface of the postzygapophyses. In dorsal view, the spine is distinctly triangular in outline as the lateral margins diverge posteriorly. The angle formed between the lateral margins of the spine is variable, but it appears to be correlated with the overall size of the skull. It ranges from about 50° in CMNH 11090, 11132, and 11068 to about 60° in the very largest axis known: CMNH 11240. The configuration of the neural spine, including its system of ridges and depressions, is probably associated with the insertion of neck musculature, probably the spinalis capitis (Holmes 1984). The central ridge quickly loses prominence as it passes ventrally along the posterior margin where it vanishes immediately above a circular depression. The circular fossa lies mesial to and slightly above the postzygapophyses. This depression is probably the site of origin of the supraneural ligament. A small depression on the anterior margin may have been the site of insertion of the ligament from the occiput. In CMNH 11090, the posterior fossa is bordered below by a medial shelf of bone between the postzygapophyses. The lateral surface of the axis neural spine is conspicuously striated.

The axis prezygapophyses are circular in outline when viewed dorsally, are buttressed from below, and extend only slightly onto the anterolateral surface of the spine. Unlike the prezygapophyses of more posterior vertebrae, they face slightly antero-dorsolaterally instead of antero-dorsomesially.

The neural canal is broadly oval when viewed anteriorly. The area between the ventral margins of contralateral pedicles is open, but may have been joined by cartilage in life.

Although the axis pleurocentrum is larger than the atlantal pleurocentrum, it is still smaller than most pleruocentra along the column. The axis intercentrum is only slightly smaller than

PHILOSOPHICAL TRANSACTIONS OF THE ROYAL SOCIETY B BIOLOGICAL SCIENCES

other anterior intercentra. It resembles the atlas intercentrum in that it lacks parapophyses, but it does bear the prominent posterolaterally directed tubercles characteristic of anterior presacral intercentra.

Ribs

The salient features of the presacral ribs in *G. burkemorani* are best seen in CMNH 11090 and CMNH 11068 (figures 3, 4 and 9). Even though rib morphology does not vary greatly from the front of the column to the back, regional variation in relatively complete specimens appears to be consistent, and the approximate position of an isolated rib can be inferred from its anatomy. Although no specimen preserves all the ribs, the presence of parapophyses and diapophyses confirms that they extended to caudal vertebra six (figure 1).

In general, the ribs are flattened proximally, with a mid-shaft cross section that is roughly semicircular in anterior presacrals to circular in posterior presacrals. The ribs are relatively short and, for the most part, only gently curved ventrally. On their posterior margin, between one half and one third of the way along the shaft, a prominent stiletto-like uncinate process may develop.

Although the atlantal ribs are not preserved in any specimen, they were probably much like those articulating with the axis and with the third vertebra. These anteriormost ribs are morphologically simpler and more gracile than other anterior presacral ribs. The tubercular facet is well developed and articulates with the broad surface of the diapophysis, whereas the capitulum appears to have been absent. The head of these ribs is slightly compressed dorsoventrally, the shaft is circular in cross section along its entire length, and no uncinate process has developed. The shaft of these ribs is gently curved at their midpoint (figure 9*a*).

Starting with the ribs on the fourth vertebra, the distal end expands to form a flattened blade that is twisted with respect to the proximal head. The torsion along the shaft causes the topologically dorsal surface of the distal portion of the rib to be directed anteriorly. Thus when the ribs are in articulation with the vertebrae and viewed dorsally or laterally, the extent of distal flair is not fully evident (figure 1). Posteriorly, in the anterior presacral region, the distal ends of the ribs become progressively wider and reach a maximum between the ninth and thirteenth vertebra. Thereafter they gradually decrease, until their shafts are cylindrical from the twentieth to the twenty-fifth vertebra. In large individuals, the anterior presacral ribs appear to have proportionately greater expansion distally than in subadults. Unfortunately, this can not be confirmed because of lack of juvenile articulated postcranial remains. The concave ventral (posterior) surface of these ribs often bears faint longitudinal striae (figure 9*e*), whereas the convex external (anterior) surface is usually unmarked.

The articular heads of the ribs from the fourth to at least the twenty-fifth vertebra are conspicuously bicipital and separated one from another by up to 5 mm (figure 9*b–h*). Viewed mesially, the capitular facet is ovoid in outline and the tubercular facet is shaped like a teardrop. The web of bone between the two facets is often compressed into a narrow ridge. In posterior trunk, sacral, and caudal ribs, the mesial outline of the proximal articular head is roughly in the shape of a figure **8**, with both articular surfaces being confluent. In these ribs, the capitulum no longer has a greater mesial projection than the tuberculum. This reflects the reduction in length of the transverse processes on posterior neural arches.

In all presacral ribs, the line that runs through the long axis of the capitular and tubercular facets lies in the plane of the shaft which is drawn out to form the uncinate flange. It appears

PHILOSOPHICAL TRANSACTIONS OF THE ROYAL SOCIETY B BIOLOGICAL SCIENCES

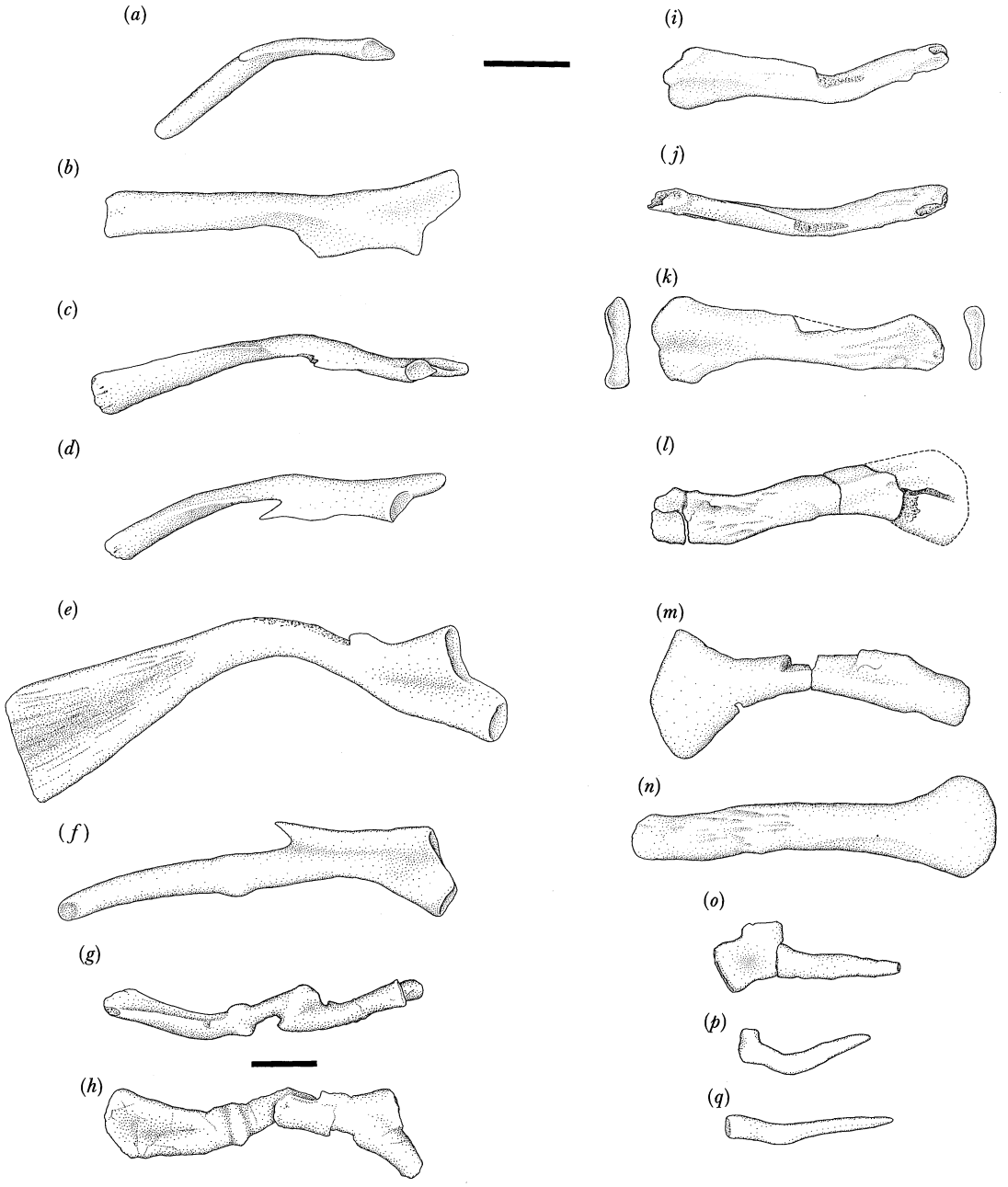

FIGURE 9. *Greererpeton burkemorani* Romer, specimen drawings of ribs. (*a*) Left axis rib of CMNH 11090 in posterior view; (*b*) left presacral six of CMNH 11090 in anterodorsal view; (*c*) left presacral seven of CMNH 11090 in posterodorsal view; (*d*) left presacral 7 of CMNH 11090 restored, dorsal view; (*e*) left presacral 11 of CMNH 11068 in posterior view; (*f*) left presacral 24 (?) slightly restored, posteroventral view (rib shows evidence of a fracture); (*g*, *h*) right anterior presacral rib of CMNH 11319 in posterodorsal and anterolateral views respectively (this rib was badly broken and fractured before death) (*i–k*) left sacral (?) or immediate presacral rib of CMNH 11090 in dorsal, posterodorsal, and anterolateral views respectively; (*l*) right sacral rib of CMNH 11090 in anterolateral view; (*m*, *n*) left and right sacral ribs of CMNH 11068 in anterolateral views; (*o*) right postsacral five (?) of CMNH 11090 in mesial view; (*p*, *q*) right and left postsacral six (?) of CMNH 11090 in mesial and lateral views respectively. Scale bar 1 cm.

PHILOSOPHICAL TRANSACTIONS OF THE ROYAL SOCIETY B BIOLOGICAL SCIENCES

as though all presacral ribs (excluding the first three cervical ribs) bore an uncinate flange. Because the uncinate flanges are so delicate few remain intact. For this reason, it is impossible to ascertain the extent to which ribs developed an uncinate process extending beyond the posterolateral margin of the uncinate flange. Flanges or processes from adjacent ribs were not nearly broad enough to effect an overlap. In *G. burkemorani* (figure 1*c*), the mesiolateral length of the flange increases from front to back along the column. The distance from the mesial margin of the tuberculum to the point where the flange merges with the shaft distally is approximately 1.5 cm on presacral six. Further back (presacral 25), this distance increases to 1.8 cm. Rib length also increases over this interval from about 4.0 cm in presacral six to about 4.5 cm in presacral 25. From presacral 30, overall rib length decreases to 3.4 cm at the sacrum in CMNH 11090.

Although the sacral region is well preserved in several specimens, a single pair of sacral ribs has been identified in CMNH 11090 and 11068 only (figure 9*k–n*). In CMNH 11068, the head of the sacral rib is expanded. Although the proximal articular surface is obscured by matrix there appear to have been two poorly differentiated facets. They appear to be slightly larger, but otherwise similar to those of other presacral ribs. The shaft of the rib immediately distal to the proximal head is gently constricted. In lateral view, the shaft expands somewhat beyond the constriction before tapering distally. No uncinate flange or process is present. The external surface of the shaft presents a flattened face, bearing longitudinal striations that presumably mark the site of ligamentous attachment to the ilium. The sacral rib is gently curved posteriorly along its entire length.

The relatively unspecialized sacral rib of *G. burkemorani* is markedly different from the short and stout rib preserved in some anthracosaurs, such as *Proterogyrinus* (Holmes 1984), *Archeria* (Holmes 1989) and *Eogyrinus* (Panchen 1966), and most microsaurs (Carroll & Gaskill 1978). In these forms, the distal end of the sacral rib abuts perpendicular to the ascending shaft of the ilium, whereas in *G. burkemorani* the ilium merely lies along the lateral margin of the posterolaterally directed rib.

Anterior caudal ribs are similar to the presacral ribs immediately in front of the sacrum. The presence of the uncinate processes could not be determined. The first five pairs show very little curvature along their entire length, whereas the last pair of caudal ribs sweep dorsally (figure 9*p*). A capitulum and tuberculum develop on some caudal ribs (figure 9*o*). The last three pairs of ribs in CMNH 11090 decrease rapidly in length, the last of them measuring only 15 mm in length (or about 56% of the length of the sacral rib).

Scales

At least two types of dermal ossification covered much of the body of *G. burkemorani*. By far the most prominent type is the gastralia; these clothe the underside of the body and appear to continue on to the lower half of the flanks. The entire dorsal body surface, including the upper flanks, appears to have been covered with ovoid scales.

The gastralia of *G. burkemorani* resemble the dorsal and ventral scales of *C. scutellatus* in possessing crenulate to punctate posterior margins (Hook 1983) (figure 10). The squamation pattern of the gastralia, clearly *en chevron*, is well preserved in many specimens. The main sequence of gastralia begins on the posteroventral surface of the interclavicle as an anteriorly directed chevron. All gastralia subjacent to the interclavicle rabbet onto its lightly sculptured

PHILOSOPHICAL TRANSACTIONS OF THE ROYAL SOCIETY B BIOLOGICAL SCIENCES

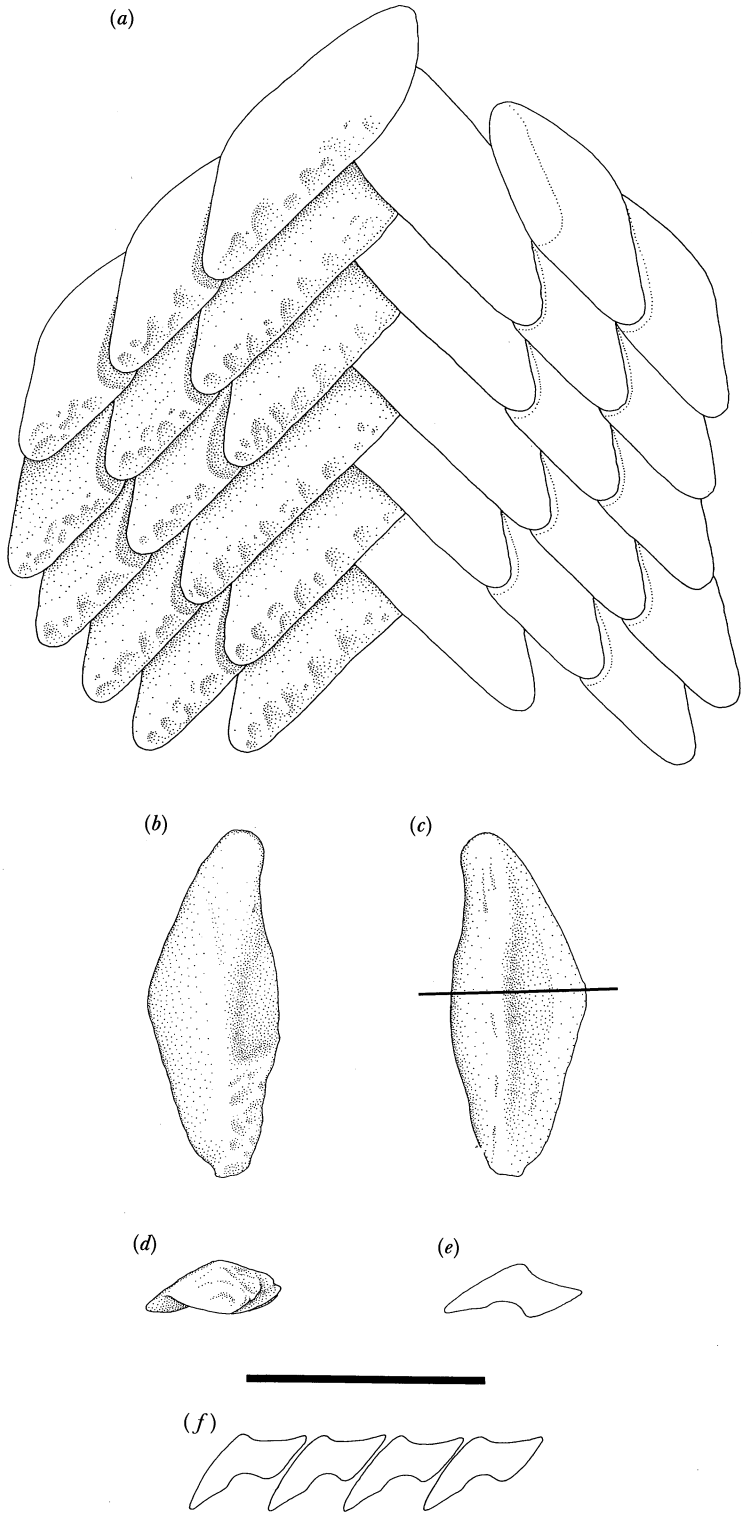

FIGURE 10. *Greererpeton burkemorani* Romer, gastralia. (*a*) Restoration of a small portion of the gastralia adjacent to the ventral midline; (*b–d*) details of one ventral scale in anteroventral, posterodorsal and posterolateral views respectively; (*e*) cross section of one scale (as sectioned in (*c*)), visceral surface is down; (*f*) four sectioned scales from adjacent rows of gastralia showing the pattern of overlap, ventral surface is up. The concave ventral margin receives the overlap of its mesial neighbour. Scale bar 1 cm.

PHILOSOPHICAL TRANSACTIONS OF THE ROYAL SOCIETY B BIOLOGICAL SCIENCES

ventrolateral and posteroventral margin. Immediately behind the pectoral girdle the posterolaterally trending rows of gastralia are formed by nine to eleven scales. The number of scales per row does not appear to increase posteriorly. Anteriorly, the opposing rows of scales meet at approximately 90° along the ventral midline (figure 10*a*). The angle may slightly decrease posteriorly. As in most early tetrapods with extensive ventral squamation, the rows abut medially in a staggered pattern, with the scales interlocking along the apex of the chevron. The largest gastralia are found among those that interlock along the midline.

Behind each clavicle and anterior to the main sequence of gastralia are a series of scales absent or undescribed in *C. scutellatus* or *P. pisciformis*, but present in *Chelydosaurus* (Fritch 1889, figure 129). They are similar to other gastralia, although most are somewhat smaller. The rows immediately behind the right clavicle are directed obliquely posteriorly towards the left-hand side of the body, whereas those behind the left clavicle are directed towards the right-hand side. In essence, these scales match those of the main sequence on the contralateral side (figure 3*a*). There are at least seven rows of these scales per side, with approximately seven scales per row. In *C. scutellatus* these scales appear to be absent, with the squamation of the main sequence forming an unbroken pattern along the ventrolateral margin of the interclavicle.

The morphology of a gastralium is relatively complex. In ventral view, most are roughly rhomboidal in outline. A section of a scale in a parasagittal plane would show that they are wedge-shaped, with the base of the wedge forming the exposed sculptured surface and the apex projecting anterodorsally, into the dermis in life. In addition to the sculptured face, each scale bears four 'articulating facets' which have varying degrees of contact with adjacent gastralia. The anteromesial facet is gently concave and underlaps the posterolateral facet on the trailing edge of its mesial neighbour. The antero-ventrolateral surface of each scale (figure 10*b*) is unsculptured, gently convex, and forms a broad area of contact for the visceral surface of the trailing edge of an adjacent scale from the preceding row (illustrated in a 'parasagittal' section, figure 10*f*). Running lengthwise along the visceral and ventral surface of each scale is a fairly pronounced ridge. In each row, the sculptured trailing edge of individual scales appears to be

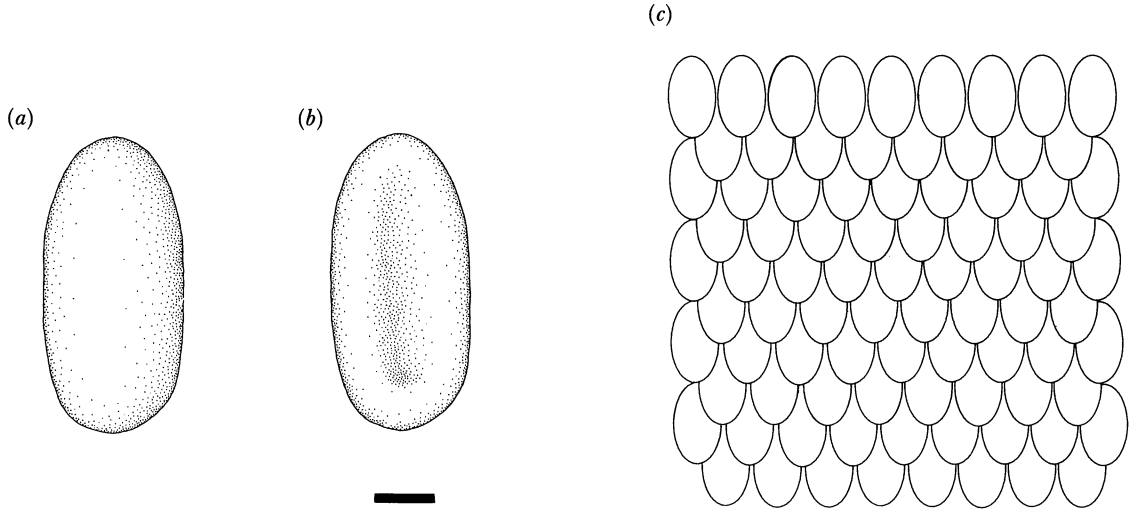

FIGURE 11. *Greererpeton burkemorani* Romer, dorsal squamation. (*a*, *b*) A single dorsal scale in dorsal and visceral views respectively; (*c*) a restoration of the 'shingled' scalation pattern. Scale bar 1 mm for (*a*) and (*b*).

PHILOSOPHICAL TRANSACTIONS OF THE ROYAL SOCIETY B BIOLOGICAL SCIENCES

reduced in degree and length of exposure further laterally. It is difficult to establish the pattern of squamation along the flanks because no unbroken series of gastralia grading into dorsal scales has been found. The gastralia-like pattern of dorsal squamation in *C. scutellatus* (Hook 1983) has not been seen in any specimen of *G. burkemorani*.

The remainder of the body appears to have been covered by small subcircular scales, well preserved in CMNH 11082 (Romer 1972, figure 3). In most specimens, these scales rarely retain a regular pattern, having been widely scattered after death. They are about 0.5 mm thick, generally 2 mm long and 1–1.5 mm wide, forming elongate ovals (figure 11). In dorsal view each scale is gently convex, whereas in ventral view an elongate groove extends almost its entire length. The groove is generally deeper at one or both ends. The pattern of overlap of the dorsal scales, as restored in figure 11*c*, resembles a shingled roof.

The appendicular skeleton

As noted in the Introduction, the limbs of *G. burkemorani* are relatively small compared with the length of the skull. In mature individuals, the pectoral and pelvic limbs are only about 60 % and 80 % respectively of the length of the skull. The marked difference between the relative lengths of the pectoral and pelvic appendages is attributed to the difference in the length of the propodials. The humerus in adults is only about 60 % of the length of the femur, whereas the antebrachium and crus are usually about the same length.

Despite the proportionately small limbs of *G. burkemorani*, the scapulocoracoids are well ossified in several individuals. Large coracoid plates are preserved in CMNH 11090, CMNH 11068 and CMNH 11319 (figures 3, 4 and 12*g*). The scapulocoracoid may be conveniently subdivided into two areas: the vertical scapular moiety and the horizontal plate-like coracoid, which has about twice the surface area of the scapula. The following description is based on the left scapulocoracoid. The unfinished dorsal margin of the scapula suggests that a cartilaginous suprascapula was present in life. In all specimens, the anterior margin of the scapula is also unfinished and presumably continued by cartilage in life. There is no evidence of more than one centre of ossification to the scapulocoracoid.

The visceral surface of the scapular portion is broadly concave (figure 12), formed by a wide, vertically oriented strip of finished bone that turns mesioventrally to form the anterior portion of the coracoid plate. The mesial and posterior surfaces of the scapula are separated by a modest ridge that sweeps ventroposteriorly from the unfinished posteromesial dorsal corner, becoming less distinct ventrally. The ridge curves mesially, tapering as it continues on to the horizontal dorsal surface of the coracoid plate. The base of this ridge bisects the coracoid plate into anterior and posterior parts.

In lateral view, the anterior border of the scapula is convex, whereas the posterior margin is strongly concave. The posterolateral margin of the concave area is formed by a ridge of equivalent size to the mesial ridge. It is attenuated somewhat as it curves posteroventrally to form the dorsolateral margin of the glenoid fossa. The area between these ridges is gently excavated, or trough-like dorsally; ventrally this area becomes increasingly convex as the bone thickens to buttress the glenoid fossa from above (figure 12*b*, *i*). Anterior to the thickened posterior border, the blade rapidly tapers to a thin plate along its margin. No supraglenoid foramen is present in any specimen. In most specimens, the vertical scapular portion of the scapulocoracoid is all that is ossified or preserved (CMNH 11070 and CMNH 11240, figure

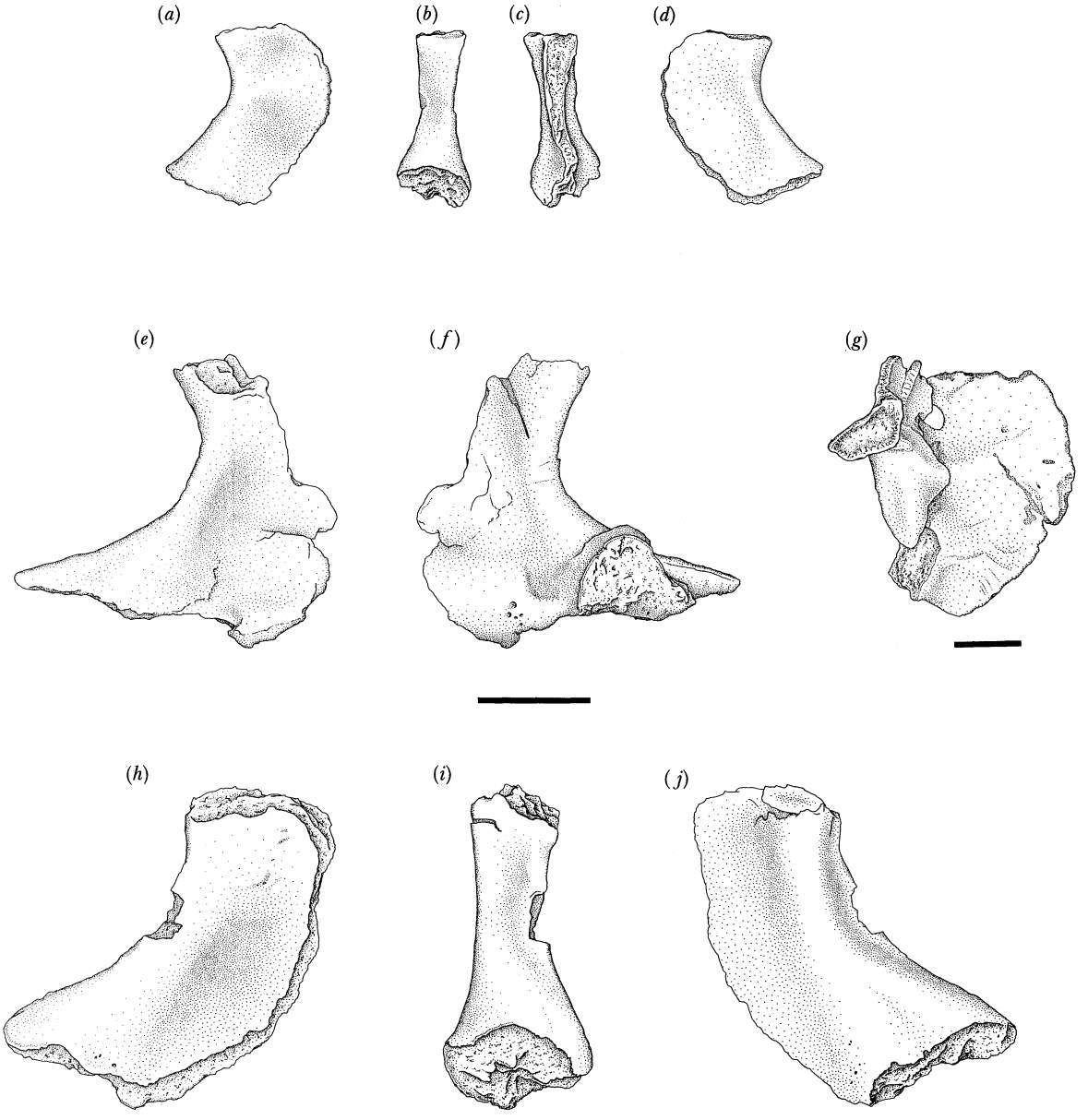

FIGURE 12. *Greererpeton burkemorani* Romer, specimen drawings. (*a–d*) The left scapulocoracoid of CMNH 11070 in mesial, posterior, anterior and lateral views respectively; (*e–g*) the left scapulocoracoid of CMNH 11319 in mesial, lateral and dorsal views respectively; (*h–j*) the left scapulocoracoid of CMNH 11240 in mesial, posterior and lateral views respectively. Scale bars 1 cm.

12 *a–d*, *h–j*). In lateral view, this crescent-like strip of bone provides no information on the size or shape of the glenoid fossa, nor of the foramina that pierce the coracoid plate. This relatively small section of the scapulocoracoid is often all that is preserved in other temnospondyl amphibians (see, for example, *Neldasaurus* (Chase 1965) and *Trimerorhachis* (Case 1935)).

The posterolateral margin of the scapulocoracoid (or the posterolateral border of the coracoid plate) is thickened, to provide support for the glenoid. If a line running along the mesially directed ridge on the coracoid plate were extended laterally it would mark the anterior

margin of the glenoid surface. Little detail of the glenoid fossa is preserved, and it appears to have been covered by a layer of cartilage in life. The concave articular surface is anteroposteriorly elongate, roughly 'teardrop' to ovoid in outline. This articular fossa, which shows no twisting along its length, would have received the convex head of the humerus.

The coracoid plate is remarkably large when compared with the size of the scapula. In dorsal aspect it is semicircular in outline, with its curved margin directed mesially. It extends from the anterior junction with the vertical scapular blade, back to buttress the posterior border of the glenoid surface (figure 13). The ventral face of the plate is finished with smooth periosteal bone. Two small foramina pierce the coracoid plate along its lateral margin. The supracoracoid foramen passes ventrolaterally through the thin curving strip of bone joining the scapular blade to the anterior coracoid plate. The glenoid foramen pierces the thickened bone just mesial to the midpoint of the glenoid.

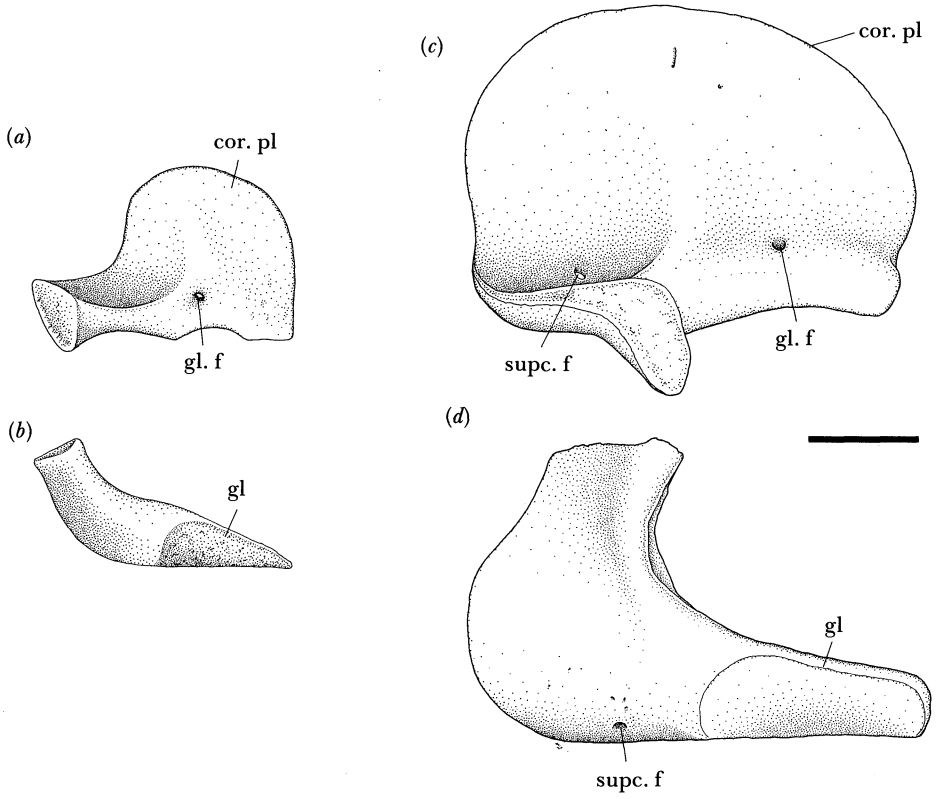

FIGURE 13. *Greererpeton burkemorani* Romer, restorations of the left scapulocoracoid. (*a*, *b*) CMNH 11090 in dorsal and left lateral views respectively; (*c*, *d*) CMNH 11319 in dorsal and left lateral views respectively. Scale bar 1 cm.

The large number of other anatomical similarities between *G. burkemorani* and its close relative *C. scutellatus* suggest that the element labelled as a cleithrum by Hook (1983, figure 12*c*, AMNH 6917) is probably its scapulocoracoid. The scapulocoracoid of *G. burkemorani*, figured by Romer (1969, figure 7) is actually a humerus, whereas the figured right radius is the scapular portion of its right (?) scapulocoracoid.

PHILOSOPHICAL TRANSACTIONS OF THE ROYAL SOCIETY B BIOLOGICAL SCIENCES

The dermal pectoral girdle

The dermal pectoral girdle of *G. burkemorani* consists of a ventromedial interclavicle, a pair of ventrolateral clavicles that abut against the interclavicle, and a pair of dorsolateral cleithra that rest against the ascending horns of the clavicles. These elements are present in nearly complete form in many specimens, notably CMNH 11090. As restored in figure 14, the shape of the pectoral girdle is very similar to that of *C. scutellatus* (Hook 1983, figure 11*b*) and other temnospondyls, including trimerorhachids and metoposaurs. The ventral dermal girdle of *G. burkemorani* formed a broad thoracic shield, as its anterior end extended forward beneath the

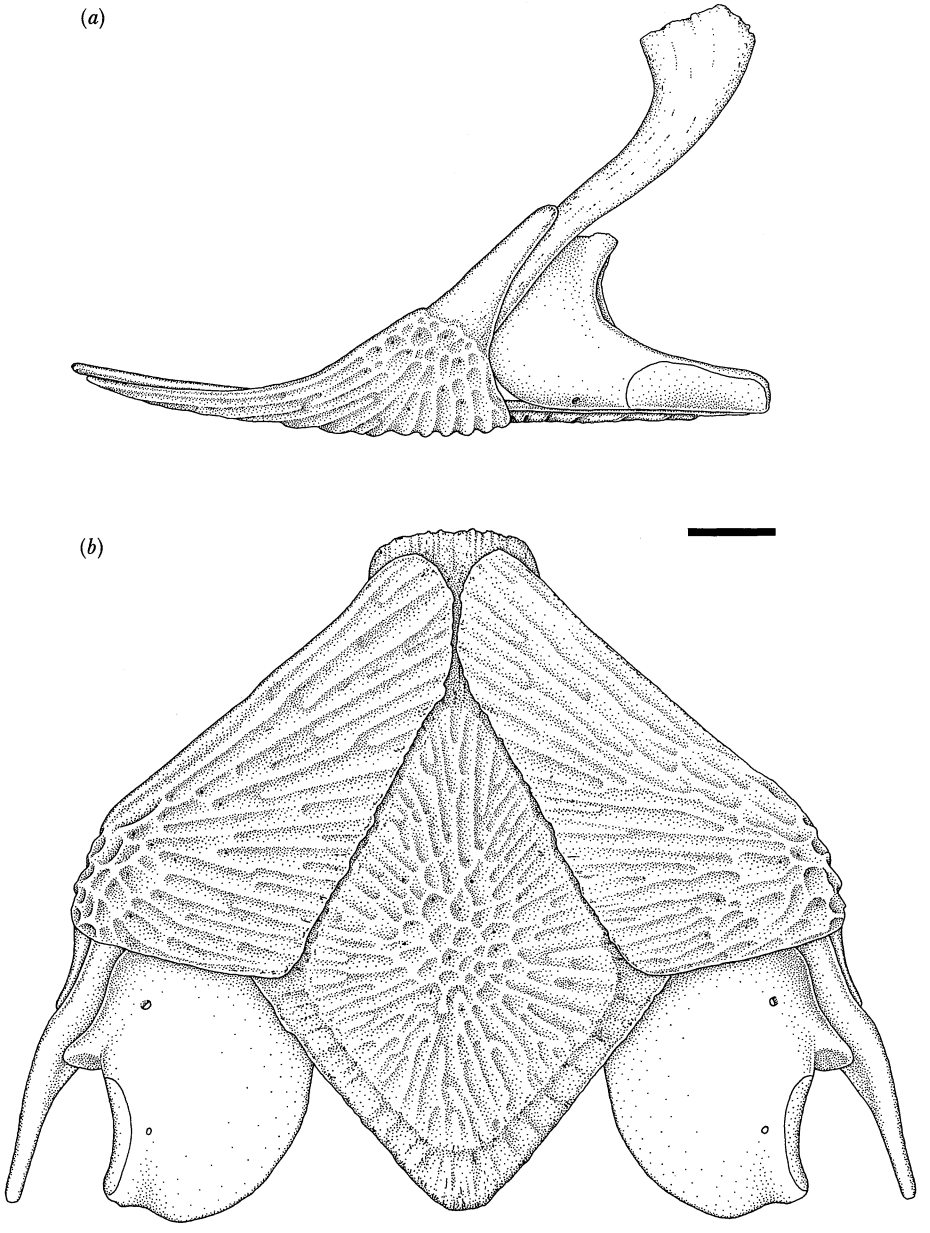

FIGURE 14. *Greererpeton burkemorani* Romer, restoration of the pectoral girdle based on CMNH 11090. (*a*) Left lateral view; (*b*) ventral view. Scale bar 1 cm.

PHILOSOPHICAL TRANSACTIONS OF THE ROYAL SOCIETY B BIOLOGICAL SCIENCES

braincase to approximately the level of the anterior end of the 'tubera parasphenoidales'. The clavicales meet anteriorly below the interclavicle with the clavicular stem angled postero-laterally so that the greatest width of the dermal pectoral girdle equals the maximum breadth of the skull.

The ventral surface of the elements forming the dermal pectoral girdle are sculptured with prominent ridges and grooves radiating from their centres of ossification. The pattern of sculpturing on the dermal shoulder girdle, like that of the skull, is reticulate near the centre of ossification, but quickly becomes linear as it radiates outward.

The interclavicle, the largest element in the pectoral girdle of *G. burkemorani*, is essentially rhomboidal in outline throughout life (figure 15). It is dorsally concave, primarily along the anteroposterior axis of the bone. The visceral surface is smooth and generally devoid of marking except for shallow irregular grooves, some of which terminate as foramina entering the bone. The ventral surface of the bone exhibits a diamond-shaped central area bearing the raised dermal sculpture discussed above. The pattern of ornamentation indicates that the centre of ossification is situated about two thirds the length of the interclavicle from the leading edge. Beyond the periphery of the heavily sculptured central area is a margin of lightly striated bone, which thins radially from the centre of ossification. In many specimens, the extent of the interclavicular margin is unknown because the thin edges of the bone were destroyed after

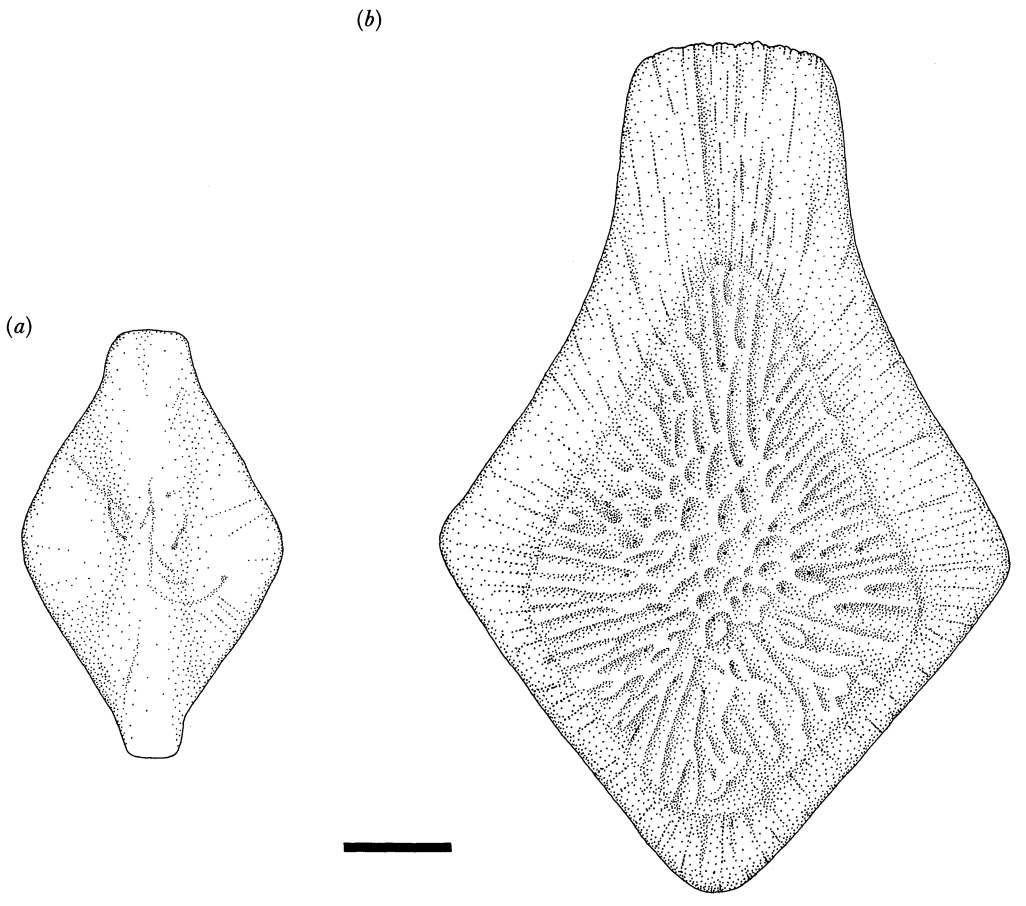

FIGURE 15. *Greererpeton burkemorani* Romer, restorations of the interclavicle. (*a*) CMNH 11320 in visceral view; (*b*) CMNH 11090 in ventral view. Scale bar 1 cm.

PHILOSOPHICAL TRANSACTIONS OF THE ROYAL SOCIETY B BIOLOGICAL SCIENCES

death. In life, this border would have provided a surface for the reception of the clavicles anteriorly and gastralia posteriorly.

The unsculptured, but striated, anteroventral portion of the interclavicle is drawn out to form a broad tongue-shaped plate that occupied a position below the parasphenoid. The significance of such an anterior extension of the pectoral girdle is uncerain, but presumably the fimbriated leading edge was important for the attachment of longitudinal throat musculature (Romer 1947). Posteriorly, the distinct tongue-shaped lappet of *C. scutellatus* (Hook 1983, figure 11) is seemingly absent in adult specimens of *G. burkemorani*, although present in immature individuals. The smallest interclavicle known (CMNH 11320) exhibits remarkable symmetry about a transverse line running through the point of greatest width (figure 15*a*). In CMNH 11320, the visceral surface of the interclavicle is gently swollen sagittally. During ontogeny the interclavicle does not remain symmetrical about its midline transverse axis. The posterior half of the element does not grow as fast as the anterior moiety of the bone. Furthermore, the overall width of this element seems to increase at a proportionately faster rate than does its length. Whether or not these changes reflect mechanical requirements due to an increase in thoracic volume or are related to the increase in the width of the skull table (relative to its length) are impossible to determine at this time.

Clavicles are preserved in a wide size range of individuals, including the tiny CMNH 11095 (Godfrey 1989, figure 2*a*). The reticulate nature of the sculpture pattern on the clavicle indicates that the centre of ossification is at its posterolateral corner, just ventral to the base of the ascending process (figure 16*a*). The lateral edge of the heavily sculptured ventral plate of the clavicle is curved upward for the posterior two thirds of its length. The margin of the sculptured moiety becomes progressively thicker posteriorly to form the support or root of the oblique ascending unsculptured cleithral process. In lateral view, the base of the ascending process is clearly delineated by the abrupt end of the heavily sculptured surface. The ascending spine is composed of a laminar and rod-like portion. The rod-like portion is not seen in lateral view because it lies mesial to the laminar portion. If the left clavicular spine were sectioned in the frontal plane, the letter **P** would describe the resulting outline. The laminar portion is a thin unsculptured plate-like, essentially vertical, extension of the posterolateral ventral clavicular plate. In a medial view, the rod-like portion of the ascending spine becomes progressively more pronounced posterodorsally. The ascending cleithral process forms an angle of about 45° to the gently convex ventral plate. The rod-like portion of the ascending process is devoid of markings except for its tip which is conspicuously striated. The laminar portion merges with the rod-like moiety of the ascending horn distally.

Internally, the clavicle bears only faint striations radiating outward from the centre of ossification toward the mesial border of the bone. The ventral plate thins mesially, and consequently is damaged in most specimens. The mesial margin of the clavicle is usually gently embayed where it abuts against the raised sculptured face of the interclavicle.

As restored by Hook (1983), the posteromesial margin of the clavicles of *C. scutellatus* extends posterior to the widest portion of the interclavicles, to terminate just anterior to the base of the parasternal lappet. On the contralateral posterior surface of the interclavicle, (Hook 1983, figure 11*b*), in the margin of the heavy sculpture are indentations that held the anterior most gastralia. They lie anterior to the posteromesial corner of the right clavicle and suggest that the whole element should be shifted anteriorly. In *G. burkemorani* and *P. pisciformis* (Panchen 1975) the posterior margin of the clavicles seldom, if ever, extends back beyond a line running transversely through the interclavicle's centre of ossification (figure 14*b*).

PHILOSOPHICAL TRANSACTIONS OF THE ROYAL SOCIETY B BIOLOGICAL SCIENCES

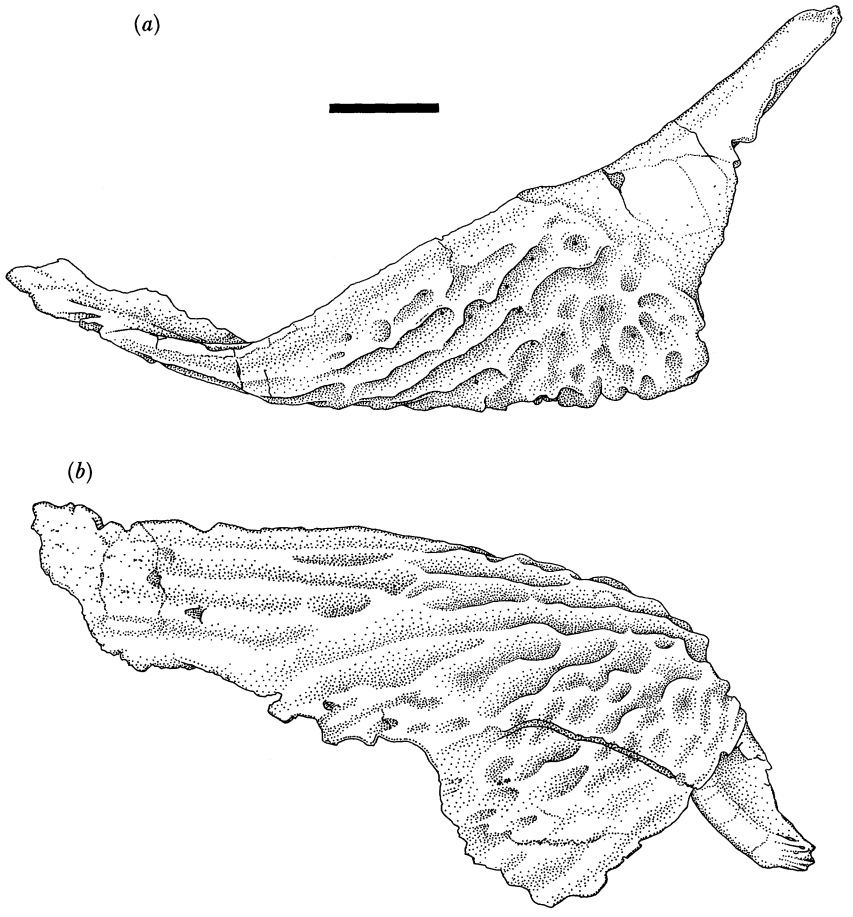

FIGURE 16. *Greererpeton burkemorani* Romer, CMNH 11319. Specimen drawings of the left clavicle. (*a*) Lateral view; (*b*) ventral view. The ventromesial margin is incompletely preserved. Scale bar 1 cm.

In adults, the thin mesial and thicker lateral margins of the clavicle form a relatively large angle between each other. This, however, does not seem to have been the case throughout life. In CMNH 11095, the smallest specimen of *G. burkemorani* known, the mesial and lateral margins of the clavicle run almost parallel to one another. The sculpturing on this clavicle is shallow.

In *G. burkemorani*, the cleithrum is a slender rod-like element, damaged or incompletely preserved in most specimens (figure 17). A thorough description was made possible by the discovery of a complete cleithrum in the juvenile specimen CMNH 11320 (figure 17 *a–c*).

In lateral view, the cleithrum appears 'cane-like' with the shaft comprising the major part of the bone. The proximal end of the shaft is bowed forward in lateral aspect and only slightly curved in anterior view. Mesially, a prominent crest arises immediately below the dorsal spatulate plate and passes ventrally where it attenuates just above the ventral tip of the shaft. The crest extends the basically elliptical section of the shaft such that in cross section its outline is 'teardrop' or subtriangular. The anterior and posterior margins of the crest present flat surfaces, variably marked with grooves or ridges, presumably to accommodate the ascending blades of the clavicle and scapulocoracoid respectively. In adults, the post-ridge area is often inset from the carina of the crest, and well marked by a groove that probably held a portion

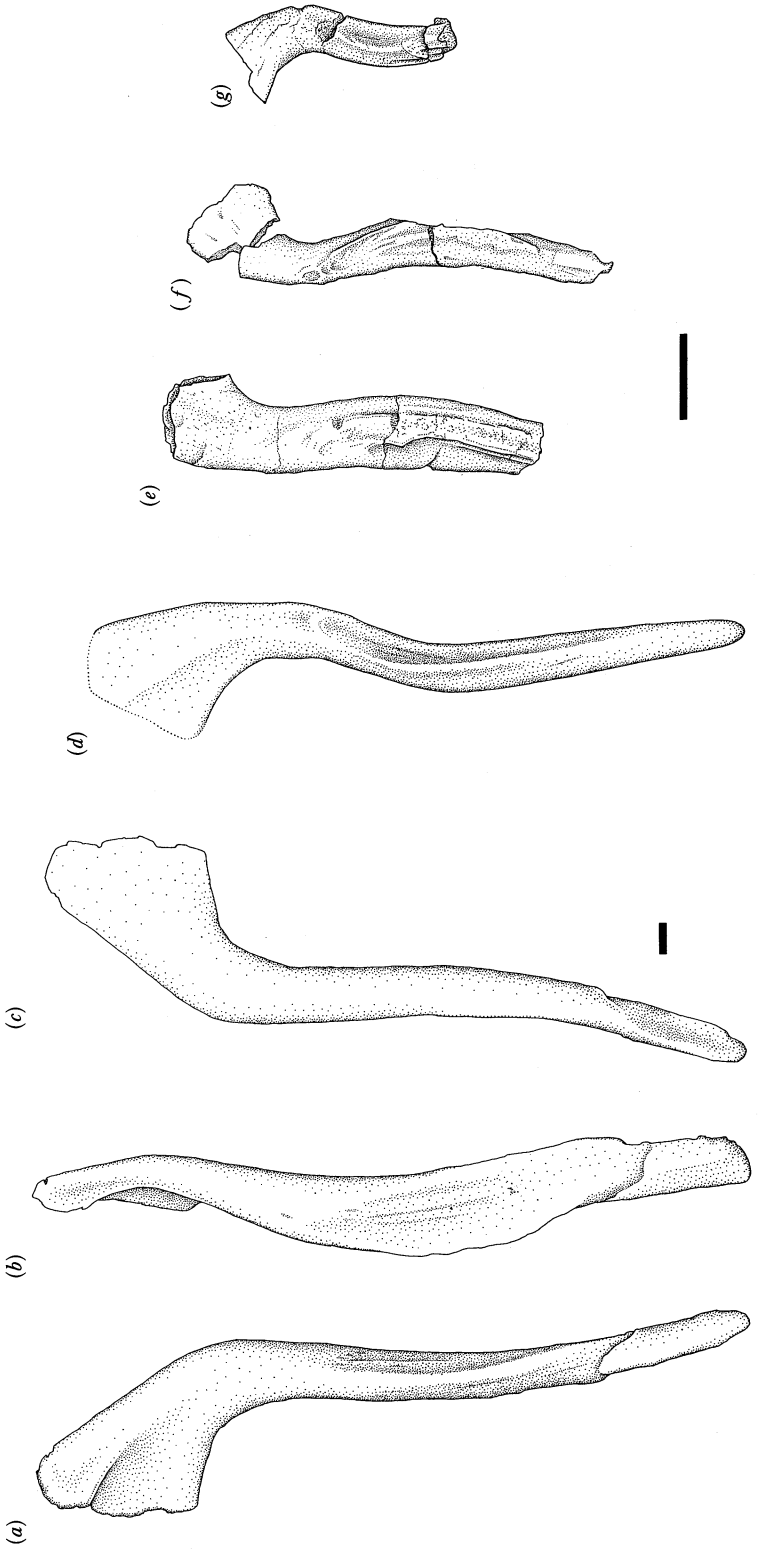

FIGURE 17. *Greererpeton burkemorani* Romer, specimen drawings of cleithra. (*a–c*) The right cleithrum of CMNH 11320 in mesial, posterior, and lateral views respectively; (*d*) the right cleithrum of CMNH 11068 in mesial view; (*e*) the left cleithrum of CMNH 11240 in mesial view; (*f*) the left cleithrum of CMNH 11233 in mesial view; (*g*) the right cleithrum of CMNH 11070 in mesial view. Scale bar 1 mm for (*a–c*) and 1 cm for (*d–g*).

PHILOSOPHICAL TRANSACTIONS OF THE ROYAL SOCIETY B BIOLOGICAL SCIENCES

of the cartilaginous scapulocoracoid plate. In all specimens in which the cleithrum is preserved in close association with the ascending clavicular spine, it rests along the posterior side of the latter.

The spatulate dorsal plate, which is generally without markings, arises smoothly by thinning of the shaft and is turned conspicuously anterodorsally. The plate in some specimens may be divided into two subequal parts: an anterior portion of relatively thin bone set off from the more robust posterior section by an escarpment. Distally, the dorsal plate usually ends abruptly in an undulating rugose margin.

In *Crassigyrinus*, Panchen (1985, figure 20*f*) has restored the clavicular spine lying in the postridge groove. Based on the remarkable similarity between the cleithra of these early tetrapods, it would not be unreasonable to suggest that in *Crassigyrinus* the cleithrum lay between the clavicular spine and the scapulocoracoid, not anterior to both (compare figure 17 with Panchen (1985), figure 20*f*).

The pectoral limb

The humerus of *G. burkemorani* is well preserved in several specimens of various sizes (figures 18 and 19), including the juvenile CMNH 11320.

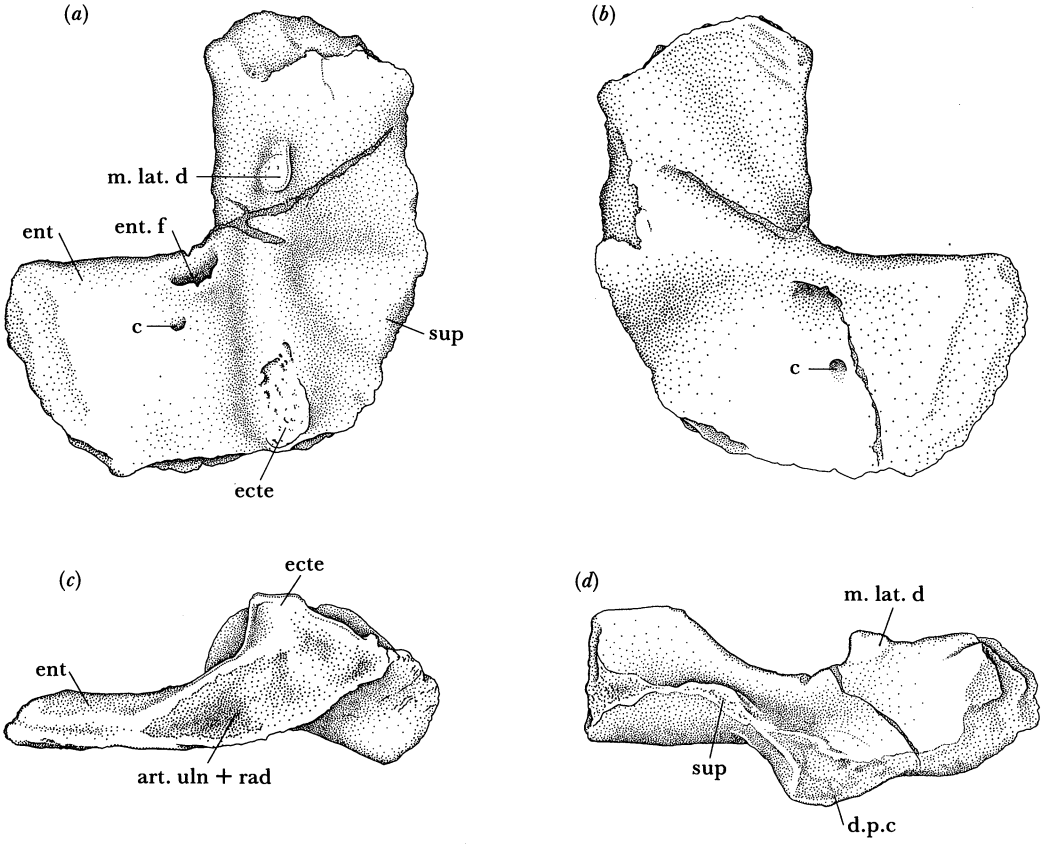

FIGURE 18. *Greererpeton burkemorani* Romer, CMNH 11090. The right humerus in (*a*) dorsal view; (*b*) ventral view; (*c*) distal (lateral) view; (*d*) preaxial (anterior) view. Scale bar 1 cm.

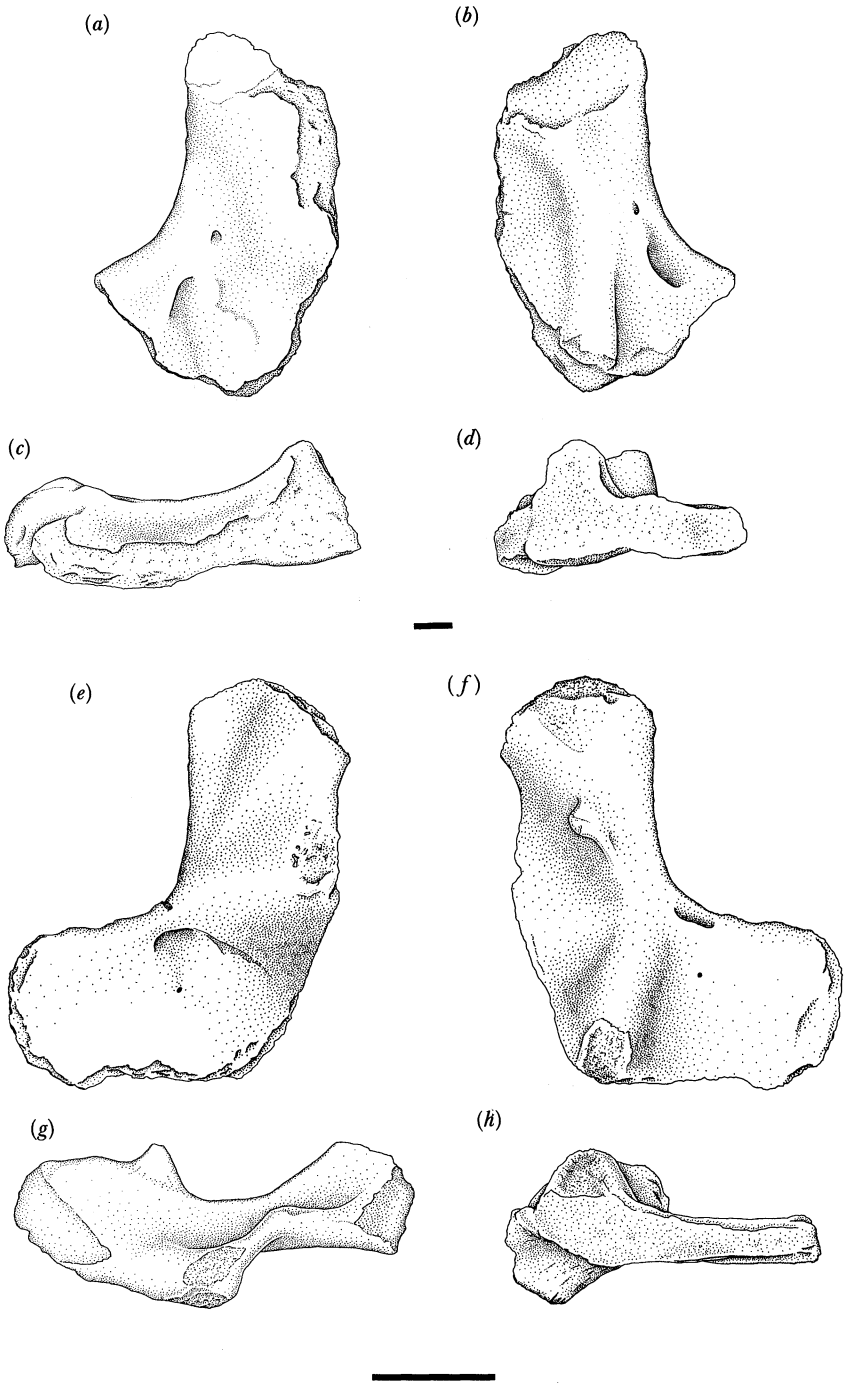

FIGURE 19. *Greererpeton burkemorani* Romer, specimen drawings of a juvenile (*a–d*) and an adult (*e–h*) humerus. (*a–d*) The left humerus of CMNH 11320 in ventral, dorsal, preaxial and distal views respectively; (*e–h*) the left humerus of CMNH 11090 in ventral, dorsal, preaxial, and distal views respectively. Scale bar 1 mm for (*a–d*) and 1 cm for (*e–h*).

PHILOSOPHICAL TRANSACTIONS OF THE ROYAL SOCIETY B BIOLOGICAL SCIENCES

The anteriormost part of the proximal articular surface forms an angle of about 90° with the long axis of the humerus. As this roughly convex strap of unfinished bone passes posteriorly, the surface bends gently ventrally to form an angle of approximately 70° with the long axis of the humerus. Very little of the caput humeri is visible in either dorsal or ventral view. The unfinished nature of this articular surface prevents a detailed analysis of the mechanics of limb movement.

A prominent processus latissimus dorsi is a conspicuous feature on the dorsal surface of the proximal humeral shaft (figures 18 and 19*f–g*). In large, well-ossified humeri the tuberosity is acuminate and directed proximodorsally (figure 4). It marks the insertion of m. latissimus dorsi.

The ectepicondyle begins as a low ridge just distal to the insertion of m. latissimus dorsi and passes diagonally (preaxially) to the anterodistal corner of the humerus, where its base becomes broader as it ascends vertically, gaining considerable exposure in anterior view (figure 18*d*). Distally, the dorsal margin of the ridge was slow to ossify.

In well-ossified specimens, the stout deltopectoral crest faces anteroventrally and slightly mesially. In some specimens this surface is weakly divided horizontally into two unequal portions. The larger, ventral portion is slightly concave and presumably marks the major insertion of m. pectoralis. Above this area, and passing on to the anterior flange, is a smaller concavity marking the site of insertion of m. deltoideus (figure 19*d*). Continuous with the deltopectoral crest distally is a relatively thin, dorsally convex flange. Along its anterior margin, the flange is almost completely finished with periosteal bone. Midway between the deltopectoral crest and the ectepicondyle, the anterior flange thickens as a shallow ridge passes posteromesially towards the entepicondyle foramen (figures 18*a* and 19*f*). This area probably marks the origin of m. supinator and is homologous with the more clearly defined supinator process of *Eryops* (Miner 1925). A more clearly defined supinator process may result in part from increased 'torsion' along the humeral shaft.

As in other early tetrapods, the adult humerus of *G. burkemorani* bears a remarkably large entepicondyle. The body of the condyle is relatively thin, more so along a line running from the entepicondyle foramen to its posterodistal corner. The condyle thickens distally, immediately behind the ectepicondyle where it forms the poorly defined ulner articulation. The entepicondyle foramen passes from the dorsal surface of the humerus in a ventrodistal and slightly anterior direction to the ventral surface. In a few specimens (CMNH 11090, figures 18 and 19*e*, *f*) the entepicondyle is pierced by a second, obliquely oriented foramen which in dorsal view lies just distal to the entepicondyle foramen. It is topologically very close and may be homologous with the c-canal in *Ichthyostega* (Jarvik 1980) and *Crassigyrinus* (Panchen 1985).

The proximoventral surface of the humerus displays two smooth, trough-like concavities separated by a low, rounded ridge. The anterior, triangularly shaped concavity begins immediately posterior to the deltopectoral crest, near the postaxial margin of the bone. It expands anteromesially and merges with the anterior margin of the humerus (figure 19*e*). The second concavity is more pronounced. It begins immediately proximal to the first concavity becoming broader and deeper as it opens below the caput humeri. It probably marks the insertion of m. coracobrachialis. The proximal margin of the low rounded ridge apparently marks the insertion of m. supracoracoideus (Holmes 1980; Smithson 1985) although no rugosities develop in *G. burkemorani*.

PHILOSOPHICAL TRANSACTIONS OF THE ROYAL SOCIETY B BIOLOGICAL SCIENCES

A low ridge passes posterodistally from the deltopectoral crest to the proximal edge of the entepicondyle and then on to the entepicondyle to form its proximoventral margin (figures 18*b* and 19*e*). Anterodistal to this ridge is the broadly concave ventral surface of the anterior (supinator) flange.

Both radial and ulnar 'condyles' were borne entirely on the distal end of the bone with no apparent ventral exposure. In most specimens of *G. burkemorani*, this area is flat to concave and was presumably filled by a large cartilaginous cap in life. In many early, presumably terrestrial, tetrapods the bulbous radial condyle (the capitellum) projects ventrally, often at right angles to the long axis of the bone. As such, the radius then formed the principal load-bearing element of the forelimb. Early amphibians that spent most, if not all, of their time in water would presumably not require this 'terrestrial' arrangement and thus either lost the ventral condyle or retained the primitive distally placed articulating surfaces.

The humerus of *G. burkemorani* resembles this element in other early tetrapods in displaying a low degree of 'torsion' along its shaft. By using the axes established by Andrews & Westoll (1970, p. 249), the angle formed between the long axis of the proximal articular surface and the horizontal plane of the entepicondyle is approximately 25–30° in adults, and the bicondylar axis (connecting the entepicondyle and ectepicondyle) measures approximately 40°.

The humerus of *G. burkemorani* appears to experience considerable morphological change during its ontogeny (figure 19). This claim is based primarily on the differences manifested by one small humerus, CMNH 11320 (figure 19*a–d*). The relatively small number of humeri available for study precluded describing relative growth in a quantitative fashion.

An adult humerus is slightly more than 20% of the length of the skull. The humerus of CMNH 11320 is slightly less than 14% of its skull length. This epipodial would seem to grow with a positive allometric coefficient even if some allowance is made for lack of ossification in juvenile humeri. The juvenile humerus differs from the adult morphology in (1) the low relief of most tuberosities, ridges and grooves and (2) a poorly developed entepicondyle. The processus latissimus dorsi is only weakly developed and just visible in anterior (preaxial) view. The ectepicondyle is strongly developed, however, rising sharply from the plane of the entepicondyle. In anterior view (figure 19*c*), the ascending ectepicondyle imparts an even concave outline to the dorsal margin of the bone.

The deltopectoral crest, a broad unfinished strip of bone confluent with the proximal surface and the anterior (supinator) flange, exhibits little relief, and does not project ventrally to the same degree as in adults. The anterior flange is poorly ossified, evidenced by the thick unfinished preaxial surface. The supinator ridge is not developed.

Unlike the adult humerus which bears a well-developed entepicondyle, that of CMNH 11320 is remarkably small. The posteromesial margin of the entepicondyle makes an angle of about 120° with the smooth posterior edge of the bone proximal to it. In mature individuals, the angle is close to 90°. In this respect the juvenile humerus resembles the humerus of *Crassigyrinus*, which forms an angle of about 140°. The distal portion of the entepicondyle is slow to ossify, so that in dorsal view the condyle is roughly triangular in outline, not rectangular as in adults. If CMNH 11320 is not anomalous, then during ontogeny the proximal edge of the condyle migrates mesially as it ossifies more completely postaxially. A large entepicondyle foramen pierces the small condyle. In CMNH 11320, a conspicuous groove passes from the ventral opening of the entepicondyle foramen distally to terminate along the unfinished margin

PHILOSOPHICAL TRANSACTIONS OF THE ROYAL SOCIETY B BIOLOGICAL SCIENCES

of the bone, as in *Crassigyrinus* (Panchen 1985). In larger specimens, the groove becomes progressively less distinct to non-existent. A second but smaller foramen, immediately anterior to the entepicondyle foramen, is difficult to interpret because it has not been described in other tetrapods.

Even though the humerus is incompletely ossified, an angle of about 25° can be measured between the long axis of the caput humeri and the plane of the entepicondyle, and the bicondylar axis measures about 30°. Both of these angles are within the adult range.

In proximal view, the radius of *G. burkemorani* (figure 20*a–f*) is almost circular in outline, whereas distally the articular surface is flattened and nearly ovoid in outline. Both articular surfaces are irregular, indicating that they were finished in cartilage. The expanded articular heads are joined by a slender shaft bearing four longitudinal ridges that produce a roughly square cross section. The two most pronounced ridges run the entire length of the bone forming the 'corners' between the sharply separated extensor and mesial, and flexor and mesial sides respectively (figure 20*d*). These ridges occur in other early tetrapods and may have marked the boundary between the extensor and flexor muscle groups (Romer 1957; Holmes 1980). The third, somewhat smaller ridge separates the flexor from the lateral surface. The last 'corner', separating the extensor from the lateral surface, is formed by a broadly rounded ridge. The mesial surface is conspicuously concave or trough-like, whereas the flexor, lateral and extensor surfaces are gently concave, essentially flat and slightly convex respectively. Thus in anterior (or extensor) view the lateral surface is almost straight, whereas the mesial margin is markedly concave (figure 20*c*). The radius appears to be devoid of surface rugosities marking the insertion or origin of brachial and propodial musculature.

The ulna *G. burkemorani* (figure 20*g–l*), as preserved in CMNH 11090, is 26% longer than the radius. In subadults, however, the epipodials are approximately the same length because the olecranon is slow to ossify. The proximal articular surface, seen end on in figure 20*k*, is shaped like an isosceles triangle, the base of which is formed by the flexor margin. Although considerably different in outline, it has approximately the same surface area as the proximal articular surface on the radius. The olecranon in *G. burkemorani* is remarkably well ossified but unfinished proximally, marking the site of insertion of the triceps muscle. As a result, the proximal articular surface gains good exposure when viewed mesially (figure 20*j*). A line passing along the inclined proximal articular face forms an angle of about 40° with the long axis of the shaft. In some early amphibians the plane of the articular facet is more nearly 90° with respect to the long axis of the bone; this presumably is a reflection of either their immaturity or degree of aquatic specialization (see *C. scutellatus* (Hook 1983, figure 12*c*) and *Crassigyrinus* (Panchen 1985, figure 22*g–h*)).

The distal articular surface forms a relatively small (the distal radial surface is between three and four times larger) anteroposteriorly compressed ovoid. It is indistinctly divided into a facet for the ulnare and a smaller one for the intermedium.

Longitudinally, the shaft is divided by two prominent ridges. Both run from the proximal articular surface and terminate immediately above the distal facets, dividing the shaft equally into broadly convex flexor and extensor moieties. A third ridge runs from the distal posterolateral corner of the shaft diagonally towards the proximomesial side, but vanishes 5 mm below the articular surface (figure 20*g*).

As for most Carboniferous tetrapods, the carpus and manus of *G. burkemorani* are incompletely preserved. The manus is most completely preserved in CMNH 11090 (figure 3).

PHILOSOPHICAL TRANSACTIONS OF THE ROYAL SOCIETY B BIOLOGICAL SCIENCES

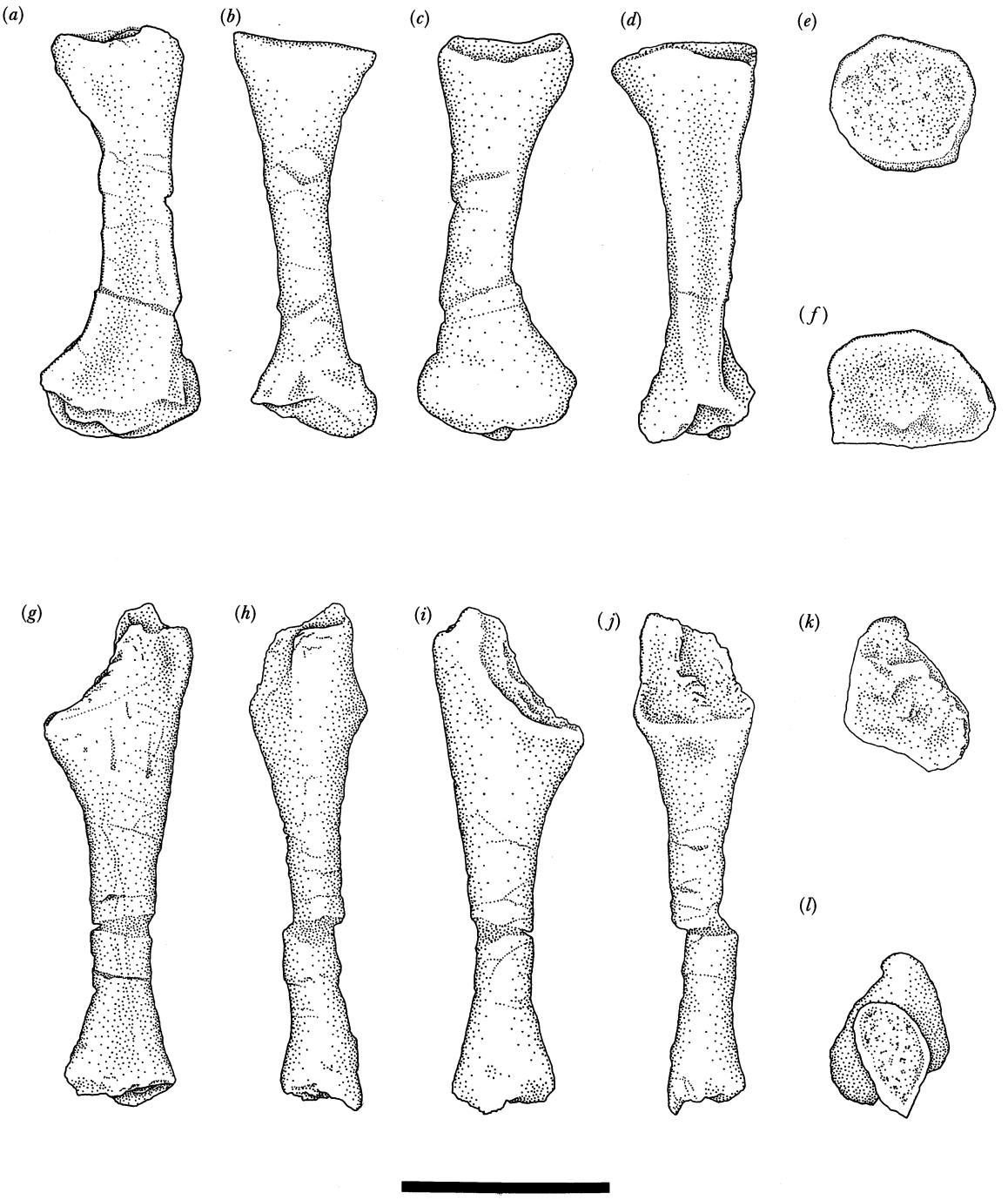

FIGURE 20. *Greererpeton burkemorani* Romer, specimen drawings of the radius and ulna. (*a–f*) The right radius of CMNH 11090 in flexor, lateral, extensor, mesial, proximal and distal views respectively; (*g–l*) the right ulna of CMNH 11090 in flexor, lateral, extensor, mesial, proximal and distal views respectively. Scale bar 1 cm.

In spite of the fact that *G. burkemorani* had diminutive limbs, this specimen preserves carpal elements, most of which are associated with the left limb. Their disarticulated state makes identification and interpretation difficult. Furthermore, several of the metacarpals have bizarre shapes that can only be regarded as the result of trauma.

PHILOSOPHICAL TRANSACTIONS OF THE ROYAL SOCIETY B BIOLOGICAL SCIENCES

The metacarpals and phalanges preserved on the right side of CMNH 11090 are similar to those present in *C. scutellatus* (Hook 1983, figure 12*d*). Each digit ends in an elongate, bluntly pointed ungual phalanx. The phalangeal formula in *G. burkemorani* remains unknown.

The pelvic girdle

The pelvic girdle in *G. burkemorani* is composed of three pairs of bones. As in other early tetrapods, the ilium and ischium are usually well represented, but the pubis appears to have been slow to ossify ontogenetically, and is only imperfectly preserved in one specimen, CMNH 11090 (figure 21*d*).

The ilium of *G. burkemorani* is typical of early Carboniferous temnospondyls. It consists of an anteroposteriorly expanded base from which rises a long narrow and undivided iliac blade. Immediately below the expanded base of the ilium, the constricted shaft is elliptical to subcircular in cross section. Posterodorsally, the blade thins mesiolaterally, but not appreciably so, and expands anteroposteriorly to a variable degree (figure 21*a*, *d*). Proximally, the blade forms an elongate oval or 'teardrop' outline in cross section. The uppermost end of the blade is concave and was probably continued by cartilage in life. The mesial surface of the iliac blade appears to be devoid of markings associated with the 'articulating' surface for the sacral rib, suggesting that a relatively weak ligamentous bond existed between the ilium and the sacral rib.

The distal (or ventral) end of the ilium is composed of an anterior, posterior and lateral salient of unfinished bone. The posterior portion forms a broad contact with the ischium whereas the smaller anterior segment abuts with the pubis. The lateral salience represents the iliac portion of acetabulum. This area displays the inverted U-shaped supra-acetabular buttress, typical of early tetrapods, which projects laterally from a gentle depression. The base of the 'U' is directed posterodorsally at an angle of between 20° and 30° from the horizontal (figures 21*a*, 22*a* and 23*a*). Below the buttress, the surface is slightly concave and appears to have been finished in cartilage. Along the margins of the inverted 'U' the ilium is finished in smooth periosteal bone to form the anterior and posterior tongue-like projections seen in *Ichthyostega* and other early tetrapods (Jarvik 1980). A pronounced ridge, beginning on the mesial surface below the iliac blade, passes diagonally anteroventrally onto the posterior and anteriormost portions of the pubis and ischium respectively, attenuating to vanish before reaching the pelvic symphysis (figure 22*b*).

The ossified portion of the pubis is roughly trapezoidal, with the narrow end directed anteriorly. The sutures with the ilium and ischium are seen on both lateral and mesial surfaces. In lateral view, the posterodorsal margin of the pubis is thickened mesiolaterally to form a buttress, which constitutes the anteroventral margin of the acetabulum. This buttress sweeps posteriorly and is confluent with that on the ischium. Below the buttress the bone appears to thin, although preservation is poor in this area. The obturator foramen pierces the pubis immediately below the suture between the pubis and ilium.

The ischium of *G. burkemorani* is well represented in the specimens studied (figure 21). The lateral surface is greatly thickened in the acetabular region to form a large buttress, which passes from the posterodorsal corner of the ischium anteroventrally on to the pubis. The posterodorsal margin of the ischium is also thickened, perhaps to resist tension and compression generated by muscular contractions during limb or tail movement. Otherwise, the ischiadic plate is of roughly uniform thickness. The lateral surface is distinctly concave posteriorly. The

PHILOSOPHICAL TRANSACTIONS OF THE ROYAL SOCIETY B BIOLOGICAL SCIENCES

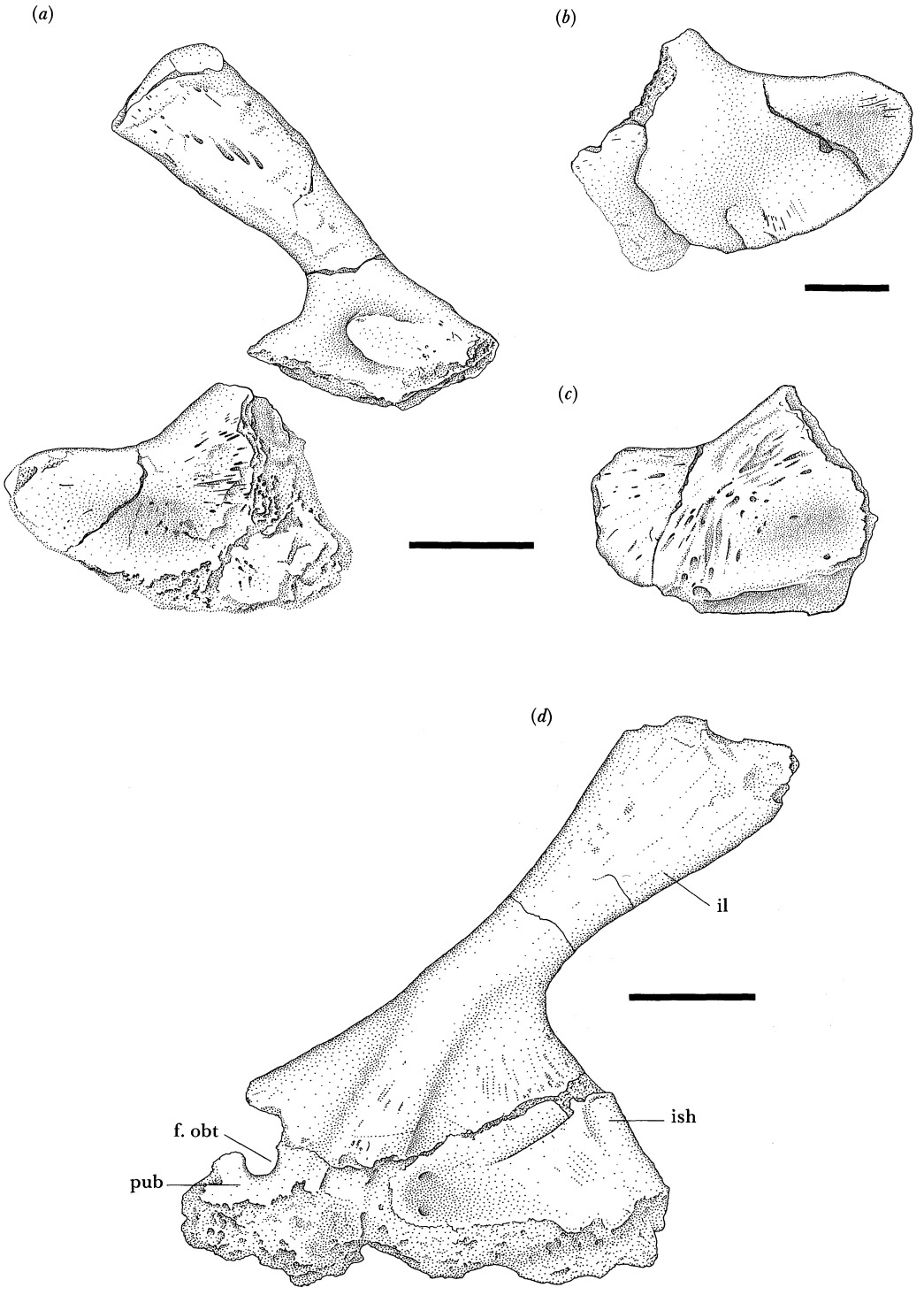

FIGURE 21. *Greererpeton burkemorani* Romer, elements of the pelvic girdle. (*a*) The right ilium and ischium of the Holotype, CMNH 10931, in lateroventral view; (*b*) the left ischium of CMNH 11068 in lateroventral view, drawn to a different scale; (*c*) left ischium of CMNH 10931 in mesiodorsal view; (*d*) the right ilium, ischium and pubis of CMNH 11090 in a mesiodorsal view. Scale bars 1 cm.

PHILOSOPHICAL TRANSACTIONS OF THE ROYAL SOCIETY B BIOLOGICAL SCIENCES

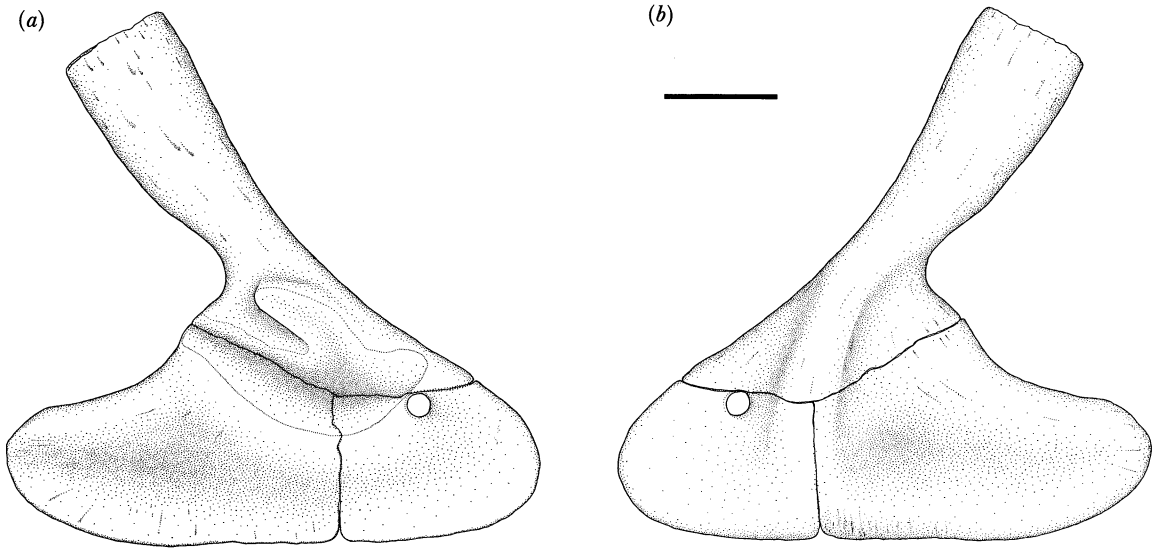

FIGURE 22. *Greererpeton burkemorani* Romer, restoration of the right half of the pelvic girdle. (*a*) Viewed laterally and slightly ventrally to provide maximum exposure; (*b*) viewed mesially and slightly dorsally. Scale bar 1 cm.

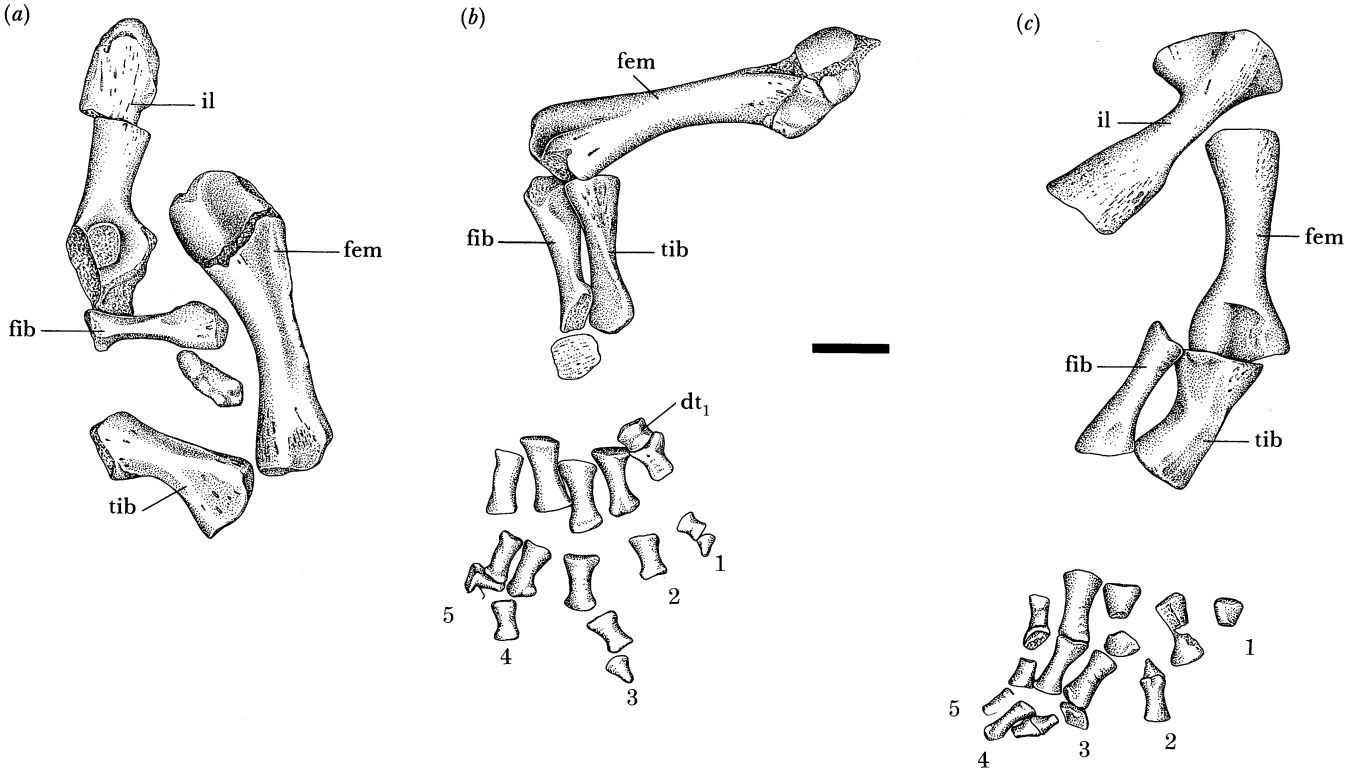

FIGURE 23. *Greererpeton burkemorani* Romer, elements of the pelvic girdle and limb. (*a*) CMNH 10931; (*b*) CMNH 11232; (*c*) CMNH 11070. Scale bar 1 cm.

PHILOSOPHICAL TRANSACTIONS OF THE ROYAL SOCIETY B BIOLOGICAL SCIENCES

posterior portion of the mesial surface is flat, whereas the anterior half to one third of this surface is occupied by a concave pocket that terminates just anterior to the puboischiadic suture. In CMNH 10931 the ventral margin is striated, and presumably represents the area of fibrous connection between the two ischia medially. Because the surface between opposing ischia is not well preserved, the angle between the two halves of the pelvic girdle cannot be established with certainty, although the width of the sacrum suggests an angle of about 90°

The pelvic limb

The femur is the longest of the limb bones and appears gracile in its proportions (figures 23 and 24). The mesially facing, band-shaped proximal articulating surface is concave, and must have been capped by cartilage in life. In a proximal view, the dorsal surface of the femur is gently convex and the ventral margin slightly concave. Measured dorsoventrally, the proximal articulating surface is broad, the greatest width being approximately 50% of its length measured along its anteroposterior axis. During ontogeny the degree of ossification of the proximal articulating surface is altered considerably. In CMNH 10931 (figure 24*a–d*), the anterior margin of the articulating surface is not separated from the adjacent internal trochanter by finished bone. With increasing size, however, this trochanter becomes progressively more distinct and in CMNH 11113 it is separated from the proximal articulating surface by a constriction between the ventral and anterior surfaces of the femur (figure 24*f*, *g*). In a slightly larger individual, CMNH 11090, it is further removed from the articulating surface by increased ossification proximally. This trend culminates in CMNH 11068, the largest femur of *G. burkemorani* known, where the trochanter is clearly distinct from the proximal articulating surface, forming a conspicuous, ventromesially directed flange (figure 24*n*). The prominent internal trochanter probably received the insertion of m. puboischiofemoralis internus.

The distal end of the femur bears two broadly convex condyles. The anterior condyle is lightly striated but otherwise featureless. The posterodorsal surface mesial to the condyle is, in adult specimens, more convex than in immature individuals. The posterior precondyle convexity in large adults is more distinct even though both ridges become separate at the same location distal to the midpoint of the shaft. The posterior condyle in the two larger specimens illustrated (figure 24*l*, *o*) extends further distally than the anterior condyle. In subadult specimens, the two condyles are of equivalent length. In the smallest femur at hand (CMNH 10931), the intercondylar fossa is shallow, but as more of the femur ossifies distally the groove deepens considerably and extends distally between the condyles. Nutritive foramina are present in the intercondylar fossa.

In CMNH 11068, the dorsally convex, crescentric tibial facet begins along the anterior margin of the distal head, passes posteriorly along the anterior condyle and turns sharply ventrally, terminating ventral to the intercondylar fossa and distal to the adductor crest. The articulating surface thus forms a boomerang-shaped condyle. An angle of about 90° is formed between the two rami of the boomerang. The fibular facet is therefore smaller, corresponding to the fibula's smaller proximal articulating surface. The fibular facet is basically subcircular in outline, and persistently concave even in the largest specimen.

The morphology of the ventral surface of the femur is similar in most respects to that of other medium- to large-sized Carboniferous tetrapods. A sharp ridge sweeps posteriodistally from the base of the internal trochanter. The intertrochanteric fossa is clearly visible in CMNH 11113. A small depression, which demarcates the distal extremity of the intertrochanteric fossa, curves

PHILOSOPHICAL TRANSACTIONS OF THE ROYAL SOCIETY B BIOLOGICAL SCIENCES

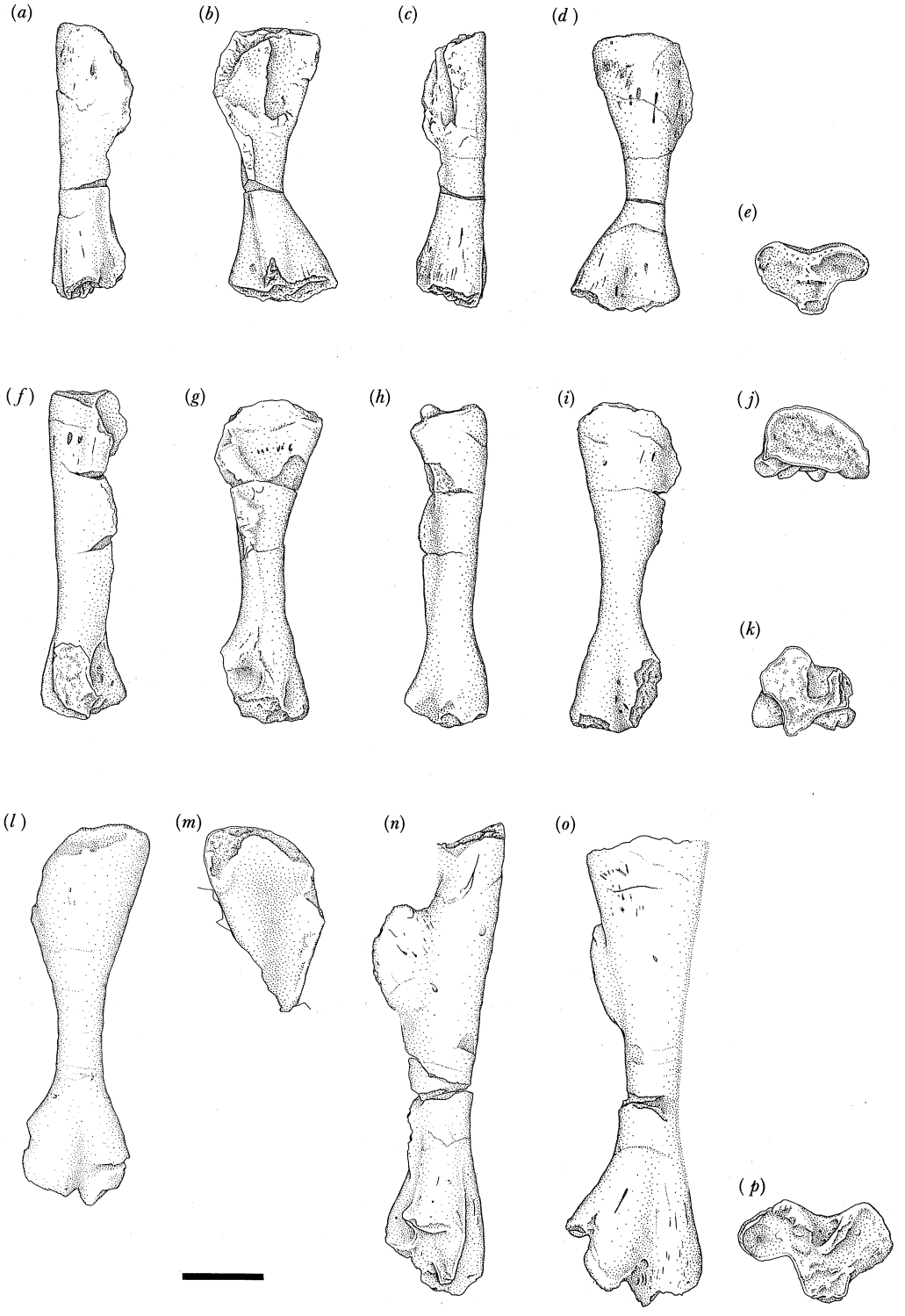

FIGURE 24. *Greererpeton burkemorani* Romer, the femur. (*a–e*) The right femur of CMNH 10931 in anterior, ventral, posterior, dorsal, and distal views respectively; (*f–k*) the right femur of CMNH 11113 in anterior, ventral, posterior, dorsal, proximal and distal views respectively; (*l*, *m*) the left femur of CMNH 11090 in dorsal and ventral views respectively; (*n*, *o*) the left femur of CMNH 11068 in anterior, dorsal, and distal views respectively. Scale bar 1 cm.

PHILOSOPHICAL TRANSACTIONS OF THE ROYAL SOCIETY B BIOLOGICAL SCIENCES

posteriorly from the internal trochanter. The depression attenuates as it passes posteriorly towards the proximal posterior branch of the ventral ridge system. This depression presumably indicates the posterior boundary of the puboischiofemoralis externus muscle (Holmes 1984).

Distal to the internal trochanter, the ridge in CMNH 10931 and CMNH 11113 appears to possess a slightly expanded or fluted region, immediately mesial to the midpoint of the shaft. This area may correspond to the fourth trochanter seen in other tetrapods, which probably received the insertion of the caudofemoralis muscle. Beyond the fourth trochanter the ridge forms the adductor crest. This crest may be distinguished from the broad ventral ridge that passes posteroventral to the tibial facet mesially, along the ventral third of the shaft. In *G. burkemorani* the two diverge somewhat, just mesial to the popliteal space. The adductor crest passes along the anterior side of the ventral crest, posteroventral to the tibial facet. In the largest femur examined (CMNH 11068, figure 24*n*, *o*), the internal trochanter and the fourth trochanter ridge do not align themselves along the shaft as they do in smaller specimens. The surprisingly large internal and fourth trochanters lie anterior to the smaller adductor crest. In this specimen (CMNH 11068), the proximoventral region is partly obscured by an ilium; the exact nature of the adductor crest's mesial configuration is therefore unknown.

The fibula has the characteristic shape seen in many early tetrapods: a thickened head with a terminal articular surface for the femur, a slim shaft, subcircular in section, and a broad, relatively thin distal segment that articulates with the tarsus (figure 25*a–f*). The fibula of *G. burkemorani* is somewhat longer than the tibia. In CMNH 11068 it is 50% of the length of the femur, whereas the tibia is only 45% of the length of the femur.

The proximal articulating surface forms a crescentic oval. The torsion along the fibula causes the long axis of the fibula's femoral articular surface to be aligned perpendicular to the long axis running through the tibia's proximal femoral articular surface. The articulating surface for the femur on the fibula is inclined towards the tibia, forming an angle of about 55° with the long axis of the bone. As preserved, the proximal articulating surface is gently concave.

The shaft of the fibula becomes increasingly constricted distally to reach its minimum girth at a point just distal to the midpoint of the shaft. The shaft at this point is oval in cross section, compresed slightly from flexor to extensor surfaces. A small ridge becomes visible on the flexor surface immediately proximal to the midpoint of the shaft. As it passes distally, it curves laterally to sweep along the outer margin of the flexor surface, terminating just above the tarsal articular surface.

Distally, the entire flexor surface is gently concave whereas the extensor surface is gently convex. Viewed distally, the distal articular surface forms a mesiolaterally elongate oval. The articular surface may be divided into two unequal parts, one facing distally and the other ventromesially. The distal articular segment, which is only approximately half the area of the ventromesial articular facet, articulates with the fibulare. The second, ventromesially directed articular surface, abutted with the large intermedium.

The two ends of the fibula are 'twisted' with respect to each other, with the effect of turning the proximolateral aspect of the head inward so that it lies in the flexor plane. The degree of torsion of the head on the shaft is between 75° and 80° in CMNH 11068.

The tibia of *G. burkemorani* is similar in most regards to that of other early tetrapods except *Ichthyostega* (figure 25*g–s*). Its maximum length is 66% of the length of the femur in CMNH 10931, and 45% in the largest individual known, CMNH 11068. This difference is a reflection of the precocious ossification of the tibia. The tibia and ulna are, in most specimens,

PHILOSOPHICAL TRANSACTIONS OF THE ROYAL SOCIETY B BIOLOGICAL SCIENCES

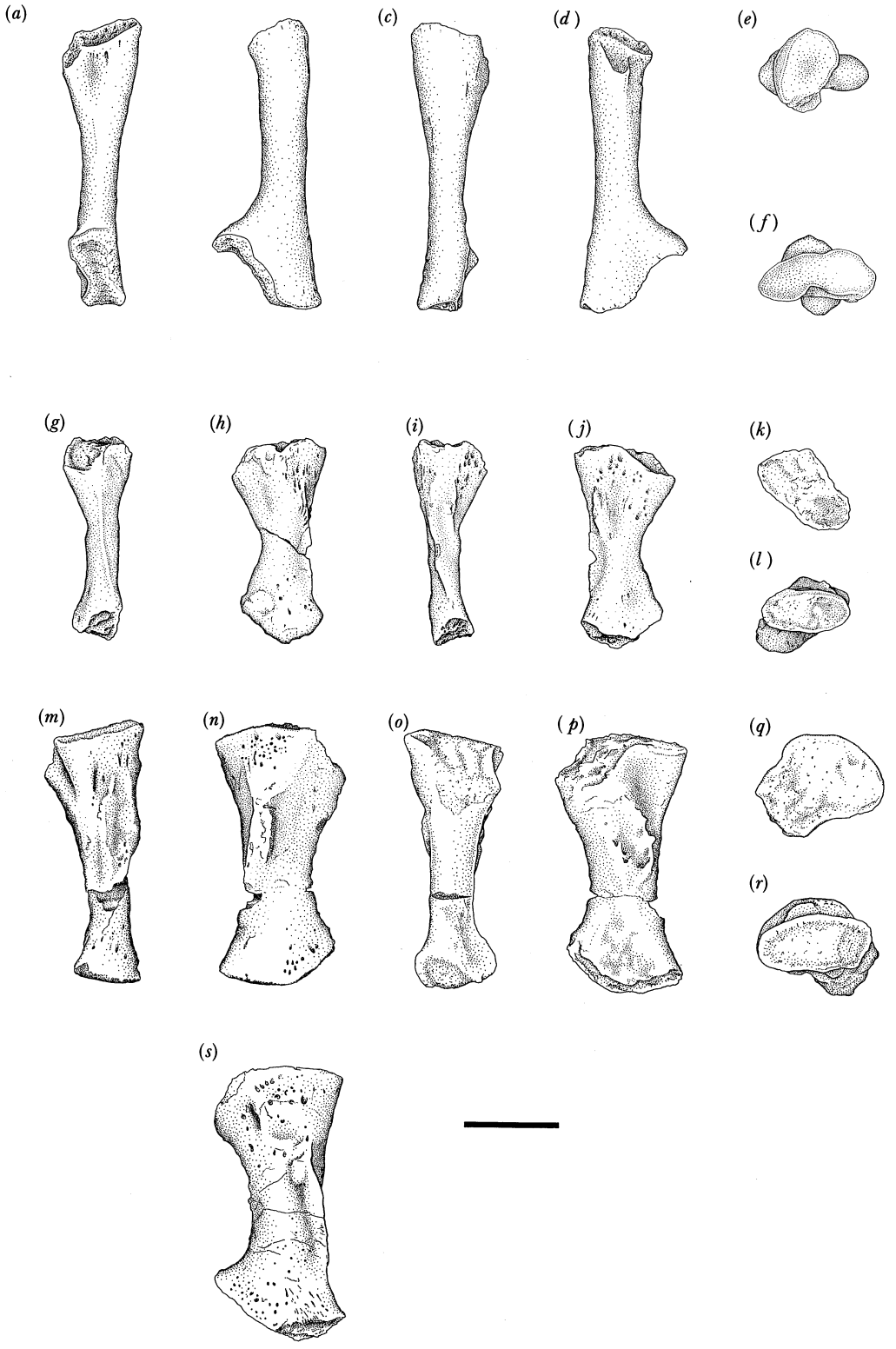

FIGURE 25. *Greererpeton burkemorani* Romer, elements of the crus. (*a–f*) The left fibula of CMNH 11068 in mesial, anterior, lateral, posterior, proximal and distal views respectively; (*g–l*) the right tibia of CMNH 10931 in mesial, anterior lateral, posterior, proximal and ventral views respectively; (*m–r*) the left tibia of CMNH 11068 in lateral, anterior, mesial, posterior, preaxial, and distal views respectively; (*s*) the right tibia of CMNH 11068 in anterior view. Scale bar 1 cm.

PHILOSOPHICAL TRANSACTIONS OF THE ROYAL SOCIETY B BIOLOGICAL SCIENCES

almost exactly the same length. In CMNH 10931, the maximum width (extensor–flexor axis), in mesial view, of the tibia is 68% relative to its broad axis (mesial–lateral; in CMNH 11068, a larger individual, the proportions remain the same). This proximal articulating surface is shaped like a gently bowed rectangle, which mirrors the strong boomerang-shaped tibial articulating facet on the femur. The entire surface is, in extensor view, broadly convex.

A cnemial crest forms a conspicuous longitudinal ridge occupying the mesial portion of the proximal extensor surface (figure 25*h*, *n*, *s*). This crest marks the point of insertion of the triceps (quadriceps) femoris muscle. It is confluent with a crest for the insertion of the m. puboischiotibialis that sweeps mesiolaterally, subsiding distally immediately proximal to the articulating surface for the tibiale. In *G. burkemorani*, however, the ridge is not as extensive mesially; thus little or no convex shape is imparted to the tibia when viewed from the extensor surface. The extensor surface lateral to the crest is gently convex.

The upper part of the flexor aspect of the tibia in CMNH 10931 is marked with longitudinal striations that could accommodate ligaments and fascia of the knee (Romer 1957). A system of rugosities and a ridge pass about one quarter of the distance down the shaft diagonally, from the centre of the flexor surface, attenuating immediately above the narrowest point of the shaft. The rugosities, more pronounced in larger specimens (figure 25*j*, *p*), presumably formed the major area of attachment for the flexor musculature of the thigh (Romer 1957). Below this rugose ridge, and extending down the mesial flexor surface of the tibia, is a low ridge. Lateral to this, and running parallel with it, is a shallow groove, which broadens distally to form a concavity occupying the entire distal flexor surface of the tibia. When viewed from the flexor aspect, the strongly convex lateral border of the bone is formed by a sharp ridge.

The distal articulating face of the tibia is roughly ovoid in outline. Viewed distally, the extensor margin is flat or convex in outline whereas the flexor surface is flat to slightly concave (figure 25*j*, *l*, *p*, *r*). The mesial portion of the articulating surface is broad and directed distally in CMNH 11068, but in subadults (CMNH 10931) the same articulating facet gains exposure mesially. This area embraces the tibiale. The lateral articulating surface, adjacent to the intermedium, is roughly equivalent in surface area to the facet. This articular surface faces distolaterally. An angle of between 46° and 58° is formed with the long axis of the bone, depending on the specimen examined and its degree of ossification.

In CMNH 10931, the distal end of the bone is 'twisted' on the shaft, so that the plane of the extensor surface on the distal end is turned mesially about 30° with respect to the proximal end of the shaft.

Elements of the tarsus of *G. burkemorani* are well preserved in CMNH 11090 and 11068 (figures 3, 23*b* and 26*a*), but in no specimen are they complete. Nevertheless, the foot may be confidently restored except for some of the distal tarsals and phalanges. The tarsus of *G. burkemorani* is remarkably similar to that of *Proterogyrinus* (Holmes 1984).

The plate-like fibulare of CMNH 11068 is almost identical to that of *Proterogyrinus*. Both dorsal and ventral surfaces are gently concave, with the mesial and distal edges of the bone raised to increase the articulating surface area. Laterally, the bone thins considerably. The flat proximal articulating surface for the fibula is wedge-shaped in outline, thickest mesially and thinning laterally. A larger triangular facet to accommodate the intermedium is set off at an angle of about 115° from the tibial surface. The facet for the third centrale and fourth distal tarsal faces mesiodistally and slightly ventrally, and is set off from the facet for the intermedium at an angle of approximately 90°. In CMNH 11090, the facet on the fibulare for the

PHILOSOPHICAL TRANSACTIONS OF THE ROYAL SOCIETY B BIOLOGICAL SCIENCES

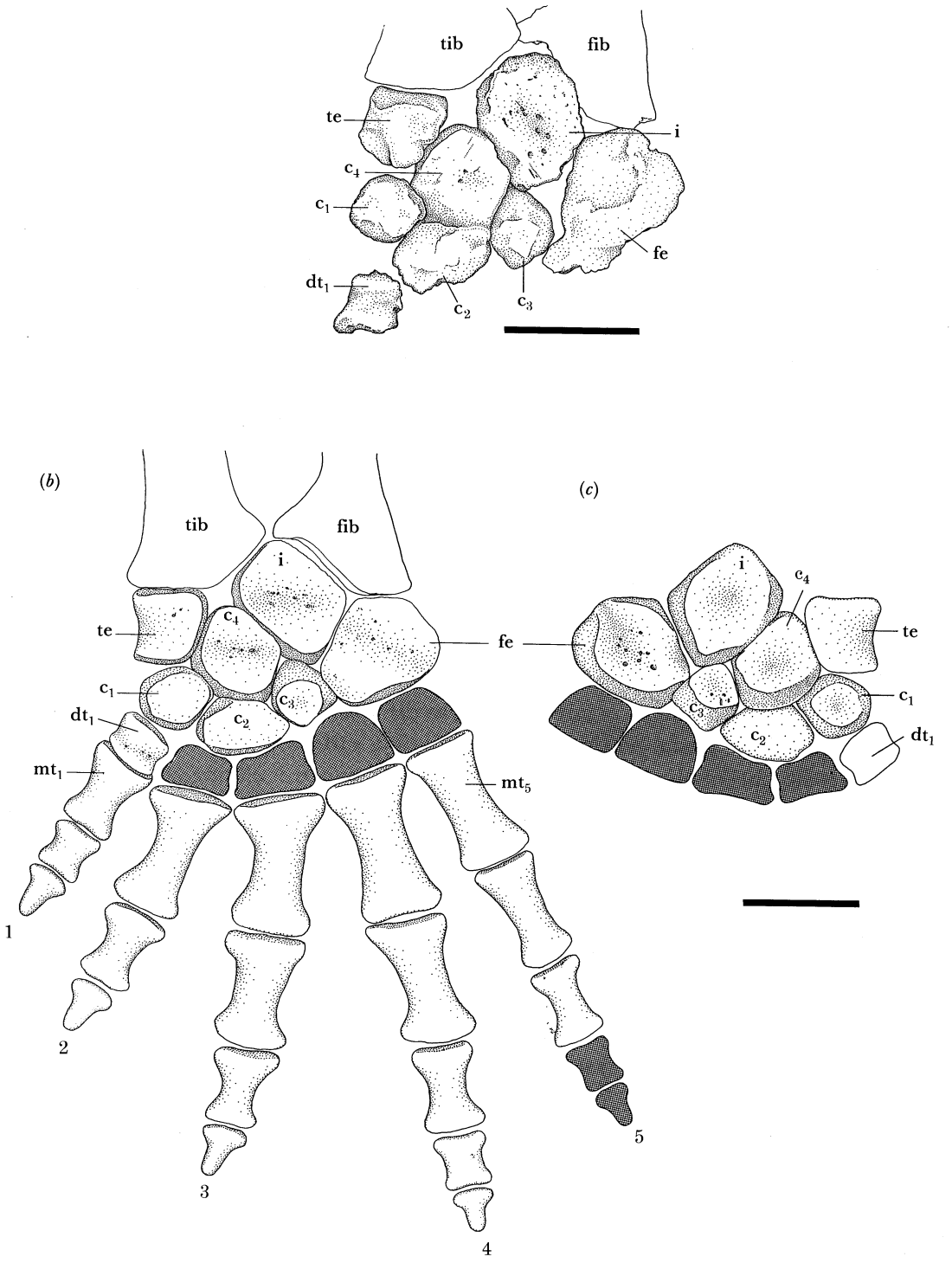

FIGURE 26. *Greererpeton burkemorani* Romer. (*a*) Specimen drawing of the left tarsus of CMNH 11068. Restoration of the left foot. (*b*) Dorsal view; (*c*) ventral view of the tarsus. 'Mechanically' shaded elements of the pes are not preserved in any known specimen. Scale bars 1 cm.

intermedium is separated from the facet for the fourth distal tarsal by a groove for the perforating artery that runs dorsoventrally. This artery passes from the mesially projecting corner of the fibulare, proximolaterally across the dorsal surface of the bone. Most of the mesially directed facet appears to abut against the third centrale. However, a small portion of this facet may have articulated with the fourth distal tarsal. A large facet to accommodate the fifth distal tarsal is also present on the fibulare. This facet is set off from that on the third centrale by an angle of between 70° and 80°. This distally directed facet tapers laterally, where the rounded lateral border of the fibulare is unfinished, and was presumably continued by cartilage in life. The ventral portion of the fibulare is not as completely finished in periosteal bone as is the dorsal surface. Both upper and lower surfaces bear clusters of minute pores, as do most other tarsal elements.

The angular relation between the articulating surfaces and general outline of the intermedium resembles closely that seen in *Proterogyrinus*. Both dorsal and ventral surfaces are gently concave, produced by the broad, raised borders of the articular facets for the fibula, tibia and other tarsal elements. This is the most massive tarsal element and all its edges bear wide surfaces for articulation with other tarsal bones, except for a very small proximal facing surface between the fibular and tibial facets where the bone thins.

The tibiale of *G. burkemorani* has only about half the surface area of either the fibulare or intermedium. In dorsal view, it is almost square in outline. The proximal head bears a wide articulating facet that abuts against the tibia. The mesial margin of this element is convex when viewed proximally. In CMNH 11090, periosteal bone on the extensor surface wraps around on to the ventral surface, completely finishing the mesial margin of the tibiale. Both dorsal and ventral surfaces of the tibiale are flat to gently convex. The lateral margin of the tibiale forms a broad facet that articulates with the mesial surface of the fourth centrale. The width of this facet (on the tibiale) is nearly as broad as the dorsal exposure of the element, producing roughly cubic proportions. The main difference between the tibiale of *G. burkemorani* and *Proterogyrinus* is that in the former it is relatively larger than in the latter, thus excluding the fourth centrale from making contact with the distal end of the tibia. The distance between the tibiale and intermedium in *G. burkemorani* is much less than in *Proterogyrinus*. The distal articular facet on the tibiale articulates with the first centrale in *G. burkemorani*.

The fourth centrale is one of the largest bones in the tarsus. It is roughly diamond-shaped, with the axis through the acute angles running approximately proximodistally. Both dorsal and ventral surfaces are finished with smooth periosteal bone, pierced only by minute foramina. The proximomesial and proximolateral surfaces articulate with the tibiale and intermedium respectively. However, unlike *Trematops* (Schaeffer 1941) and *Proterogyrinus*, the fourth centrale does not appear to gain contact with the tibia, nor does it articulate with the fibulare as in *Trematops*. The distomesial, distal, and distolateral facets articulate with the first, second, and third centralia respectively. The roughly circular first and third centralia are both much smaller than the fourth. The second centrale is intermediate in size, being roughly equal in size to the tibiale.

In CMNH 11090, co-ossification occurs between the first and second, and third and fourth, centralia such that two roughly 'figure **8**' shapes result (figure 3). Although fusion is nearly complete, each centrale is still discernable. CMNH 11090 is presumably anomalous in this respect, although an analogous co-ossification occurs between the fourth centrale and tibiale in a large *Proterogyrinus* specimen. The tarsus is restored with each centrale separate as seen in the larger specimen, CMNH 11068.

PHILOSOPHICAL TRANSACTIONS OF THE ROYAL SOCIETY B BIOLOGICAL SCIENCES

Of the five specimens of *G. burkemorani* that preserve elements of the pes (CMNH 11090, 11068, 11069, 11232, and USNM 22576), only one distal tarsal (probably the first) is preserved in CMNH 11090 and CMNH 11232. It forms a rectangular block of bone, which in life probably articulated with the first centrale. Except for the proximal and distal articulating facets, this element is finished with smooth periosteal bone. The remaining four distal tarsals in the pes were either poorly ossified or destroyed during preparation. They have been restored as keystone-shaped elements after the pattern seen in *Trematops* and *Proterogyrinus*.

In CMNH 11090, a small nodule of bone is preserved immediately mesial to the tibiale and first centrale. If the centralia have been properly identified, this element may represent a pretarsale, somewhat like that in *Trematops* (Schaeffer 1941).

The metatarsals and phalanges are not unlike those in other early tetrapods (figures 23*b*, *c*). The first metatarsal is significantly shorter than the other four, approaching in size the second phalanx of the third or fourth digits. The remaining four metatarsals are very much alike, differing only slightly in length. As in most primitive tetrapods the fourth is the longest.

Although the pes is not complete in any known specimen, digits 1 and 3, and 2, 3, and 4, are complete in CMNH 11232 and USNM 22576 respectively, permitting a composite restoration of the phalangeal fomula as 2, 2, 3, 4, 3 (4?). This phalangeal formula is the same as that in *Amphibamus lyelli* (Hook & Baird 1984) and may represent the pattern of early temnospondyls. Each digit ends in a robust, bluntly pointed ungual phalanx.

Discussion

Depositional environment

Northern West Virginia and southwestern Pennsylvania was covered by an epicontinental sea in the early Carboniferous (Busanus 1974). Tectonic activity during the latter part of the Mississippian produced a general retreat of the sea to the southwest yielding the terrestrial–fluvial–lacustrine deposits characteristic of the Mauch Chunk Group. At Greer, West Virginia, the Bluefield Formation, which forms the lower subdivision of the Mauch Chunk Group, is exposed as four units (from bottom to top): the Lillydale Shale, the Glenray Limestone, the Bickett Shale, and the Renolds Limestone. The Bickett Shale, from which all vertebrate remains were recovered, appears to represent a local, geologically momentary fluvio-deltaic sequence deposited along the northwest margin of the retreating sea. Rapid lateral changes in lithology from thin-bedded red or green shales to massive red siltstones or grey-green micaceous channel sandstones characterize the Bickett Shale and reflect local depositional environments (Busanus 1974, 1976). The invertebrate fauna within this unit is limited to a non-marine or brackish water bivalve, an inarticulate brachiopod and a suite of ostracods. Many of the vertebrate remains are disarticulated and fragmentary, forming bone beds that could represent final lag concentrations (Elliott & Taber 1982). The mixture of isolated vertebrate remains in these bone beds led Busanus (1974) and Elliott & Taber (1982) to conclude that the elements were probably transported by moving water of rather high energy levels for some distance before deposition.

In addition to the bone beds, only one known long and narrow lenticular grey-green sandstone deposit produced articulated vertebrate remains. The degree of skeletal articulation suggests a depositional environment with at least temporary quiet water conditions. The

PHILOSOPHICAL TRANSACTIONS OF THE ROYAL SOCIETY B BIOLOGICAL SCIENCES

unusually high density of vertebrate remains suggests a sudden mass death, although the cause(s) remains unclear. The absence of mudcracks in this deposit prompted Busanus (1974) to hypothesize that a sudden temporary influx of salt water from the sea to the southwest may have been responsible. Bathing of the fluvio-deltaic complex by minor transgressions of the sea is believed to have occurred periodically during deposition of the Bickett Shale. An alternative thesis suggests that the Greer lithology represents alluvial plain deposits, with the red and green coloration the result of oxidized floodplains.

Along with *G. burkemorani*, this deposit produced fully articulated skeletons of the lungfish *Tranodis castrensis* and partly articulated skeletons of the anthracosaur *Proterogyrinus scheelei* (figure 27). Other vertebrate remains collected from Greer by the Museum of Comparative Zoology, the Cleveland Museum of Natural History, the West Virginia Geological and Economic Survey, and the West Virginia University include numerous *Gyracanthus* spines, one shark spine (M. Williams (CMNH), personal communication), a tooth plate that may represent a form similar to *Uronemus* (Elliott & Taber 1982), clusters of scales and teeth of palaeoniscoids, isolated cranial and postcranial elements of a large rhizodontiform crossopterygian (possibly *Strepsodus*) and at least two other unnamed tetrapods (Godfrey 1988).

Palynological analysis of the grey-green sandstone associated with one specimen of *G. burkemorani* provided no information on the flora in the vicinity of the depositional environment (J. McAndrews, personal communication 1982).

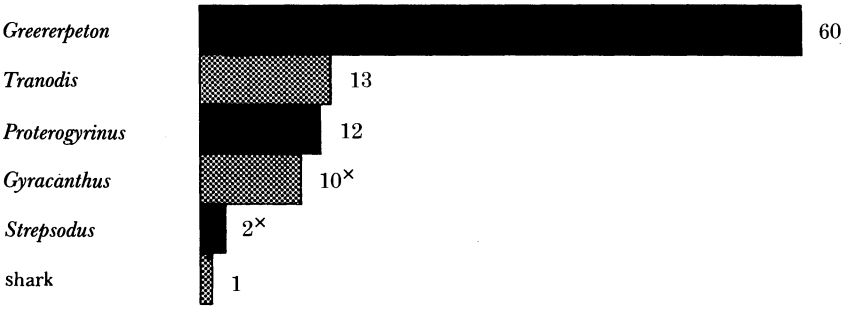

FIGURE 27. Census of the vertebrate fossils recovered from Greer. The superscript × indicates that fragmentary remains of these forms are abundant.

Ecology of Greererpeton

Comparison of the anatomy of *G. burkemorani* with that of the living giant salamanders (Cryptobranchidae) provides some useful insights into its possible mode of life.

There are two extant species of Asian giant salamanders, *Andrias davidianus* and *A. japonicus*. The Japanese giant salamander, *A. japonicus*, is the larger and may attain a length of more than 1.5 m (Freytag 1974), about the same size as an adult *G. burkemorani*. The head and body are strongly depressed except for the terminal two thirds of the tail, which is strongly compressed laterally. The tail is short, only slightly more than one third of the snout–vent length. Both pectoral and pelvic limbs are stout, with four and five digits respectively (Stejneger 1907).

All giant salamanders live entirely submerged, chiefly on the floor of shallow streams and rivers with clear, fast-flowing water. *Andrias japonicus* usually lives at depths between 2 and 8 m, where it hides beneath rocks, in cavities or other dark recesses. Small and middle-sized individuals are found near the surface of the water, whereas older giant salamanders prefer

PHILOSOPHICAL TRANSACTIONS OF THE ROYAL SOCIETY B BIOLOGICAL SCIENCES

deeper water, and migrate downstream in large rivers. These salamanders are active primarily at night and feed on fishes, frogs, crustaceans, earthworms and insects.

The head and body of *G. burkemorani* were also dorsoventrally compressed in life; a conclusion based on the height of the skull, the dermal pectoral girdle, and the curvature of the ribs. In most cases, isolated skulls and all articulated skeletons of *G. burkemorani* are preserved with the frontal plane parallel to the bedding plane (figures 2, 3, and 4), whereas the caudal portion of articulated specimens lies with its sagittal plane parallel to the bedding horizon (figure 3). This pattern of preservation strongly suggests that *G. burkemorani* was dorsoventrally compressed from snout to vent whereas its tail was laterally compressed. Its limbs are of similar proportions to those of *Andrias*. A well-developed lateral line system in the dermal bone of the skull in *G. burkemorani* strongly suggests that it spent its entire life in water. The dorsally directed orbits in adults may have been an adaptation to exploit a benthonic environment. The bias towards large individuals in the Cleveland collection (Godfrey 1989, figure 1) may reflect habitat selection or segregation with respect to individual size. If, as in *Andrias*, young of *G. burkemorani* lived in shallow water with older individuals migrating 'downstream' to deeper water, then the highly productive deposit at Greer might accurately reflect the ratio of juveniles to adults living in the vicinitiy of the depositional environment.

Relationships of Greererpeton

The complex taxonomic history of the family Colosteidae, the position of *G. burkemorani* within the family, and the plesiomorphic status of the family within the context of the Temnospondyli have been addressed recently by Smithson (1982) and Hook (1983). Their results need not be repeated here, as I do not wish to contest their findings. Nevertheless, a description of the postcranial skeletal anatomy of *G. burkemorani* has prompted a re-examination of the distribution of apomorphic skeletal features among some early tetrapods. To simplify the task, only four of the earliest and most completely known tetrapods were included in the analysis: *Ichthyostega* sp., *Crassigyrinus scoticus*, *Greererpeton burkemorani* and *Proterogyrinus scheelei*. Each taxon is a basal member of a larger tetrapod assemblage: the Ichthyostegalia, the Palaeostegalia, the Temnospondyli, and the Anthracosauria respectively. Many of the characters (Appendix 3) were compiled from publications by Clack & Holmes (1988), Gaffney (1979), Holmes (1984), Jarvik (1980), Panchen (1985), Panchen & Smithson (1987), Schultze (1986), Schultze & Arsenault (1985), and Smithson (1982, 1985). Osteolepiform fish (more specifically panderichthyid osteolepiform fish) form the outgroup for this analysis (Holmes 1985; Schultze & Arsenault 1985; Shultze 1986; Panchen & Smithson 1987). The results are presented in figure 28*a*.

On the basis of the distribution of the characters among the four taxa, the most parsimonious cladogram is that of figure 28*a*. The arrangement of the taxa in figure 28*a* differs, however, from those of Smithson (1985) and Panchen (1985). Smithson hypothesized that all early tetrapods could be placed on one of two major branches. The first branch of the dichotomy included the ichthyostegalians, temnospondyls, microsaurs and their descendents, the extant amphibians. This assemblage was united by three synapomorphies: (1) an akinetic skull in which the ventral otic fissure was retained; (2) a platybasic skull; and (3) ribs bearing uncinate processes. The other branch included all remaining tetrapods: anthracosaurs, diadectomorphs, *Crassigyrinus*, loxommatoids, aistopods, nectrideans, and amniotes. These forms (1) retained cranial kinesis between the skull table and cheek; (2) eliminated the ventral otic fissure; and

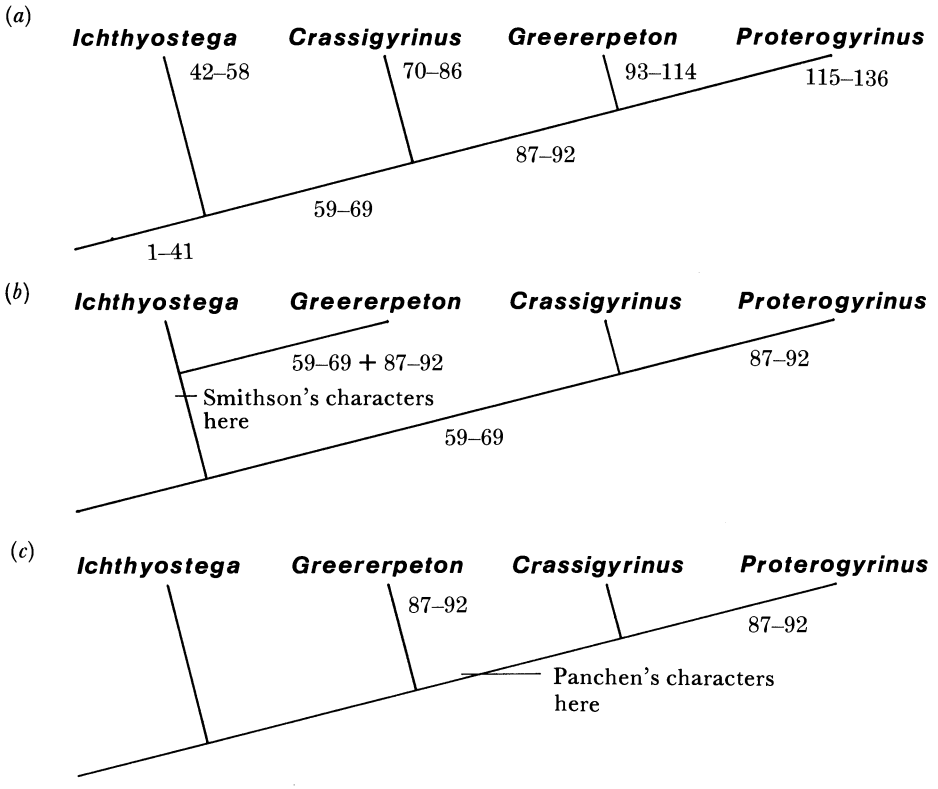

FIGURE 28. (*a*) Cladogram illustrating hypothesis of the relationships among some early tetrapods. The numbers correspond to the characters listed in Appendix 3. (*b*, *c*) Rearrangement of the four taxa in (*a*) to illustrate their implied relationships as proposed by Smithson (1985) and Panchen (1985) respectively (see text). In (*b*) and (*c*), the numbers presented correspond to the characters listed in (*a*) that would have to occur independently in the given lineage.

(3) their basal articulation exhibited clearly defined articulating surfaces (Smithson 1985). Smithson had to assume, however, that ichthyostegid characters traditionally viewed as having been lost before the appearance of other major groups of tetrapods ('... the suboperculum, caudal fin rays, the ventral otic fissure and the notochordal tunnel, as well as a reduction in size of the cleithrum and the development of : an open lateral line sulci, a peg and socket basal articulation and a craniocervical joint' (Smithson 1985, p. 395)), did so independently on both sides of the dichotomy (figure 28*b*). Study of the skeletal anatomy of *Ichthyostega*, *G. burkemorani* and *Proterogyrinus* has brought several more characters to light. If *G. burkemorani* were in fact more closely related to *Ichthyostega* than *Proterogyrinus*, the loss or acquisition of characters 59 though 69 and 87 through 92 would have had to occur independently on both sides of the dichotomy (figure 28*b*). Even though many of these characters are 'loss' characters, for all to have occurred independently on both sides of the dichotomy seem quite unlikely. If my scheme is to be accepted, Smithson's three characters are either primitive or homoplastic in *Ichthyostega* and *G. burkemorani*.

Although Panchen (1985) did not comment on the position of *Ichthyostega* and *G. burkemorani*, he proposed a sister-group relationship between *Crassigyrinus* and anthracosaurs (*Proterogyrinus*, as in figure 28*b* or 28*c*) that would exclude *G. burkemorani* from its possible sister-group relationship with *Proterogyrinus*. Although this relationship is based primarily on four characters ((1) the dermal ornament on the skull roof and dermal pectoral girdle; (2) the tabular horns;

PHILOSOPHICAL TRANSACTIONS OF THE ROYAL SOCIETY B BIOLOGICAL SCIENCES

(3) the lack of posttemporal fossae; and (4) the histology of the teeth), they present the best challenge to the arrangement of the taxa in figure 28*a*. The node defined by the fewest number of characters in figure 28*a* occurs between *Crassigyrinus* on the one hand and *G. burkemorani* and *Proterogyrinus* on the other. The node is defined almost exclusively by 'loss' characters, which may or may not be as reliable as possessing evolutionary novelties to demonstrate monophyly unequivocally. It is possible that characters 87 through 92 occurred polyphyletically, i.e. on one branch leading to *G. burkemorani* and on another leading to *Crassigyrinus* and *Proterogyrinus* (figure 28*c*). If the hypothesis presented in figure 28*a* is correct then Panchen's four features are either primitive or homoplastic within the Tetrapoda.

I thank Dr R. L. Carroll under whose guidance this project was undertaken. I am indebted to Dr M. Williams and the Cleveland Museum of Natural History for their permission to study *G. burkemorani*. Collection and most of the preparation of the specimens was done by the staff of the Cleveland Museum supported by the United States National Science Foundation, grant G.B.-35474.

I also thank Dr D. Baird, Dr H. Bjerring, Dr R. Carroll, Dr J. Chorn, Dr R. Holmes, Dr R. Hook, Dr E. Jarvik, Dr A. Panchen, Dr H.-P. Schultze, Dr D. Walsh and Dr C. Wellstead for liberal exchange of information and contributing to stimulating discussions on the origin and evolution of early tetrapods.

I am grateful to Mrs. P. Gaskill for preparing specimen drawings 3, 5, and 23. My thanks are due to Mr. C. Schaff (Museum of Comparative Zoology, Harvard University) for the loan of comparative skeletal material, Dr J. McAndrews (Royal Ontario Museum) for palynological work, and Mr R. Lamarche and Mr G. L'Heureux (McGill) for photographic work. Editorial comments by Dr R. Carroll, Dr R. Holmes, Dr B. Hook, Dr H.-P. Schultze, Dr D. Walsh, Ms C. Wright and two anonymous reviewers significantly improved this paper.

This research was supported by the Natural Sciences and Engineering Research Council of Canada and McGill University.

Appendix 1. Specimens studied

CMNH (Cleveland Museum of Natural History)

10931. Holotype, crushed skull and scattered postcranial material. Figured specimen, Romer (1969).

10939. Disarticulated skeleton, poorly preserved, no skull.

11034. Skull and some postcranial material, associated with 11036 and 11082. Figured specimen, Romer (1972).

11036. Good skull and postcranial elements. Figured specimen, Romer (1972).

11068. Largest complete skull and skeleton, associated with 11069 and 11070. Figured specimen, Smithson (1982).

11069. Complete subadult skull, lacking postcranial skeleton except anterior cervical region.

11070. Good subadult postcranial skeleton, no skull.

11072. Compressed skull, no braincase, stapes or postcranial material.

11073. Good skull, disarticulated anterior axial elements.

11073(2). Second individual with the same number. Severely crushed skull of a subadult.

PHILOSOPHICAL TRANSACTIONS OF THE ROYAL SOCIETY B BIOLOGICAL SCIENCES

11079. Right half of a skull, includes a good braincase. Figured specimen, Smithson (1982). Braincase figured by Godfrey (1989).

11082. Good skull and postcranial material. Figured specimen, Romer (1972).

11090. Best-preserved and most complete specimen known. Portions of this specimen were figured by Carroll (1980) and Smithson (1982).

11092. Articulated posterior presacral and caudal vertebrae, includes portions of the pelvic girdle and limb.

11093. Good, but incomplete, subadult skull, no postcranial material known.

11095. Smallest specimen known; partial skull and clavicle. Figured specimen, Godfrey (1989).

11113. Incomplete juvenile skull, scattered postcranial elements and an isolated femur; probably not from the same individual. Figured specimen, Godfrey (1989).

11129. Anterior segment of the snout, premaxilla.

11130. Virtually complete skull, little postcranial material. Stapes figured by Smithson (1982) and Godfrey (1989).

11131. Fairly complete skull, poorly exposed axial skeleton.

11132. Good skull and articulated skeleton.

11133. Lower mandible attached to 11132.

11219. Fairly good skull, but poorly preserved postcranial skeleton. Associated with 11220.

11220. Fairly complete skull, lacks the left cheek and the lower left mandible.

11231. Incomplete and poorly preserved skull. Braincase figured, Godfrey (1989).

11232. Right pelvic limb, well preserved.

11233. Skull and postcranial remains.

11234. Severely distorted skull, includes some elements of the anterior postcranial skeleton.

11238. Disarticulated remains of the entire skeleton.

11240. Partial skull and skeleton of one of the largest individuals known. Stapes figured by Smithson (1982).

11241. Incompletely prepared skull and postcranial skeleton, associated with pelvic limb elements of *Proterogyrinus*.

11319. Large crushed skull. Braincase figured by Smithson (1982) and Godfrey (1989).

11320. Good skull and anterior postcranial skeleton of a juvenile. Figured specimen, Godfrey (1989).

FN 23. Anterior presacral elements of the axial and pectoral skeleton.

USNM (United States National Museum)

22576. Anterior portion of two skulls and one skeleton.

PHILOSOPHICAL TRANSACTIONS OF THE ROYAL SOCIETY B BIOLOGICAL SCIENCES

Appendix 2. postcranial measurements

CMNH	interclavicle length/cm	interclavicle width (maximum)/cm
10931	5.3‡	—†
11036	—	5.8‡
11070	5.7‡	—†
11073	7.7‡	5.5‡
11090	7.7	5.5
11233	5.5‡	5.1‡
11240	—†	5.3‡
FN 23	7.5‡	6.9
11320	3.4‡	2.2

CMNH		clavicle length/cm	clavicle width/cm	cleithrum length/cm
10931	right	4.7	2.6‡	—†
	left	4.6	2.9	—†
11036	left	—†	—†	5.5‡
11068	right	—†	—†	7.6‡
	left	—†	—†	6.4‡
11069	right	5.3	2.8‡	—†
11070	right	—†	—†	2.8‡
	left	3.7‡	2.3	3.7
11073	right	6.2	2.8‡	4.7‡
11090	right	4.9	3.8	5.8
	left	5.0	2.8‡	2.6‡
11095	left	1.4	0.7	—†
11233	right	—†	—†	4.0‡
	left	4.8‡	—†	4.7‡
11240	right	6.8	4.0‡	—†
	left	5.5‡	4.3‡	—†
FN 23	right	4.2‡	3.8	—†
	left	6.3	3.0	—†
11320	right	—†	—†	2.6
USNM 22576	left	—†	—†	5.6

CMNH		humerus length/cm	ulna length/cm	radius length/cm
10931	left	2.6	—†	—
11036	left	—†	1.6	1.6
11068	right	3.5	—†	—†
	left	—†	2.7	2.0
11070	right	2.4	1.6	—†
	left	1.9	—†	1.5
11073	right	2.6	—†	—†
11090	right	2.9	2.4	1.9
	left	3.2	2.2	1.8
11320	right	0.9	—†	—†
USNM 22576	left	2.8	—†	—†

† Element missing.
‡ Element incomplete, obscured by matrix or other bone.

PHILOSOPHICAL TRANSACTIONS OF THE ROYAL SOCIETY B BIOLOGICAL SCIENCES

APPENDIX 2 (*cont.*)

CMNH		femur length/cm	tibia length/cm	fibula length/cm
10931	right	3.5	2.2	—†
	left	4.0	2.2	—†
11068	right	6.1	2.6	—†
	left	5.9	2.7	3.1
11070	right	—†	—†	—†
	left	3.1	2.0	2.0
11090	right	4.9	—†	2.7
	left	5.0	2.4	—†
11092	right	4.0	2.0	—†
	left	4.0	2.0	2.1
11113	right	4.2	—†	—†
11132	left	4.1	2.2	—†
11220	right	4.1	2.3	—†
11232	right	5.1	2.2	2.1
11236	right	3.7‡	2.1	—†
	left	3.9	—†	—†
11238	right	5.1	—†	—†

† Element missing.
‡ Element incomplete, obscured by matrix or other bone.

APPENDIX 3. CHARACTERS USED IN FIGURE 28

A question mark (?) follows those characters of which the level of apomorphy remains uncertain.

Tetrapod autapomorphies include:

(1) a single pair of nasal bones;
(2) parietals that are wider than the frontals;
(3) postparietals that are shorter than the parietals;
(4) a tabular tubercle (or tuberosity) on this element's occipital surface;
(5) a jugal that forms at least half of the ventral margin of the orbit;
(6) a medial abutment of the pterygoids anterior to or below the cultriform process;
(7) no operculum;
(8) no median gular;
(9) no submandibulars;
(10) a 'peg and socket' basicranial articulation;
(11) a fenestra ovalis in the otic capsule (?), not yet known in *Ichthyostega* or *Crassigyrinus*;
(12) a stapes (?), not yet known in *Ichthyostega* or *Crassigyrinus*;
(13) an unossified laterosphenoid region of the braincase (but see Clack & Holmes (1988));
(14) a sphenethmoid that is Y-shaped anteriorly and V-shaped posteriorly (?);
(15) loss of tusk and replacement pits on at least one of the coronoids;
(16) some lateral line organs (neuromast system) held in canals, no longer covered by bone (lower mandible);
(17) dermal sculpturing consists of deep polygonal pits or troughs surrounded by raised ridges;

PHILOSOPHICAL TRANSACTIONS OF THE ROYAL SOCIETY B BIOLOGICAL SCIENCES

(18) neural arch elements of the atlas–axis complex consist of paired pro- and atlas arches, and a relatively massive axis arch, condition not yet known in *Ichthyostega*;

(19) well-developed pre- and postzygapophyses;

(20) ribs that are well developed and turned ventrally;

(21) ribs that extend from the atlas neural arch to caudal 5 or 6;

(22) the loss of all the bones above the cleithrum;

(23) a large dorsally expanded scapular blade;

(24) a shaft-like cleithrum;

(25) a large interclavicle with a ventral exposure that is longer than the ventral exposure of either the clavicle or scapulocoracoid;

(26) a preaxial keel on the humerus that extends from the caput humeri to the ectepicondyle;

(27) an entepicondyle that is square to rhomboidal in dorsal view;

(28) an olecranon on the ulna;

(29) carpal and tarsal elements;

(30) distinct digits (dactyli);

(31) at least one pair of sacral ribs;

(32) a long posterolaterally directed sacral rib that lay against the mesial face of the ilium (distal end did not abut at about right angles with the ilium);

(33) a pubis, ischium and ilium form each half of the pelvic girdle;

(34) an anterior and posterior tongue-like projection on either side of the supra-acetabular buttress;

(35) a laterally directed acetabulum (?);

(36) a pubo-ischiadic plate that is pierced by at least one foramen (two foramina may be the primitive number for tetrapods, see *Ichthyostega* and *Proterogyrinus*);

(37) a well-developed adductor crest on the femur (?);

(38) two canals that pierce the distal end of the femur (may represent an autopomorphy of *Ichthyostega*);

(39) wrist and knee joints that are hinge-like, whereas elbow and ankle joints are rotary;

(40) an articular condyle on the distal end of the tibia;

(41) an intermedium that articulates directly with the tibia and fibula.

Apomorphies of *Ichthyostega* include:

(42) loss of intertemporal (variable in *Greererpeton*) and a broad postorbital–parietal contact, also occurs in *Greererpeton*;

(43) an orbital margin from which the lacrimal is excluded, also occurs in *Crassigyrinus*;

(44) a premaxilla that does not contribute to the formation of the internal naris;

(45) loss of cranial kinesis, also occurs in *Greererpeton* (might be primitive for tetrapods);

(46) no trace of denticles on the palate;

(47) prominent flanges that descend from the dermal skull roof to hold the braincase;

(48) a small foramen that pierces the pterygoid on either side of the cultriform process;

(49) loss of abdominal gastralia (?);

(50) ribs that possess large uncinate flanges, some of which are pierced by one or two foramina (might be primitive for tetrapods);

(51) a long and slender parasternal process on the interclavicle (?) (might be primitive for tetrapods);

PHILOSOPHICAL TRANSACTIONS OF THE ROYAL SOCIETY B BIOLOGICAL SCIENCES

(52) a supraglenoid process on the scapulocoracoid;
(53) a radius that articulates on the ventral surface of the humerus;
(54) a large and conspicuous longitudinal keel or carina along the lateral margin of the ulna;
(55) a posterior iliac process (?), might be homologous with that seen in *Proterogyrinus* (might be primitive for tetrapods);
(56) an iliac canal (?);
(57) a tibia that is L-shaped in cross section;
(58) a phalangeal formula of 2 (3?), 3, 3, 3, 3 for the pes (primitive pattern for tetrapods remains unknown).

The following synapomorphies unite *Crassigyrinus*, *Greererpeton*, and *Proterogyrinus*:
(59) parietals that no longer extend anterior to a transverse line through the midpoint of orbit length;
(60) an otico-occipital moiety of the parasphenoid that bears a longitudinal median groove or trough in ventral view;
(61) loss of palatal teeth along the mesial margin of the internal nares;
(62) loss of the fossa hypophyses (buccohypophysial foramen) on the parasphenoid;
(63) a dentary that no longer extends posteriorly to the level of the articular;
(64) no subopercular;
(65) loss of caudal fin rays;
(66) loss of the notochordal tunnel beneath the braincase in adults (?);
(67) a unipartite braincase in which the parasphenoid bridges the fissure between the ethmoid and otico-occipital moieties and extends posteriorly, but not all the way back to the posterior margin of the basioccipital;
(68) basipterygoid processes that evince troughs or foramina for vascular and/or nervous tissue along their mesial margins (?);
(69) posterolateral unsculptured margins on the ventral surface of the interclavicle on to which the gastralia rabbet.

Apomorphies of *Crassigyrinus* include:
(70) loss of posttemporal fossae (might be primitive for tetrapods, posttemporal fossae may not be homologous with osteolepiform fossa Bridgei);
(71) loss of vomerine fangs (?), also lost in *Proterogyrinus*;
(72) large quadrangular orbits;
(73) constricted parietals and frontals between the orbits (?);
(74) a deep cheek below the orbit;
(75) an orbital margin from which the lacrimal is excluded;
(76) parasymphysial tusks that are not bounded laterally by the marginal tooth row, also present in *Greererpeton*;
(77) pterygoids that do not meet anterior to the cultriform process (retention of, or a reversal to, an osteolepiform configuration (?));
(78) additional tusk-like teeth on the palate;
(79) anthracosaur-like dermal ornament;
(80) a fenestra between the premaxillae;
(81) tusk peaks along the dentary;

PHILOSOPHICAL TRANSACTIONS OF THE ROYAL SOCIETY B BIOLOGICAL SCIENCES

(82) a series of pits on the mesial surface of the dentary below the tooth row;
(83) a precoronoid (coronoid 1) that extends forward to contribute to the formation of the symphysis (coronoid 1 may include an adsymphysial tooth-plate which would then make it primitive, an adsymphysial tooth-plate is present in osteolepiform fish);
(84) no well-formed postzygapophyses;
(85) conspicuous sulci along the anterolateral and posteromesial margins of the clavicles;
(86) minute forelimbs.

The following synapomorphies unite *Greererpeton* and *Proterogyrinus*:
(87) loss of the anterior tectal;
(88) loss of the preopercular;
(89) loss of the ectepicondyle foramen;
(90) loss of the canal 'd' on the humerus;
(91) *tubera parasphenoidales*;
(92) four centralia in the tarsus (level remains uncertain as the condition in *Crassigyrinus* and *Ichthyostega* remain unknown to the author).

Apomorphies of *Greererpeton* include:
(93) loss of the intertemporal (variable) and a broad postorbital–parietal contact;
(94) loss of cranial kinesis;
(95) a postparietal–exoccipital contact;
(96) interpterygoid vacuities;
(97) an elongate prefrontal;
(98) a prefrontal–maxilla suture that excludes the lacrimal from the narial margin;
(99) loss of the squamosal embayment;
(100) a single pair of premaxillary tusks;
(101) a large notch in the dentary to accommodate the premaxillary tusk;
(102) parasymphysial tusks that are not bounded laterally by the marginal tooth row;
(103) *tubera parasphenoidales* that are divided by a prominent median ridge;
(104) dentary teeth that are larger than maxillary teeth;
(105) two pairs of teeth on the precoronoid (coronoid 1);
(106) a single elongate Meckelian fenestra;
(107) a dorsoventrally compresed skull and postcranial skeleton;
(108) approximately 40 presacral vertebrae;
(109) a small posterolaterally directed uncinate process on some of the ribs;
(110) no supraglenoid foramen;
(111) a single undivided iliac blade;
(112) a four-digit manus with a phalangeal formula of 2, 2, 3, 3 (?), and a phalangeal formula of 2, 2, 3, 4, 3 (or 4) for the pes;
(113) gastralia with a crenulated posterior margin;
(114) dorsal scalation consists of a mosaic of small ovoid scales.

Apomorphies of *Proterogyrinus* include:
(115) biramic tabular horns;
(116) a tabular–parietal suture;
(117) loss of the posttemporal fossa;

PHILOSOPHICAL TRANSACTIONS OF THE ROYAL SOCIETY B BIOLOGICAL SCIENCES

(118) opisthotics that are fused medially to form an occipital plate, no supraoccipital dorsal to the foramen magnum;

(119) a vena capitis dorsalis foramen;

(120) a median retractor pit anterior to the dorsum sellae;

(121) a jugal that enters the lower skull margin (processus alaris);

(122) an ectopterygoid that is excluded from the subtemporal fossa;

(123) loss of vomerine fangs;

(124) a descending flange on the pterygoid;

(125) light dermal sculpture;

(126) a surangular crest;

(127) two large Meckelian fenestrae;

(128) pleurocentra that are complete ventrally;

(129) at least 32 presacral vertebrae;

(130) cervical ribs that are greatly expanded into flattened plates distally;

(131) a short sacral rib, the distal end of which rests (at about right angles, as seen in dorsal view) against the mesial surface of the ilium;

(132) ascending clavicular spine becomes wider dorsally;

(133) ilium biramic;

(134) fourth centrale intervenes between the tibiale and intermedium to make contact with tibia;

(135) tibiale and fourth centrale fuse;

(136) a phalangeal formula of 2, 3, 4, 5, 4 and 2, 3, 4, 5, 5 for the manus and pes respectively.

(Some of the apomorphies attributed to the four taxa are in fact autapomorphies for larger assemblages of which they are members; the levels of apomorphy have not been specified.)

References

Andrews, S. M. & Westoll, T. S. 1970 The postcranial skeleton of *Eusthenopteron foordi* Whiteaves. *Trans. R. Soc. Edinb.* **68**, 207–329.

Busanus, J. W. 1974 Paleontology and paleoecology of the Mauch Chunk Group in Northwestern West Virginia. M.Sc. thesis, Bowling Green State University.

Busanus, J. W. 1976 Faunal distribution within the Greerbrier–Mauch Chunk Transition (Chesterian: Elviran) along the Chestnut Ridge Anticline. [Abstract.] *Abstracts of the northeast and southeast sections of the G.S.A. annual meeting* **8**, number 2.

Carroll, R. L. 1970 The ancestry of reptiles. *Phil. Trans. R. Soc. Lond.* B **257**, 267–308.

Carroll, R. L. 1980 The hyomandibular as a supporting element in the skull of primitive tetrapods. In *The terrestrial environment and the origin of land vertebrates*, Systematics Association special volume no. 15 (ed. A. L. Panchen), pp. 293–317. London: Academic Press.

Carroll, R. L. & Gaskill, P. 1978 The Order Microsauria. *Mem. Am. Phil. Soc.* **126**, 1–211.

Case, E. C. 1935 Description of a collection of associated skeletons of *Trimerorhachis*. *Contr. Mus. Paleontol. Univ. Mich.* **4**, 227–274.

Chase, J. N. 1965 *Neldasaurus wrightae*, a new rhachitomous labyrinthodont from the Texas Lower Permian. *Bull. Mus. Comp. Zool. Harv.* **133**, 153–225.

Chorn, J. D. 1984 A trimerorhachid amphibian from the Upper Pennsylvanian of Kansas. Ph.D. thesis, University of Kansas.

Clack, J. A. & Holmes, R. 1988 The braincase of the anthracosaur *Archeria crassidisca* with comments on the interrelationships of primitive tetrapods. *Palaeontology* **31**, 85–107.

Elliott, D. K. & Taber, A. C. 1982 Mississippian vertebrates from Greer, West Virginia. *Proc. West Virginia Acad. Sci.* **4**, 73–80.

PHILOSOPHICAL TRANSACTIONS OF THE ROYAL SOCIETY B BIOLOGICAL SCIENCES

Freytag, G. E. 1974 Urodeles and caecilians. In *Grzimek's animal life encyclopedia*, volume 5 – Fishes II/Amphibians (ed. B. Grzimek), pp. 315–316. New York: Van Nostrand Reinhold Company.
Fritsch, A. 1889 *Fauna der Gaskohle und der Kalksteine der Permformation Bohemens*, volume 2. Prague.
Gaffney, E. S. 1979 Tetrapod monophyly: a phylogenetic analysis. *Bull. Carnegie Mus. nat. Hist.* **13**, 92–105.
Godfrey, S. J. 1988 Isolated tetapod remains from the Carboniferous of West Virginia. *Kirtlandia* **43**, 27–36.
Godfrey, S. J. 1989 Ontogenetic changes in the skull of the Carboniferous tetrapod *Greererpeton burkemorani* Romer, 1969. *Phil. Trans. R. Soc. Lond.* B **323**, 135–153.
Hanken, J. 1982 Appendicular skeletal morphology in minute salamanders, genus *Thorius* (Amphibia: Plethodontidae): growth regulation, adult size determination, and natural variation. *J. Morph.* **174**, 57–77.
Holmes, E. B. 1985 Are lungfishes the sister-group of tetrapods? *Biol. J. Linn. Soc.* **25**, 379–397.
Holmes, R. 1980 *Proterogyrinus scheelei* and the early evolution of the labyrinthodont pectoral limb. In *The terrestrial environment and the origin of land vertebrates*, Systematics Association special volume no. 15 (ed. A. L. Panchen), pp. 351–376. London: Academic Press.
Holmes, R. 1984 The Carboniferous amphibian *Proterogyrinus scheelei* Romer, and the early evolution of tetrapods. *Phil. Trans. R. Soc. Lond.* B **306**, 431–527.
Holmes, R. 1989 Manuscript in preparation.
Hook, R. W. 1983 *Colosteus scutellatus* (Newberry), a primitive temnospondyl amphibian from the Middle Pennsylvanian of Linton, Ohio. *Am. Mus. Novit.* **2770**, 1–41.
Hook, R. W. & Baird, D. 1984 *Ichthycanthus platypus* Cope, 1977, reidentified as the dissorophoid amphibian *Amphibamus lyelli*. *J. Paleont.* **58**, 697–702.
Hotton, N. 1970 *Mauchchunkia bassa* gen. et sp. nov., an anthracosaur (Amphibia, Labyrinthodontia) from the Upper Mississippian. *Kirtlandia* **12**, 1–38.
Howie, A. A. 1972 On a Queensland labyrinthodont. In *Studies in vertebrate evolution* (ed. K. A. Joysey & T. S. Kemp), pp. 51–64. New York: Winchester Press.
Jarvik, E. 1980 *Basic structure and evolution of vertebrates* (2 volumes). London: Academic Press.
Miner, R. W. 1925 The pectoral limb of *Eryops* and other primitive tetrapods. *Bull. Am. Mus. nat. Hist.* **51**, 145–312.
Moulton, J. M. 1974 A description of the vertebral column of *Eryops* based on the notes and drawings of A. S. Romer. *Breviora* **428**, 1–44.
Panchen, A. L. 1966 The axial skeleton of the labyrinthodont *Eogyrinus attheyi*. *J. Zool.* **150**, 199–222.
Panchen, A. L. 1975 A new genus and species of anthracosaur amphibian from the Lower Carboniferous of Scotland and the status of *Pholidogaster pisciformis* Huxley. *Phil. Trans. R. Soc. Lond.* B **269**, 581–640.
Panchen, A. L. 1985 On the amphibian *Crassigyrinus scoticus* Watson, from the Carboniferous of Scotland. *Phil. Trans. R. Soc. Lond.* B **309**, 505–568.
Panchen, A. L. & Smithson, T. R. 1987 Character diagnosis, fossils and the origin of tetrapods. *Biol. Rev.* **62**, 341–438.
Parrington, F. R. 1948 Labyrinthodonts from South Africa. *Proc. zool. Soc. Lond.* **118**, 426–445.
Romer. A. S. 1947 Review of the Labyrinthodontia. *Bull. Mus. comp. Zool. Harv.* **99**, 1–366.
Romer, A. S. 1957 The appendicular skeleton of the Permian embolomerous amphibian *Archeria*. *Contr. Mus. Paleontol. Univ. Mich.* **13**, 103–159.
Romer, A. S. 1969 A temnospondylous labyrinthodont from the Lower Carboniferous. *Kirtlandia* **6**, 1–20.
Romer, A. S. 1970 A new anthracosaur labyrinthodont *Proterogyrinus scheelei*, from the Lower Carboniferous *Kirtlandia* **10**, 1–16.
Romer, A. S. 1972 A Carboniferous labyrinthodont amphibian with complete dermal armor. *Kirtlandia* **16**, 1–8.
Schaeffer, B. 1941 The morphology and functional evolution of the tarsus in amphibians and reptiles. *Bull. Am. Mus. nat. Hist.* **78**, 395–472.
Schultze, H.-P. 1986 Dipnoans as sarcopterygians. *J. Morph.* suppl. 1, 39–74.
Schultze, H.-P. & Arsenault, M. 1985 The panderichthyid fish *Elpistostege*: a close relative of tetrapods? *Palaeontology* **28**, 293–309.
Smithson, T. R. 1982 The cranial morphology of *Greererpeton burkemorani* Romer (Amphibia: Temnospondyli). *Zool. J. Linn. Soc.* **76**, 29–90.
Smithson, T. R. 1985 The morphology and relationships of the Carboniferous amphibian *Eoherpeton watsoni* Panchen. *Zool. J. Linn. Soc.* **85**, 317–410.
Smithson, T. R. & Thomson, K. S. 1982 The hyomandibular of *Eusthenopteron foordi* Whiteaves (Pisces: Crossopterygii) and the early evolution of the tetrapod stapes. *Zool. J. Linn. Soc.* **74**, 93–103.
Steen, M. 1937 On *Acanthostoma vorax* Credner. *Proc. Zool. Soc. Lond.* B **107**, 491–500.
Stejneger, L. 1907 Herpetology of Japan and adjacent territory. *Bull. U.S. natn. Mus.* **58**, 1–577.

PHILOSOPHICAL TRANSACTIONS OF THE ROYAL SOCIETY B BIOLOGICAL SCIENCES

Abbreviations used in the figures

ang	angular
art	articular
art. rad., uln.	articular facets for the radius and ulna on the humerus
at	atlas arch
ax	axis arch
b.p	basal process
basi	basioccipital
c	canal c
c1	1st centrale
c2	2nd centrale
c3	3rd centrale
c4	4th centrale
clav	clavicle
clei	cleithrum
cor. pl	coracoid
cul	cultriform process
d	dentary
d.n	dentary notch
d.p.c	deltopectoral crest
dscl	dorsal dermal scales
dtl	first distal tarsal
ecte	ectepicondyle
ent	entepicondyle
ent. f	entepicondyle foramen
f. obt	obturator foramen
fe	fibulare
fem	femur
fib	fibula
gas	gastralia
gl	glenoid
gl. f	glenoid foramen
ha	haemal arch
hum	humerus
i	intermedium
ic	intercentrum
icl	interclavicle
il	ilium
ish	ischium
m	maxilla
m. lat. d	tuberosity for m. latissiumus dorsi
mt1	first metatarsal
mt5	fifth metatarsal
na	neural arch
pa	parasphenoid
pc	pleurocentrum
pp	postparietal
pra	prearticular
prm	premaxilla
psp	postsplenial
pt	pterygoid
pub	pubis
q	quadrate
rad	radius
rib	rib
sac. rib	sacral rib
sc	scapulocoracoid
sph	sphenethmoid
stap	stapes
sup	supinator flange
supc. f	supracoracoid foramen
sur	surangula
te	tibiale
tib	tibia
uln	ulna
un. pr	uncinate process
1–5	digits

PHILOSOPHICAL TRANSACTIONS OF THE ROYAL SOCIETY B BIOLOGICAL SCIENCES

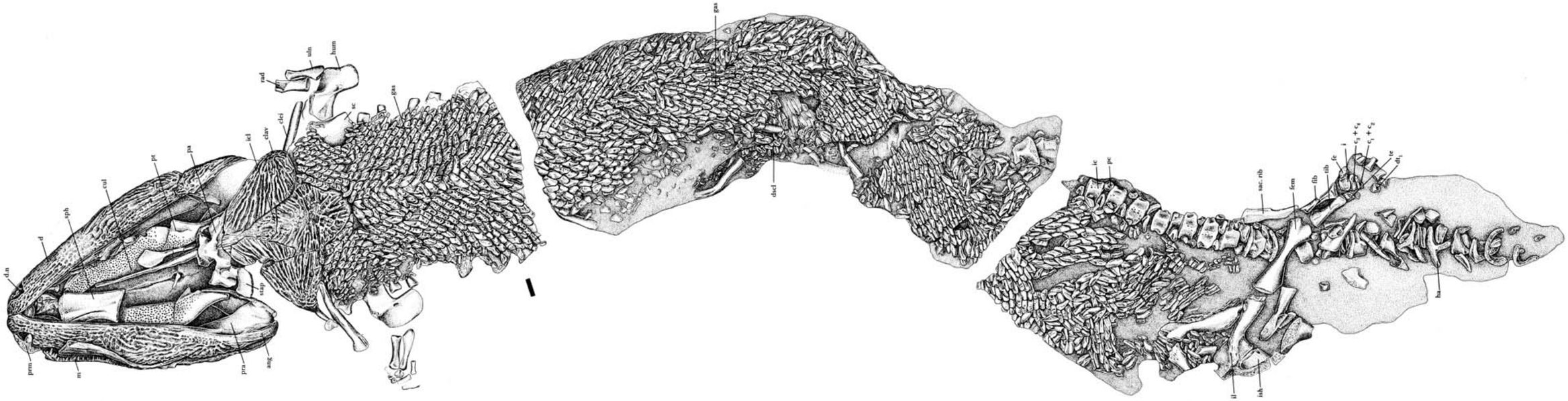

FIGURE 3*a*. *Greererpeton burkemorani* Roner, CMNH 11090. Articulated skeleton in ventral view. Scale bar 1 cm.

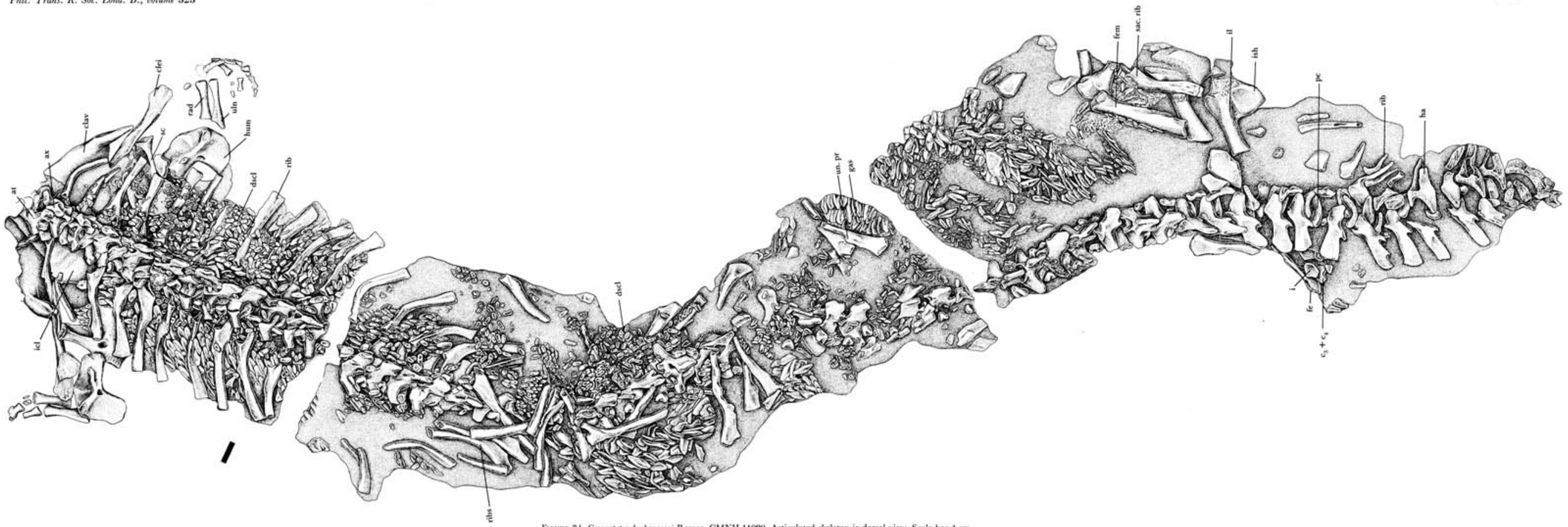

FIGURE 3*b*. *Greererpeton burkemorani* Romer, CMNH 11090. Articulated skeleton in dorsal view. Scale bar 1 cm.

PHILOSOPHICAL TRANSACTIONS OF THE ROYAL SOCIETY B BIOLOGICAL SCIENCES